

South Dakota State University

Open PRAIRIE: Open Public Research Access Institutional Repository and Information Exchange

Electronic Theses and Dissertations

2019

Evaluating Green Solvents and Techniques in Extraction Methods

Shanmugapriya Dharmarajan
South Dakota State University

Follow this and additional works at: <https://openprairie.sdstate.edu/etd>

 Part of the [Analytical Chemistry Commons](#)

Recommended Citation

Dharmarajan, Shanmugapriya, "Evaluating Green Solvents and Techniques in Extraction Methods" (2019). *Electronic Theses and Dissertations*. 3658.
<https://openprairie.sdstate.edu/etd/3658>

This Dissertation - Open Access is brought to you for free and open access by Open PRAIRIE: Open Public Research Access Institutional Repository and Information Exchange. It has been accepted for inclusion in Electronic Theses and Dissertations by an authorized administrator of Open PRAIRIE: Open Public Research Access Institutional Repository and Information Exchange. For more information, please contact michael.biondo@sdstate.edu.

EVALUATING GREEN SOLVENTS AND TECHNIQUES IN EXTRACTION
METHODS

BY

SHANMUGAPRIYA DHARMARAJAN

A dissertation submitted in partial fulfillment of the requirements for the

Doctor of Philosophy

Major in Chemistry

South Dakota State University

2019

DISSERTATION ACCEPTANCE PAGE

Shanmugapriya Dharmarajan

This dissertation is approved as a creditable and independent investigation by a candidate for the Doctor of Philosophy degree and is acceptable for meeting the dissertation requirements for this degree. Acceptance of this does not imply that the conclusions reached by the candidate are necessarily the conclusions of the major department.

Douglas Raynie

Advisor

Date

Department Head

Date

Dean, Graduate School

Date

ACKNOWLEDGEMENTS

I express my deepest gratitude to my advisor, Dr. Douglas Raynie, for his relentless support, constant encouragement and guidance throughout this journey. I thank him for being patient with me during my difficult times, having profound belief in my abilities, and offering countless opportunities to develop my skills. I thank my advisory committee members, Dr. Jihong Cole-Dai, Dr. Brian Logue, Dr. Matthew Miller and Dr. Hemachand Tummala for their invaluable advices and the constructive feedback throughout my graduate study.

I extend my sincere thanks to Dr. Logue and the Department of Chemistry and Biochemistry for motivating me with the Logue Academic Excellence Award. I gratefully acknowledge Dr. Fathi Halaweish, Dr. Ronald Hirko and Dr. Matthew Miller for teaching great classes and helping me develop my teaching skills. I sincerely appreciate Dr. Kasiviswanathan Muthukumarappan and his lab for providing samples for my research and letting me use some of their instruments. I thank CEM Corporation for the funding and the opportunity to work on their prototype extractor.

I appreciate my labmates Tanvir Amit, Sampson Asare, Jadhav Balawanthrao, Eric Boakye, Ganesh Degam, Victor Essel, George Gachumi, Hiran Kandala, John Kiratu, Vara Prasad, and Changling Qui for their academic and personal support. I am grateful to my fellow co-workers and staff, Department of Chemistry and Biochemistry, Graduate School, International Student Affairs and Indian Student Association.

My heartfelt thanks go to my friends Vijay Sundaram and Anand Rajendran for sharing best moments and caring for me during my stay in Brookings. I am greatly indebted to my mother Seethalakshmi Dharmarajan for her love and sacrifices. I extend

my acknowledgements to my family members and well-wishers for their blessings and encouragement. No words will be enough to express my thanks to my husband, Saravanan Ramasamy, without whom I could have not come this far. Finally, I thank my beloved son Kabilan Ramasamy for making me comprehend my inner strength.

TABLE OF CONTENTS

LIST OF TABLES	ix
LIST OF FIGURES	xii
ABSTRACT	xviii
1 Introduction and Background.....	1
1.1 Green Analytical Chemistry.....	1
1.1.1 Trends in Green Analytical Chemistry.....	2
1.1.2 Solvent Reduction and Replacement.....	2
1.2 Green Extraction Techniques	4
1.2.1 Assisted or Accelerated Extraction Techniques.....	5
1.2.2 Alternative Solvent Techniques:	7
1.2.3 Microextraction Techniques.....	7
1.2.4 Solid-Phase Extraction Techniques.....	7
1.2.5 Previous Works Done in Our Research Lab	8
1.3 The Objectives of this Study	10
2 Comparison of Green Solvents during Chemical Extraction of soybean oil	11
2.1 Introduction	11
2.1.1 Accelerated Solvent Extraction.....	11
2.1.2 Green Solvents	14
2.1.3 Soybean Oil.....	23
2.1.4 Solvent Extraction and Diffusion Coefficient.....	26

2.1.5 Hot-ball Model of Extraction	28
2.2 Experimental Methods	33
2.2.1 Materials and Reagents	33
2.2.2 Solubility Study in Computational Method.....	33
2.2.3 Viscosity Study.....	34
2.2.4 Extraction of Soybean oil using Accelerated Solvent Extractor	34
2.2.5 Application of the Hot-ball Model to Extraction Data.....	35
2.2.6 IR Spectroscopy	38
2.2.7 Esterification of Extracted Soybean Oil.....	38
2.2.8 GC-MS Characterization	39
2.3 Results and Discussion.....	40
2.3.1 Experimental Design	40
2.3.2 Sample Pretreatment.....	42
2.3.3 Effect of Particle Size on Extraction Yield	44
2.3.4 Solubility of Soybean Oil Components in Green Solvents	47
2.3.5 Viscosity of Green Solvents at Different Temperature	57
2.3.6 Characterization of extracted oil	60
2.3.7 ASE Extraction Results and Hot-ball model Comparison	62
2.3.8 <i>n</i> -Hexane Extraction and Hot-ball Model Results	66
2.3.9 2-MeTHF Extraction and Hot-ball Model Results.....	72

2.3.10	<i>alpha</i> -Pinene Extraction and Hot-ball Model Results.....	77
2.3.11	CPME Extraction and Hot-ball Model Results	82
2.3.12	Ethyl Lactate Extraction and Hot-ball Model Results.....	87
2.3.13	TBME Extraction and Hot-ball Model Results.....	92
2.3.14	Comparison of Extraction Efficiency of Green Solvents.....	97
2.4	Summary and Conclusions.....	107
3	Extraction of SOyBEAn oil using A Prototype Automated Extractor.....	110
3.1	Introduction	110
3.1.1	Automated Soxhlet Extraction	110
3.1.2	Prototype Automated Extractor from CEM	111
3.2	Experimental Methods	116
3.2.1	Materials and Reagents	116
3.2.2	Extraction of Soybean Oil Using CEM’s Prototype Extractor.....	116
3.3	Results and Discussion.....	118
3.3.1	Validating the CEM Extractor using the Hot-Ball Model.....	118
3.3.2	Comparison of Extraction Efficiency of ASE and the CEM Prototype Extractor.....	125
3.4	Summary and Conclusions.....	128
4	Efficiency of Adsorbents in Accelerated Solvent Extraction.....	129
4.1	Introduction	129

4.1.1 Use of Adsorbents in Extraction	129
4.1.2 In-Cell Cleanup during Accelerated Solvent Extraction.....	131
4.2 Experimental Methods	136
4.2.1 Materials and Reagents	136
4.2.2 Oil Adsorption Study in ASE.....	136
4.2.3 Oil Adsorption Study in CEM Prototype Extractor	139
4.3 Results and Discussion.....	140
4.3.1 Efficiency of Different Adsorbents in ASE Extraction.....	140
4.3.2 Efficiency of Different Adsorbents in CEM Extraction.....	142
4.3.3 Effect of Temperature on the Performance of Adsorbents.....	143
4.3.4 Effect of Adsorbent Concentration on the Performance of Adsorbents.....	147
4.4 Summary and Conclusions.....	151
5 Conclusion and Future Work	152
6 REFERENCES.....	156

LIST OF TABLES

Table 1.1 Comparison of Soxhlet, Soxtec, ASE, MAE, and ultrasound for greenness. (Table adapted from Driver 2009) ³¹	8
Table 2.1 GSK scores for the some common organic solvents and the solvents we used in our research. (Data obtained from Henderson <i>et al</i> 2011) ⁵¹	16
Table 2.2 List of green solvents (along with <i>n</i> -hexane) used to study the extraction of soybean oil and the physical properties of those solvents. ⁵²⁻⁵³	17
Table 2.3 Typical composition of soybeans (dry weight basis). ⁶¹ The amount of oil is 21%, which is the potential analyte in our extraction studies.....	23
Table 2.4 Major fatty acid methyl esters obtained from the hydrolysis and derivatization of triglycerides in soybean oil. ⁶¹	24
Table 2.5 Results of ASE extraction of oil from different size soybean particles using <i>n</i> -hexane (temperature is 100 °C).....	45
Table 2.6 Structure and σ -surface of the fatty acid triglycerides in soybean oil used for the COSMO solubility calculation.....	50
Table 2.7 Structure and σ -surface of the <i>n</i> -hexane and green solvents used for the COSMO solubility calculation.....	51
Table 2.8 Predicted solubility probability of triglycerides of major soybean fatty acids in different solvents. Green color represents high solubility (100%-60%), yellow color represents moderate solubility (60%-20%), and red color represent low solubility (20%-0%).....	56
Table 2.9 Results of accelerated solvent extraction (ASE) of soybean oil using <i>n</i> -hexane as solvent (particle size is 513 μ m, temperature is 100 °C).....	67
Table 2.10 Hot-ball model results for the ASE extraction of soybean oil using <i>n</i> -hexane.	69

Table 2.11 Results of accelerated solvent extraction (ASE) of soybean oil using 2-MeTHF as solvent (particle size is 513 μm , temperature is 100 $^{\circ}\text{C}$).	73
Table 2.12 Hot-ball model results for the ASE extraction of soybean oil using 2-MeTHF	75
Table 2.13 Results of accelerated solvent extraction (ASE) of soybean oil using <i>alpha</i> -pinene as solvent (particle size is 513 μm , temperature is 100 $^{\circ}\text{C}$).	78
Table 2.14 Hot-ball model results for the ASE extraction of soybean oil using α -pinene.	80
Table 2.15 Results of accelerated solvent extraction (ASE) of soybean oil using CPME as solvent (particle size is 513 μm , temperature is 100 $^{\circ}\text{C}$).	83
Table 2.16 Hot-ball model results for the ASE extraction of soybean oil using CPME.	85
Table 2.17 Results of accelerated solvent extraction (ASE) of soybean oil using ethyl lactate as solvent (particle size is 513 μm , temperature is 100 $^{\circ}\text{C}$).	88
Table 2.18 Hot-ball model results for the ASE extraction of soybean oil using ethyl lactate	90
Table 2.19 Results of accelerated solvent extraction (ASE) of soybean oil using TBME as solvent (particle size is 513 μm , temperature is 100 $^{\circ}\text{C}$).	93
Table 2.21 Comparison of percent of soybean oil extracted in ASE using different solvents at different times.	98
Table 2.22 Comparison of percent of soybean oil recovered in ASE using different solvents at different times.	99
Table 2.23 Linear regression analysis for the plot of $\ln(m/m_0)$ vs. extraction time for different solvents.	102

Table 2.24 Calculated extraction time equivalent to $t_r = 1$ and diffusion coefficient for ASE extraction of soybean oil using different solvents (particle size = 513 μm).	105
Table 3.1 Results of soybean oil extraction using <i>n</i> -hexane in the CEM prototype extractor (particle size is 513 μm , temperature is 100 $^{\circ}\text{C}$).....	120
Table 3.2 Hot-ball model results for soybean oil extraction using <i>n</i> -hexane in the CEM prototype extractor.	122
Table 4.1 Amount of Adsorbent and Oil used for Initial Study of selectivity of adsorbents	137
Table 4.2 Amount of adsorbents and oil used to study the effect of temperature and the effect of adsorbent's concentration on adsorption efficiency.	138
Table 4.3 ASE extraction results for different adsorbents	150

LIST OF FIGURES

Figure 1.1 Relative contribution of green extraction techniques in recent literature based on the data reported by Berton <i>et al.</i> ⁸	5
Figure 1.2 Comparison of extraction methods based on the complexity and selectivity. (Image adapted from chromacademy.com)	9
Figure 2.1 Schematic diagram of accelerated solvent extraction (ASE) system describes flow of pressurized solvent during the extraction process (image adapted from Richter et al 1996) ³⁹	12
Figure 2.2 Image of Dionex™ ASE™ 350 Accelerated Solvent Extractor used in this research work. (Image obtained from ThermoFisher Scientific).....	12
Figure 2.3 Chart combines the environment, health, and safety (EHS), and cumulative energy demand (CED) of some common solvents. (Image adapted from Byrne <i>et al.</i> 2016) ¹⁴	15
Figure 2.4 The plot defines the three regions i) an equilibrium region dominated by solute partitioning, ii) a diffusion region controlled by solute diffusion, and iii) a transitional region. (Image adapted from Raynie 2000) ⁶⁸	27
Figure 2.5 Theoretical plots of hot-ball model.	30
Figure 2.6 Flow chart showing the process involved in the comparison of efficiency of green solvent in ASE extraction of soybean oil.....	41
Figure 2.7 Soybeans before and after grinding	42
Figure 2.8 Sieving process of ground soybean sample.....	43
Figure 2.9 The percent yield of different size soybean particles following the sieving process.....	43

- Figure 2.11** Computer predicted σ -profile (charge density profile) of solvents and solute compounds (Generated in COSMO Software). This chart compares the distribution of positive and negative charges on the surface of solvent and solute molecules. 52
- Figure 2.12** Computer predicted σ -potential of soybean triglycerides compounds (Generated in COSMO Software). This chart shows the chemical potential of the four different triglycerides compounds are more or less same..... 52
- Figure 2.13** Computer predicted σ -potential of soybean hexane and green solvents (Generated in COSMO Software). This chart shows that the chemical potential of the solvents varies with polar, nonpolar, protic and aprotic nature of the compounds. 53
- Figure 2.14** Comparison of change in viscosity of solvents at different temperature. 58
- Figure 2.15** Reaction scheme show the conversion of fatty acids (from triglyceride) in the soybean oil into methyl esters using Lewis acid catalyzed esterification..... 61
- Figure 2.16** Photograph of the reaction setup used for methyl esterification of fatty acids in soybean oil. 61
- Figure 2.17** Picture of extracts (that contains oil) collected from ASE. As the amount of solvent used is about 30 mL, a concentration and drying process was required after extraction..... 62
- Figure 2.18** Example of qualitative comparison of experimental plot of percent recovery vs. extraction time, obtained from *n*-hexane extraction, with the theoretical hot-ball model plot. 64
- Figure 2.19** Example of qualitative and quantitative comparison of experimental plot of $\ln(m/m_o)$ vs. reduced time, obtained from CPME solvent extraction, with the theoretical hot-ball model plot..... 65
- Figure 2.20** Percent of oil recovered out of total extractable oil in soybean sample using *n*-hexane at different extraction times. Particle size is 513 μm 67

- Figure 2.21** Plot of $\ln(m/m_0)$ vs. extraction time for *n*-hexane scaled to the reduced time (t_r) to compare with the hot-ball model..... 69
- Figure 2.22** Comparison of IR spectra of commercial soybean oil and soybean oil extracted in ASE using *n*-hexane..... 71
- Figure 2.23** Gas chromatogram shows the presence of fatty acid methyl ester derivatives from soybean oil extracted in ASE using *n*-hexane..... 71
- Figure 2.24** Percent of oil recovered out of total extractable oil in soybean sample using 2-MeTHF at different extraction times. Particle size is 513 μm 73
- Figure 2.25** Plot of $\ln(m/m_0)$ vs. extraction time for 2-MeTHF scaled to the reduced time (t_r) to compare with the hot-ball model..... 75
- Figure 2.26** Comparison of IR spectra of commercial soybean oil and soybean oil extracted in ASE using 2-MeTHF. 76
- Figure 2.27** Gas chromatogram shows the presence of fatty acid methyl ester derivatives from soybean oil extracted in ASE using the green solvent 2-MeTHF..... 76
- Figure 2.28** Percent of oil recovered out of total extractable oil in soybean sample using *alpha*-pinene at different extraction times. 78
- Figure 2.29** Plot of $\ln(m/m_0)$ vs. extraction time for *alpha*-pinene scaled to the reduced time (t_r) to compare with the hot-ball model. 80
- Figure 2.30** Comparison of IR spectra of commercial soybean oil and soybean oil extracted in ASE using *alpha*-pinene. 81
- Figure 2.31** Gas chromatogram shows the presence of fatty acid methyl ester derivatives from soybean oil extracted in ASE using the green solvent *alpha*-pinene. 81
- Figure 2.32** Percent of oil recovered out of total extractable oil in soybean sample using CPME at different extraction times. 83

Figure 2.33 Plot of $\ln(m/m_0)$ vs. extraction time for CPME solvent was scaled to the reduced time (t_r) to compare with the hot-ball model.....	85
Figure 2.35 Gas chromatogram shows the presence of fatty acid methyl ester derivatives from soybean oil extracted in ASE using the green solvent CPME.	86
Figure 2.36 Percent of oil recovered out of total extractable oil in soybean sample using ethyl lactate at different extraction times.....	88
Figure 2.37 Plot of $\ln(m/m_0)$ vs. extraction time for ethyl lactate was scaled to the reduced time (t_r) to compare with the hot-ball model.....	90
Figure 2.38 Comparison of IR spectra of commercial soybean oil and soybean oil extracted in ASE using ethyl lactate.	91
Figure 2.39 Gas chromatogram shows the presence of fatty acid methyl ester derivatives from soybean oil extracted in ASE using the green solvent ethyl lactate.....	91
Figure 2.40 Percent of oil recovered out of total extractable oil in soybean sample using TBME at different extraction times.	93
Table 2.20 Hot-ball model results for the ASE extraction of soybean oil using TBME .	95
Figure 2.41 Plot of $\ln(m/m_0)$ vs. extraction time for TBME solvent was scaled to the reduced time (t_r) to compare with the hot-ball model.....	95
Figure 2.42 Comparison of IR spectra of commercial soybean oil and soybean oil extracted in ASE using TBME solvent.	96
Figure 2.43 Gas chromatogram shows the presence of fatty acid methyl ester derivatives from soybean oil extracted in ASE using the green solvent TBME.	96
Figure 2.44 Percent of oil extracted from soybean using different solvents at different extraction times. As the y-axis is an extended % extraction, zero intercept is not shown.	98

Figure 2.45 Percent of oil recovered from soybean using different solvents at different extraction times.	99
Figure 2.47 Comparison of diffusion coefficients of green solvents with <i>n</i> -hexane.	105
Figure 2.48 Comparison of the overall efficiency of green solvents based on the time required for 99% oil recovery.	106
Figure 3.1 The prototype energized dispersive extraction from CEM Corporation.	112
Figure 3.2 The sample holder (Q-cup) used in CEM EDGE. (Image obtained from CEM.).....	113
Figure 3.3 The energized dispersive extraction process in CEM prototype extractor. (Image obtained from CEM).....	115
Figure 3.4 An upgraded version of automated energized dispersive extraction EDGE from CEM. (Image obtained from CEM)	115
Figure 3.5 Percent oil recovered from the soybean sample using <i>n</i> -hexane at different extraction times in the CEM prototype extractor. The average particle size is 513 μm	120
Figure 3.6 Plot of $\ln(m/m_0)$ vs. extraction time for <i>n</i> -hexane scaled to the reduced time (t_r) to compare with the hot-ball model.....	122
Figure 3.7 Comparison of IR spectra of commercial soybean oil and soybean oil extracted in the CEM prototype extractor using <i>n</i> -hexane.	124
Figure 3.8 Gas chromatogram shows the presence of fatty acid methyl ester derivatives from soybean oil extracted in the CEM prototype extractor using <i>n</i> -hexane.	124
Figure 3.9 Comparison of percent recovery from ASE and CEM's prototype extractor.	126
Figure 3.10 Comparison of $\ln(m/m_0)$ curves from ASE and the CEM prototype extractor.	127

Figure 4.1 Schematic image shows the sample and adsorbent packing in ASE extraction cell.....	137
Figure 4.2 Adsorption of soybean oil by different adsorbents during ASE extraction (at 100 °C) using <i>n</i> -hexane.....	141
Figure 4.3 Adsorption efficiency of five different adsorbents during the CEM extraction.	143
Figure 4.4 Effect of temperature on the performance of silica in adsorbing soybean oil during ASE extraction as a function of adsorbent:oil.....	145
Figure 4.5 Effect of temperature on the performance of florisil in adsorbing soybean oil during ASE extraction as a function of adsorbent:oil	146
Figure 4.6 Effect of temperature on the performance of activated carbon in adsorbing soybean oil during ASE extraction as a function of adsorbent:oil.....	147
Figure 4.7 Effect of oil to adsorbent weight ratio on the performance of silica at different temperatures.....	148
Figure 4.8 Effect of oil to adsorbent weight ratio on the performance of florisil at different temperatures.	148
Figure 4.9 Effect of oil to adsorbent weight ratio on the performance of activated carbon at different temperatures.	149

ABSTRACT

EVALUATING GREEN SOLVENTS AND TECHNIQUES IN EXTRACTION
METHODS

SHANMUGAPRIYA DHARMARAJAN

2019

Of all analytical techniques, extraction is a huge solvent-consuming process that could adversely impact the environment. Use of petroleum-based solvents for extraction of oilseeds is still a common practice, despite the potential fire hazard and the toxic water pollution. The rising awareness of chemical activities created immense need for sustainable development schemes and strategies that should address the environmental impact without compromising the yield. In the course of developing green extraction techniques, automation, alternative solvents, and selective extractions are the growing trend. This dissertation aligns with that progress by surveying green solvents, comparing their performance during oil extraction, examining a prototype automated extraction system, and studying the efficiency of selective adsorbents.

Green solvents are of great interest as they are sourced from renewable feedstock and pose little or no danger to the environment. But their application in analytical chemistry is not widely appreciated. This dissertation aimed to study the extraction efficiency of green solvents during accelerated solvent extraction of soybean oil. Five green solvents, 2-methyltetrahydrofuran (2-MeTHF), alpha-pinene, cyclopentyl methyl ether (CPME), ethyl lactate, and t-butyl methyl ether (TBME), were chosen based on the literature, solubility, and viscosity. Using the GSK solvent-scoring system obtained from literature, the ecological and economic impact of these solvents were roughly identified

with respect to *n*-hexane. As the solubility of analytes can influence the initial part of the extraction, relative solubility of triglycerides (of the major soybean fatty acids such as linoleic acid, oleic acid, palmitic acid, and stearic acid) in the green solvents was theoretically predicted using a computer program. Also, the viscosities of the green solvents at different temperatures was investigated prior to the extraction study.

Soybean, the most dominant oilseed in the market with rich protein and oil content, was used as the sample for the extraction study. As the initial analysis indicated that the lower size particles give greater oil recovery, soybean particles of average diameter 513 μm were chosen for the elaborate extraction evaluation. For a small-scale fast extraction of analytes from solid and semisolid samples, accelerated solvent extraction (ASE) is a powerful and sophisticated device. This fully automated extraction system uses very little solvent at elevated temperature and pressure and is able to run several queued experiments at programmed conditions. To rely on the results from ASE of soybean oil using green solvents, the hot-ball model was used as a validating tool. The hot-ball model gives a theoretical extraction profile for an ideal spherical matrix that can be used to evaluate and validate any experimental extraction results.

As diffusion plays a major role in the kinetics of extraction, comparing the diffusion coefficient of green solvents was the key approach. Upon assessing the performance of green solvents with respect to percent oil recovery, CPME demonstrated the highest diffusion coefficient and highest % recovery for soybean oil. A remarkable 99% recovery was attained within 30 min, which is 17 times faster than *n*-hexane. These results suggest CPME as a promising green alternative solvent for soybean oil extraction.

The second part of this dissertation examines a new green extraction system. A prototype automated extractor from CEM was investigated in terms of its extraction efficiency. The knowledge obtained from previous ASE extraction studies were used to gauge the capabilities of this instrument, and the hot-ball model was used to validate the results.

Adsorbents are a significant part of the post-extraction cleanup process and studying their efficiency could reveal their ability to green the analytical techniques. The mechanism of adsorption is complex, and it varies with each adsorbate-solvent-adsorbent system. The last part of the dissertation aimed to investigate the oil adsorption efficiency of five adsorbents – silica, florisil, activated carbon, alumina and diatomaceous earth – during ASE extractions at different temperatures and concentration. Results showed that activated carbon has remarkable tendency to retain oil, at low temperatures and high adsorbent concentrations.

1 INTRODUCTION AND BACKGROUND

1.1 Green Analytical Chemistry

The concept of sustainable development and protection of the environment emerged in the scientific community in the late 20th century. To address the increasing concern about the impact of chemical activities on environment, Anastas and Warner formulated the 12 principles to define green chemistry in 1998.¹ As the awareness grew, the responsibility to practice environmental friendly chemistry spread across all areas in the discipline. The key principles of green chemistry, which insist a contribution from analytical chemistry, include prevention of waste, use of non-toxic substances, use of safer solvents and auxiliaries, design for energy efficiency, reduction of derivatives, real-time analysis for pollution prevention, and inherently safer chemistry for accident prevention.²⁻³ Thus the demand for developing green analytical methodologies shaped at both the industrial and the laboratory scale.

To meet the increasing needs in everyday life, a rapid expansion of manufacturing technology became unavoidable. But by employing the green chemistry principles in the designing of these technologies, an exploitation of the environment can be avoided. As the size of industrial production goes up, the amount of chemicals used in the analytical steps such as extraction, purification, and identification would also increase. To curb generating large amount of waste, a modification of existing analytical technologies incorporating green measures is necessary. Identifying the ways to cut down chemical wastes, and using of safer chemicals are the two significant efforts that analytical chemists can definitely contribute.³ This initiative toward environmental protection set a stage for a new area of research called “green analytical chemistry”.

1.1.1 Trends in Green Analytical Chemistry

The primary objective of green analytical chemistry is to not only lower the environmental impact of the analyses, but also to provide the information crucial to make decisions regard to environmental and human health. To meet these objectives, new innovative models should be introduced in the two main schemes of analytical chemistry, the sample preparation and the signal generation.

In recent years, the trends in green analytical chemistry took a direction toward advancing the sensitivity of analytical devices to determining analytes at low concentration in complex sample matrix, particularly in environmental analysis.⁴ If fast, precise and accurate result at ppb level is the goal, this may not be achieved without a progression in developing of new sample preparation procedures. The traditional sample preparation methods consist of operations such as preservation and pretreatment of the sample, calibration and preparation of equipment, extraction of analytes from the sample matrix, separation of the extract from undesired co-extracts, removal of solvent, drying and further purification before chromatographic analysis. These analytical steps are crucial in testing of toxic substances in food, plants and environmental samples.⁵ But ironically, this procedure generates greater toxic substances than what is being tested. Many efforts were made in recent years to automate some of these tedious and exhausting procedures in order to maximize the reliability, and at the same time minimize the use of chemicals.⁶⁻⁸

1.1.2 Solvent Reduction and Replacement

Solvent are used in large quantities especially in the purification stage, as they play a vital role in increasing the recovery. A study reports that out of all types of

materials used to manufacture an active pharmaceutical ingredient, non-aqueous solvents constituted 80-90% by mass.⁹ Until the advent of green chemistry, the impact of lavish solvent usage on the environment had been underestimated. Solvents represent about 75-80% of harmful impact on environmental health out of all materials used in pharmaceutical companies in 2005.¹⁰⁻¹¹ The solvent market was one of the profitable areas for petroleum industries, despite the unsustainable nature of petroleum based solvents. The process of fabricating solvents is energy consuming in every step, which itself causes damage to the environment. A wide range of techniques have been introduced in the last decade to reduce the use of solvents in small scale analytical processes (discussed in section 1.2). The scaling up of these techniques to an industrial level is still a goal.³

The choice of solvent is another important factor influencing the percent recovery in sample preparation steps. A solvent neither participates in reaction with the components of sample nor is it directly responsible for the composition of the extract, but its physical properties such as polarity, viscosity, and boiling point are crucial in carrying out an extraction. Thus unnecessary use of environment-damaging solvents would devalue the fortune of extracts obtained in the process. Though hydrocarbon solvents are cheap and have the ability to dissolve a wide variety of oils, their low water solubility poses danger to aquatic lives.¹² The consequence of using undesirable solvents can be eliminated by opting for green solvents. Around the world, a growing number of inquiries on harmful solvents force many countries to restrict the application of widely used solvents such as toluene, dichloromethane, chloroform, DMF, etc.¹³

Among the several methods developed to define and index green solvents, the one based on the net cumulative energy demand (CED) of solvents is common. The difference between the energy required to produce a solvent and the energy reclaimed at final stage of solvent is used to calculate the CED of the solvent.¹⁴ Other considerations in assessing greenness of solvents include fire and explosion safety, toxicity to humans, water and air hazard, reaction and decomposition, etc. However, users do not always entail the selection tools, but some basic understanding of solvents can be used to choose an alternative solvent with minimum safety concern, low toxicity and little impact on the environment. Solvents sourced from renewable feedstock are promising candidates.¹⁵ Many unconventional bio-based solvents were incorporated in recent solvent selection guides, as discussed in section 2.1.2. Efficiency of these green solvents in analytical techniques is not quite recognized, and this is a fresh area of research.

1.2 Green Extraction Techniques

The reduction of chemical wastes in sample preparation is a cornerstone of green analytical chemistry. As new technologies rapidly developed in the new millennium, the already widespread green initiatives carefully utilized them to improve sample preparation methods. Miniaturization and automation of extraction techniques remarkably increased the precision and accuracy, and at the same time reduced the amount of sample, solvent and energy consumption.⁸ Some other advantages along this line include effective use of labor, reduced exposure to dangerous substances, preventing accidents at workplace, fewer consumables, better waste management, and reduction of residue accumulation. A brief account of the promising green extraction techniques is

discussed in this Introduction. In **Figure 1.1** relative contribution of green extraction techniques showed that assisted or accelerated extraction techniques contributed the most (43%). The other extraction techniques such as solid-phase extraction techniques, microextraction techniques and alternative solvent techniques contributed 29%, 22% and 6% respectively.

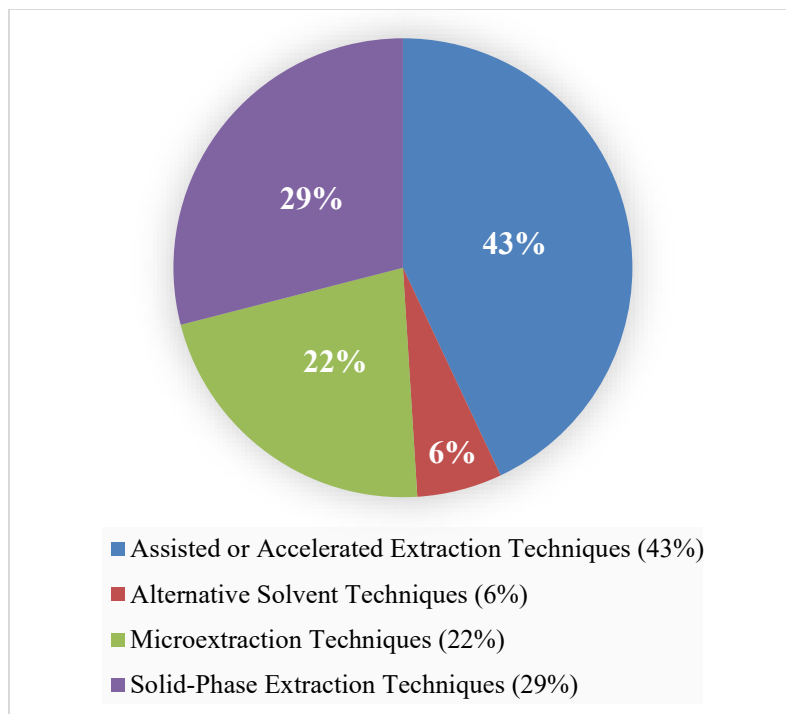


Figure 1.1 Relative contribution of green extraction techniques in recent literature based on the data reported by Berton *et al.*⁸

1.2.1 Assisted or Accelerated Extraction Techniques

In order to increase the mass transfer of analytes into a solvent of low volume, the physical condition of the medium is altered in the assisted or accelerated extraction techniques. Many recent reports provide evidence that the extraction efficiency can be enhanced with the aid of high pressure, ultrasound and microwave.⁸

Pressurized fluid extraction (PFE) or accelerated solvent extraction (ASE) is a commonly used techniques for environmental, food and biological samples.¹⁶⁻¹⁹

Compared to the conventional open vessel Soxhlet extraction (SE), the solvent in ASE extraction cell reaches high temperature and pressure that increases the solvent penetration, sample solubility, and analyte diffusion rate. ASE is more automated and a much safer extraction technique that requires only about 30-35 mL of solvent for 10 grams of sample, and most extraction can be done in 30 min.¹⁷ In this dissertation, the majority of extraction study is conducted using ASE. The option of carrying out in-cell cleanup is an addition advantage of ASE that is discussed in detail in section 4.1.2.

Microwave assisted extraction (MAE) is another prominent green extraction techniques that reduces solvent usage to as low as 30 mL per 10 grams of sample.²⁰ Microwave radiation generates heat directly at the molecules of polar solvents, which is more energy efficient than using of heating chambers. The increased temperature in sealed vessels elevates the pressure, which subsequently lowers the viscosity of solvent and promotes analyte diffusion. In case of non-polar solvents, a microwave-active polar counterpart is mixed to receive the radiation. Some common solvent mixtures for MAE are toluene-methanol, hexane-acetone, cyclohexane-isopropanol, and xylene-dichloromethane.^{21 22}

Ultrasound assisted extraction (UAE) employs high-energy ultrasound to disintegrate and disperse the solid sample into liquid solvent. As this strategy increases the surface-to-volume ratio to assist analyte extraction, a very low volume of sample is sufficient in most cases.²³ A focused ultrasonic probe immersed in solution is often used to increase the concentration of soundwaves. This method was reported for extraction of toxic substance (eg., polybrominated diphenyl ethers) in environmental and biological samples.^{24 25}

1.2.2 Alternative Solvent Techniques:

Supercritical fluid extraction (SFE), cloud point extraction (CPE), and ionic liquids (ILs) are some of the alternative solvent techniques that fit in the concept of green sample preparation methods. SFE uses solvents at temperature and pressures above their critical points, which ultimately increases the diffusivity of those solvent for better extraction efficiency. Supercritical carbon dioxide, is a widely used solvent for this purpose.²⁶ CPE utilizes the amphiphilic nature of surfactants to abstract analytes that are not readily soluble in water, by micelles formation.²⁷ ILs, such as 1-octyl-3-methylimidazolium hexafluorophosphate, possess high thermal stability, and low vapor pressure, and ability to dissolve wide range of analytes. The last two alternative solvent techniques were barely studied, but existing reports indicate that a proper selection of solvents could notably increase the extraction efficiency.²⁸

1.2.3 Microextraction Techniques

Liquid-phase microextractions (LPME) are suitable for aqueous samples, where an extracting organic solvent and a dispersing solvent are introduced into liquid phase sample to create a microemulsion. Due to the increased surface contact, increased mass of analyte from the aqueous sample matrix is transferred to the organic solvent. This method was reported to work best with environmental water samples, semi-solid sediments, milk and plant, and animal tissues.²⁹⁻³⁰

1.2.4 Solid-Phase Extraction Techniques

Solid-phase extraction (SPE) techniques use a multilayer column filled with sorbents for the selective extraction of analytes from the sample dissolved in eluent. Dispersive solid-phase extraction (d-SPE) uses sorbents that can be dispersed into the

sample solution for increased surface contact, and selective extraction. This method is commonly employed in QuEChERS (more detailed discussion is given in section 4.1.1). Solid-phase microextraction (SPME) is a solventless technique that uses sorbent coated thin-silica fiber to adsorb analytes from sample.

1.2.5 Previous Works Done in Our Research Lab

Our research group has been engaged in exploring and comparing different extraction techniques for past several years. Previously, we had investigated the efficiency and greenness of different extraction methods such as Soxhlet, accelerated solvent extraction, microwave assisted extraction, ultrasound assisted extraction, and Soxtec (automated Soxhlet).³¹ **Table 1.1** shows the comparison of energy score, extraction temperature, solvent volume, and typical extraction time of the different extraction methods. With smallest volume, extraction time, and energy, the performance of ASE and MAE stand out among the other modern techniques.

Table 1.1 Comparison of Soxhlet, Soxtec, ASE, MAE, and ultrasound for greenness. (Table adapted from Driver 2009)³¹

Technique	Green Energy Score	Extraction temperature (°C)	Solvent volume (mL)	Typical extraction time (minutes)
Soxhlet	3	39	150	480 – 1440
Soxtec	3	39	45	30 – 60
ASE	2	100	30	30
MAE	2	100	30	30
Ultrasound	2	39	150	30

The application of ASE for the extraction of beeswax from honeycomb, cappings, slumgum, and filter cakes using supercritical CO₂ was investigated.³² We had also investigated the effects of temperature, pressure, and time on extraction yield, and the

efficiency of common adsorbents such as silica gel, diatomaceous earth, florisil, alumina oxide, and activated charcoal in discoloring of extracted beeswax.³²

A list of extraction methodology was compared with a viewpoint of complexity and selectivity in extraction (Figure 1.2).³³ Pressurized fluid extraction (PFE or ASE) is a solvent-based technique, where polarity match between the analyte and the extraction phase is the key to selectivity.

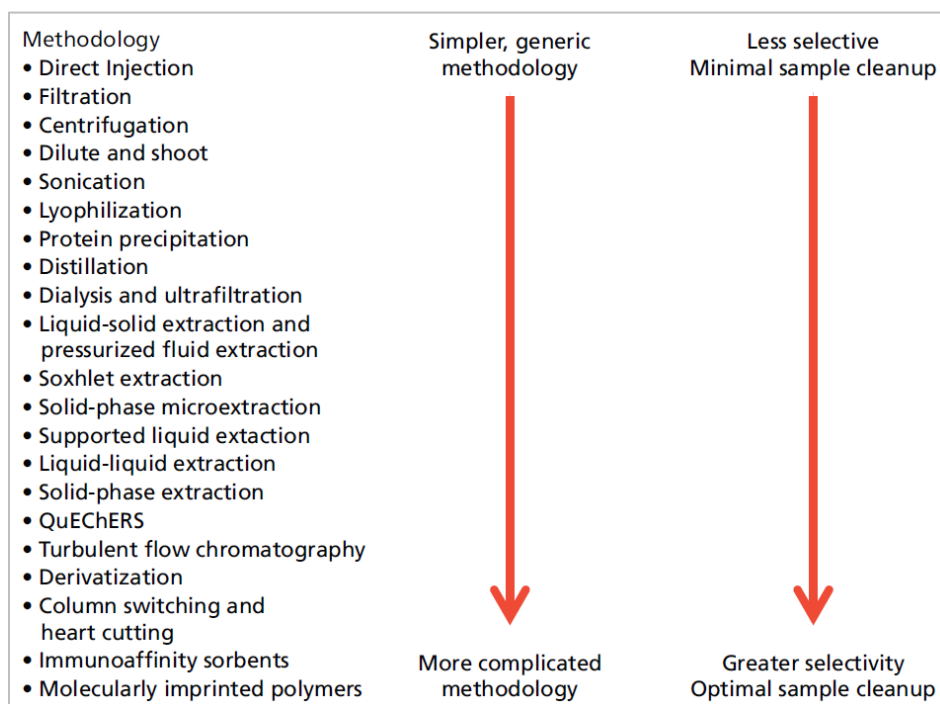


Figure 1.2 Comparison of extraction methods based on the complexity and selectivity. (Image obtained from chromacademy.com)

ASE can be used for complete extraction of various classes of compounds. This technique is accepted by US EPA, US Contract Laboratory Program, US ASTM, and in other countries like China and Germany. Also, methods using ASE for determination of polycyclic aromatic hydrocarbons and chlorinated hydrocarbons have been validated in National Oceanic and Atmospheric Administration (NOAA).³⁴

1.3 The Objectives of this Study

The overall objective of this dissertation is a continuing effort of exploring green analytical techniques. The main focus is to study the performance of green solvents and adsorbents during a seed oil extraction using automated solvent extraction systems. Also, the experiments were designed to understand the effect of diffusion in small scale and short-time extractions.

The specific objectives are summarized as

- (i) Compare the extraction efficiency of green solvents using a green extraction technique.
- (ii) Propose green alternatives to the commonly used hydrocarbon solvent *n*-hexane for soybean oil extraction.
- (iii) Validate the green solvent extraction technique using the hot-ball model and diffusion study.
- (iv) Explore and examine a prototype automated extraction system.
- (v) Compare the oil adsorption efficiency of a few common adsorbents during accelerated solvent extraction.

2 COMPARISON OF GREEN SOLVENTS DURING CHEMICAL EXTRACTION OF SOYBEAN OIL

2.1 Introduction

2.1.1 Accelerated Solvent Extraction

Accelerated solvent extraction (ASE) uses small volume of organic solvents at high pressures and temperatures to extract analytes from samples. ASE is one of the modern extraction techniques that have been developed in last two decades to replace the classical ways of extractions. Various techniques like automated Soxhlet extraction,³⁵ microwave extraction,³⁶ sonication extraction,³⁷ supercritical fluid extraction,³⁸ and accelerated solvent extraction have been developed to reduce both the volume of solvent required and time of sample preparation.³⁴

Extraction with ASE is performed at elevated temperature (50-200 °C) and pressure (500 – 3000 psi) conditions for short times (5-10 min). A sample cartridge packed with solid or semisolid sample is preheated and filled with extraction solvent under the programmed extraction conditions. A compressed gas is used to flush the solvent that contains extracted analyte from the cartridge into a collection vessel.³⁹ Unlike the Soxhlet, where the solvent temperature is below the boiling point, in ASE the solvent temperature is maintained above the atmospheric boiling point. As the sample cell in ASE is pressurized, the solvent remains in liquid state even above its boiling point. Thus the volume of solvent required for ASE extraction is relatively small (about 90% less than Soxhlet extraction).⁴⁰ This pressurized fluid extraction method takes less time to recover maximum extractable analyte that is due to the 1) solubility and mass transfer effect, and 2) disruption of surface equilibria.

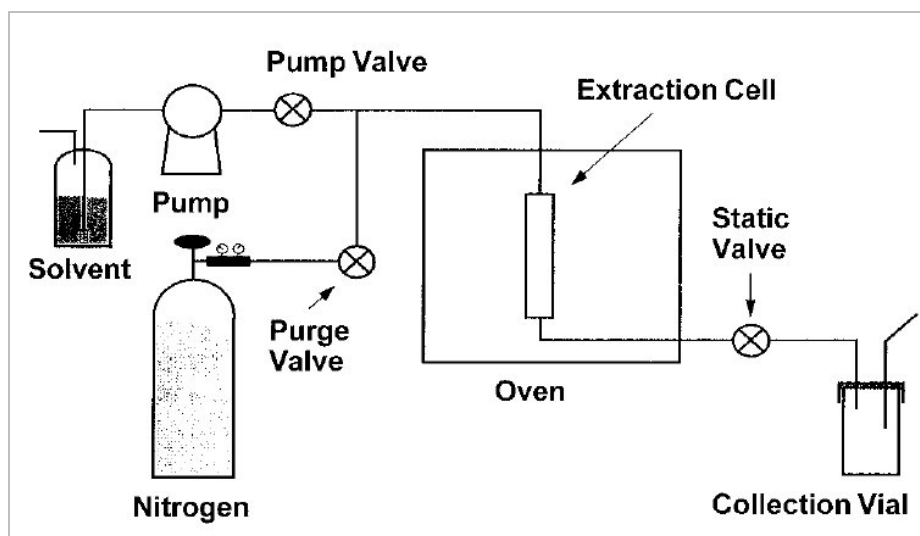


Figure 2.1 Schematic diagram of accelerated solvent extraction (ASE) system describes flow of pressurized solvent during the extraction process (image obtained from Richter et al 1996)³⁹



Figure 2.2 Image of Dionex™ ASE™ 350 Accelerated Solvent Extractor used in this research work. (Image obtained from ThermoFisher Scientific).

Accelerated solvent extraction is a trademark name of an instrument manufactured by Dionex for pressurized fluid extraction. **Figure 2.1** shows the schematic diagram of an ASE unit that describes the flow of pressurized solvent through the extraction cell and the flow of extract into a collection flask. **Figure 2.2** shows the actual model (Dionex™ ASE™ 350) that was used in this research work. It consists of extraction cells that are heated in an oven and pressurized with solvent pumped from a reservoir using compressed gas. The cell is rinsed after extraction and the solvent with extract is collected in a collection vial.

The enhanced performance of ASE over the other extraction techniques was reported by Richter *et al.*³⁹ The use of elevated temperature increases the ability of solvent to dissolve the analyte.⁴¹ It is difficult to obtain the relationship between the temperature and the diffusion rate for a multicomponent analyte, but in general, the diffusion rate increases with the temperature. The introduction of fresh solvent during the static extraction increases the concentration gradient, and hence enhances the mass transfer (Fick's first law of diffusion).⁴² This will result in an escalated extraction rate.

In this research work, we used the Accelerated Solvent Extraction to compare the efficiency of different green solvents in extracting oil from soybean sample. The operating conditions of ASE was optimized for the green solvents and the soybean sample.

2.1.2 Green Solvents

The goal of green chemistry is to lower the effect of chemicals on human health and practically avoid contamination of the environment. This should be achieved through adapting our classical techniques to alternative, environmentally friendly reactions or extraction media and at the same time make effort to increase reaction or extraction rates.

Solvents have received great attention under the growth of the green chemistry field. Though solvent is not an active part of composition of a reaction product and does not directly alter the mechanism of a chemical process, a large volume of solvent is normally used in extraction or purification steps.⁴³⁻⁴⁵ Because solvents have no effect on the function of the chemical processes, it is unnecessary to use toxic or environmentally hazardous solvents.¹⁴ While less polar solvents, like hydrocarbons, possess the ability to dissolve a wide variety of oils in extraction and separation processes, their low water solubility leads to bioaccumulation and aquatic toxicity.¹² Common solvents like dichloromethane, chloroform, benzene, and toluene are suspected of being carcinogenic to humans and lead to ozone depletion.⁴⁶⁻⁴⁷ There are several restrictions from “Registration, Evaluation, Authorization and Restriction of Chemicals” (REACH) of Europe on the chemicals like toluene, chloroform, and dichloromethane.⁴⁸ Amide-containing solvents have high polarity and are used in reactions where a wide range of reagents need to be dissolved. Amide-containing solvents like N,N-dimethylformamide (DMF), N,N-dimethylacetamide (DMAc), and N-methylpyrrolidinone (NMP), as well as certain hydroxyethers and chlorinated solvents have fallen under scrutiny because of their environmental risk factors. To evade these restrictions, replacement strategies look for solvents of close structural similarity that are not yet covered by the regulatory affairs,

ignoring the fact that these replacements could often have same health and environmental hazards.

Categorizing solvents based on the regulatory assessment and the environment, health and safety (EHS) profiles requires a sophisticated selection tool. The approach of replacing conventional solvents with greener bio-based organic solvents should also address the performance of solvent, and the energy demand in production and implication of green solvents. The net cumulative energy demand (CED) in producing a solvent is the difference in the amount energy required to produce the solvent and the amount of energy recovered at end in various ways (incineration, recycling, etc.).⁴⁹ **Figure 2.3** shows the incorporation of the energy demand and the EHS scores of different solvents that will give a big picture of the impact of solvents.

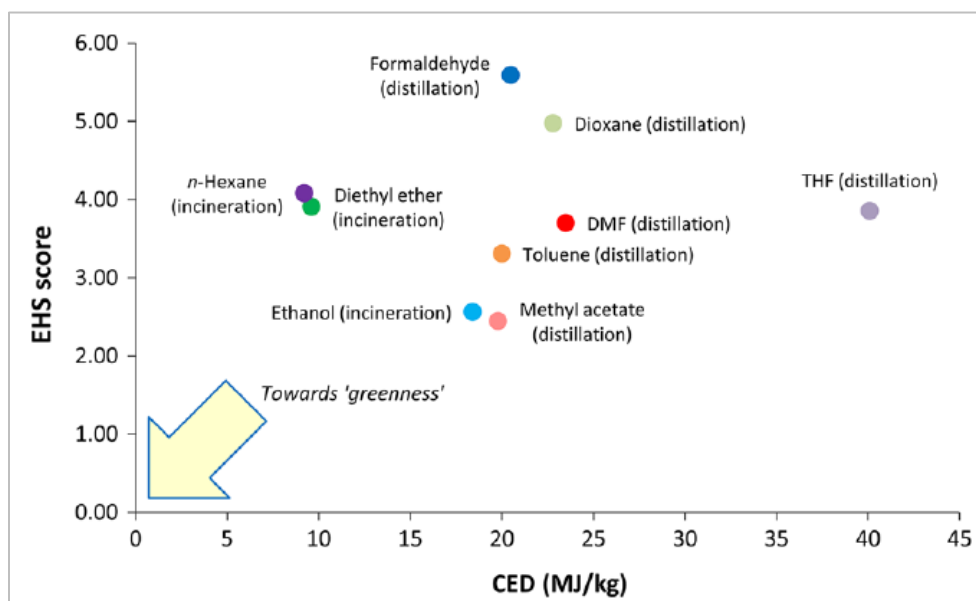


Figure 2.3 Chart combines the environment, health, and safety (EHS), and cumulative energy demand (CED) of some common solvents. (Image obtained from Byrne *et al.* 2016)¹⁴

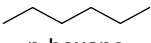
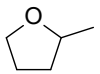
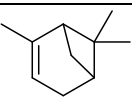
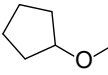
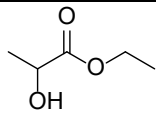
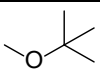
GlaxoSmithKline (GSK) has published different versions of a solvent selection guide with a detailed breakdown of different EHS scores.⁵⁰⁻⁵¹ This guide serves the purpose of identifying and comparing alternatives to common but hazardous solvents for medicinal and other scale-up chemical laboratories. The selection guide uses a scale of 1 to 10 to estimate the life-cycle environmental impact relative to the other solvents in the dataset. It also incorporates factors like waste generation, health effects, flammability /explosion, reactivity, and stability of the solvents. **Table 2.1**, adapted from the GSK's selection guide, shows the scores of some common solvents along with the some less common greener solvents that are used in our research. Greater numbers in a scale of 1 to 10 indicate the greenness of the solvent.

Table 2.1 GSK scores for the some common organic solvents and the solvents we used in our research. (Data obtained from Henderson *et al* 2011)⁵¹

Solvent	MP °C	BP °C	Waste	Environment Impact	Health	Flammability / explosion	Reactivity / stability	Life cycle score
Water	0	100	4	10	10	10	10	10
Ethanol	-114	78	3	8	8	6	9	9
Methanol	-98	65	4	9	5	5	10	9
Ethyl acetate	-84	77	4	8	8	4	8	6
Acetone	-95	56	3	9	8	4	9	7
Toluene	-95	111	6	3	4	4	10	7
Benzene	6	80	5	6	1	3	10	7
Diethyl ether	-116	35	4	4	5	2	4	6
Tetrahydrofuran	-108	65	3	5	6	3	4	4
Dimethyl Formamide	-61	153	4	6	2	9	9	7
Acetonitrile	-45	82	2	6	6	6	10	3
Carbon tetrachloride	-23	77	4	5	3	4	10	7
Dichloromethane	-95	40	3	6	4	6	9	7
Chloroform	-64	61	3	6	3	6	9	6
<i>n</i> -hexane	-95	69	5	3	4	2	10	7
2-Methyltetrahydrofuran	-137	78	4	5	4	3	6	4
<i>alpha</i> -pinene	-62	157	NA	NA	4	7	NA	NA
Cyclopentyl methyl ether	-140	106	6	4	4	5	8	4
Ethyl lactate	-23	154	7	5	4	8	10	NA
<i>t</i> -Butylmethyl ether	-109	55	4	5	5	3	9	8

In this dissertation these five less common but greener solvents were selected to study their efficiency of extraction of oil from a natural product (soybean). **Table 2.2** shows the structure and properties of the five green solvents used in our research.

Table 2.2 List of green solvents (along with *n*-hexane) used to study the extraction of soybean oil and the physical properties of those solvents.⁵²⁻⁵³

Solvents	CAS	Molecular Weight (g mol ⁻¹)	Boiling Point (°C)	Flash point (°C)	Viscosity at 25 °C (C _p)	Energy to Evaporate 1 kg of Solvent (kW·h)
 n-hexane	110-54-3	86.16	69	-23	0.32	0.121
 2-Methyltetrahydrofuran	96-47-9	86.13	78	-12	0.56	0.126
 alpha-Pinene	80-56-8	136.24	157	32	1.32	0.144
 Cyclopentyl methyl ether	5614-37-9	100.16	106	-1	0.55	0.132
 Ethyl lactate	97-64-3	118.13	154	46	2.44	0.014
 t-Butylmethyl ether	1634-04-4	88.15	55	-28	0.35	NA

(a) 2-Methyltetrahydrofuran (2-MeTHF):

Typical ether solvents like diethyl ether, tetrahydrofuran (THF), 1,2-dimethoxyethane (DME), and 1,4-dioxane have been widely used in synthesis and extraction for a long time because of their high solubility for a wide range of organic compounds. However, their characteristics like low boiling point, easy peroxide formation, and poor solvent recovery make them unfit for green chemistry.⁵⁴

2-MeTHF is a green alternative to dichloromethane (DCM) and tetrahydrofuran (THF), as it is derived from the natural renewable resources like bagasse and corncobs. 2-

MeTHF is an aprotic polar solvent and has similar physical properties of toluene. Also, it has a low peroxide-formation ability compared to THF. Although, 2-MeTHF is structurally similar to THF, it has a higher boiling point (78 °C) than THF (65 °C) that makes it a suitable solvent for high temperature reactions and extractions. Also, 2-MeTHF has a low heat of vaporization, which prevents the loss of solvent during reflux and saves energy during the distillation.⁵³

In an evaluation of green solvents for the substitution of *n*-hexane in the extraction of natural pigments, Varon *et al* used computer simulation to predict the physiochemical properties and solubility for various solvents, and then performed solid-liquid extraction to compare the efficiency of extraction.⁵⁵ 2-MeTHF was reported to give better yield than *n*-hexane in the extraction of carotenoids from carrot. It was shown that 2-MeTHF had a higher percent recovery of 80% compared to *n*-hexane, 68%. This promising report revealed that green solvents like 2-MeTHF has greater potential to replace *n*-hexane for the extraction of natural products. Moreover, the energy of evaporation of 1 kg of 2-MeTHF was reported to be 0.126 kW h, which is very close to the energy of evaporation of *n*-hexane, 0.121 kW h. In this dissertation, the solubility and diffusion coefficient of 2-MeTHF for the extraction of soybean oil were calculated and compared with other solvents.

(b) *alpha*-Pinene:

alpha-Pinene (or α -Pinene) is a terpene and possess a bicyclic hydrocarbon structure with two isoprene units. Terpenes are a large class of natural organic compounds found chiefly in citrus fruits, conifer resins, and in many other plants with different physical and chemical properties. Limonene, linalool, carvone, pinene, carotene, lycopene, and cymene are some of the well-known terpenes. Some of the terpenes are viable alternatives to petroleum solvents like *n*-hexane, as they are derived from low-cost agricultural waste, low toxic, and biodegradable.⁵²

Pinenes (both α and β -pinene) are extracted from pine resin or pine oil. Pinenes are used to produce insect repellent, varnishes, and solvents to thin paint. Pinenes are now becoming valuable solvents, as their solubility-related properties are very similar to *n*-hexane, and likely behave the same way in dissolving natural oils in extraction processes. However, since pinene has slightly higher dielectric constant, it exhibits more dissociating power than *n*-hexane. Considering the safety point of view, *alpha*-pinene has higher flash point (32 °C) compared to *n*-hexane (-23 °C), so it is less flammable.⁵³ The viscosity and density of *alpha*-pinene is greater than *n*-hexane, which can be a setback in extraction efficiency. Also, it may require more energy consumption related to recovery of solvent, as the boiling point of *alpha*-pinene is 157 °C. α -Pinene has been reported to be used in extraction of lipids from yeast⁵³ and oil from microalgae.⁵² But to our knowledge, there is no literature that reports a comparison of extraction efficiency of α -pinene with *n*-hexane and other green solvents for soybean oil extraction.

(c) Cyclopentyl methyl ether (CPME):

Cyclopentyl methyl ether (CPME) offers a green solvent for chemical processes by not only decreasing the solvent waste, but also laboratory safety due to CPME's unique composition which resists the formation of peroxides.⁵⁴ This makes CPME more stable than THF for longer times, and reduced the frequency of peroxide testing. Also, because CPME is more hydrophobic and has a limited miscibility in water (1.1g/100g at 23°C), it provides a greater selectivity over THF in many synthesis processes. CPME has a higher boiling point (106 °C) compared to THF that offers a higher reaction temperature and reduces the reaction time. With a low heat of vaporization, loss of solvent can be avoided during the reflux process and saves energy during the recovery. These properties contribute to green chemistry through a reduction in the total amount of solvents used, waste solvent created, and carbon dioxide emissions produced. CPME can reduce costs due to its high recovery rate (90%). Wide synthetic utility and a detailed toxicity study suggest CPME as a green and sustainable solvent of choice for modern chemical transformations.⁵⁶ CPME can be efficiently manufactured at low cost by the methylation of cyclopentanol or through an addition reaction of methoxide to cyclopentene, these two methods provide a good operating condition and better atom economy.

CPME has been reported to give better yield than *n*-hexane in the extraction of carotenoids from carrots. In a study of green solvents for the substitution of *n*-hexane in the extraction of natural pigments, Varon *et al* used computer simulation programs to predict the physiochemical properties and solubility for various solvents, and then performed solid-liquid extraction to compare the efficiency of extraction.⁵⁵ It was reported that CPME had a percent recovery of 95%, compared to 68% for *n*-hexane. This

promising report revealed that green solvents like CPME have greater potential to replace *n*-hexane for the extraction of natural products. Moreover, the energy of evaporation of 1 kg of CPME was reported to be 0.132 kWh, which is very close to the energy of evaporation 0.121 kW h for *n*-hexane.

(d) Ethyl lactate:

Ethyl lactate is a significant lactate ester. Since lactic acid is a common functional group in many natural metabolites in biological systems, ethyl lactate is not a potential health risk, because it readily converts into alcohol and lactic acid in a metabolic hydrolysis. The low toxicity of ethyl lactate, even in high concentration, is reflected in the FDA approval in food flavors and pharmaceutical products.⁵⁷ The environmental impact of ethyl lactate is very low, as it can fully biodegrade in a short time. This environmentally benign green solvent completely biodegrades into CO₂ and water. The vapor of ethyl lactate itself has no impact on ozone depleting. Ethyl lactate possesses a high flashpoint that makes it safe to work with. Ethyl lactate is synthesized from renewable low-cost agricultural waste (carbohydrate products), therefore industrial production of this green solvent does not require a petrochemical source. This reduction of energy and cost of production favors the replacement of traditional solvents by ethyl lactate for large- scale extractions.

Literature sources show that ethyl lactate is currently used for cleaning purposes, manufacturing of electronic devices, paint, and pharmaceutical products.⁵⁸ The polarity of ethyl lactate is moderate that makes it miscible in both hydrophilic and hydrophobic liquids. The specific topography of ethyl lactate allows it to form hydrogen bonds with

other solvents.⁵⁸ This hydrogen bond donor and acceptor property offers an excellent solvent property, and recent studies report an excellent efficiency of ethyl lactate in the extraction of natural products from plant matrices.⁵⁷

The physical properties of ethyl lactate show that it has a moderate viscosity. This could be a critical consideration in estimating its extraction efficiency, but it can be suitable for different types of industrial applications.⁵⁹

(e) t-Butyl methyl ether (TBME):

t-Butyl methyl ether is considered as a green solvent, for its high score in preventing waste, environmental hazard, health hazard, reactivity, and life cycle. TBME has a relatively low boiling point (55 °C) compared to *n*-hexane. So, in the solvent recovery standpoint, TBME consumes less energy than *n*-hexane. Although TBME is flammable, it is still a potential alternate to other more highly flammable ether solvents such as diethyl ether and carcinogenic ether solvents such as 1,4-dioxane, and 1,2-dimethoxyethane.

TBME has been used for extraction of lipids from cells and tissues.⁶⁰ The advantage of using TBME in place of chloroform for extraction of lipids from cells was reported that it has faster and cleaner recovery due to the low density and viscosity of TBME. Furthermore, compared to other ether solvents, TBME is relatively more stable, with less peroxide-formation ability.

2.1.3 Soybean Oil

Soybeans are one of the important oilseeds that have rich protein (40% by weight), and oil (21% by weight) content, and it dominates the market as 70% of total oilseed meals produced every year is soybean meal.⁶¹ The typical composition of soybean seed is shown in the **Table 2.3**. The defatted solid left after the oil extraction is called soybean meal. Soybean meal accounts for between 51% and 76% of money earned in the process of extraction of soybeans.

Table 2.3 Typical composition of soybeans (dry weight basis).⁶¹ The amount of oil is 21%, which is the potential analyte in our extraction studies.

Components	Weight %
Protein	40 %
Carbohydrate	29 %
Oil	21 %
Lysine	2.5 %
Threonine	1.5 %
Cysteine	0.7 %
Methionine	0.5 %
Tryptophan	0.5 %
Ash	4.5 %

Soybean oil has a unique composition among other common vegetable oils with a higher content of linoleic acid (54%) in triglyceride form.⁶² The relative amount of different triglycerides found in the oil can be measured by converting them into fatty acid methyl esters (FAME). **Table 2.4** shows the average amount of fatty acid methyl esters

typically present in soybean oil.⁶¹ This composition makes soybean oil more stable towards oxidation and well suited to use as a salad oil, frying oil, margarine, etc.

Table 2.4 Major fatty acid methyl esters obtained from the hydrolysis and derivatization of triglycerides in soybean oil.⁶¹

Major FAME	Typical (%)
Methyl Linoleate	54 %
Methyl Oleate	23 %
Methyl Palmitate	11 %
Methyl Stearate	4 %

Nowadays, the major methods of extracting oil from oilseeds are by screw pressing, by extruding-expelling or through the use of organic solvents. Solvent extraction is currently the most efficient way of extracting soybean oil, which is commonly used in the laboratory scale. It is reported that the average residual oil, left in the soybean meal after extraction, is only 1.2% in the solvent extraction method, compared to the 6.3% residual oil in screw-pressed and 7.2% residual oil in extruding-expelling methods.⁶¹ The high-protein and low-oil contents obtained in solvent-extracted soybean meal is desired for feeding poultry and swine. This makes solvent-extraction a widely used soybean oil recovery method, and it accounts for the 98% of soybean processed in United States.

Currently, the main solvent used for soybean oil extraction is the petroleum distillate containing a mixture of hexane isomers. The hexanes (mixture of isomers) contains about 45% to 70% of *n*-hexane. As discussed in the section 2.1.2, the hydrocarbons have high environmental and health impact (lower scores in the GSK scale). Also, *n*-hexane is considered as a neurotoxin in United States. The maximum

workplace exposure level has been set to be 500 ppm for *n*-hexane, and at higher concentration it was proven as toxic.⁴⁸ Industrial scale extraction of soybean oil involves a large volume of *n*-hexane that pose a fire hazard, as its flash point is low, and thus the flammability/explosion score is also very low (**Table 2.1**).^{50, 63} Also with the low vaporization point the loss of solvent during the distillation is high and that ends up in the waste stream.

With the increasing environment and health concern of *n*-hexane, and the legislative pressure against the use of hydrocarbons, there is a significant interest in alternative solvents.⁶⁴ Supercritical carbon dioxide (scCO₂) is a considerable alternative as it requires only mild treatment and sensory characteristic. Several research attempts have used scCO₂ for the extraction of soybean oil, and the results show that this alternative solvent's extraction yields are lower than the typical *n*-hexane's extraction yield of 20%. Using supercritical CO₂ as solvent at 300 bar and 40 °C, Nodar *et al* (2013) has reported 19.5% extraction, Stahl *et al* (1980) has reported 16.4% extraction,⁶⁵ and Friedrich *et al* has reported 19.9% extraction.⁶⁶ However the use of scCO₂ may not be an energy- and cost-efficient extraction process.^{62, 67} Phan *et al* has evaluated the use of a switchable-polarity solvent system (SPS) where the solvent's polarity and hydrophilicity can be switched back and forth. The results show that alternative solvents can recover soybean oil less efficiently than *n*-hexane. To our knowledge, there is no preceding work that reported the use of green solvents for the extraction of soybean oil. This dissertation study reports the results of extraction of soybean oil using five green solvents, as well as the role of diffusion, application of hot-ball model, and effect of particle size.

2.1.4 Solvent Extraction and Diffusion Coefficient

Extraction can be defined as moving of one or more compounds from one phase to another. Extraction takes place by partitioning of compound between two immiscible phases. Extraction of soybean oil studied in this dissertation is a type of solid to liquid extraction, where the analyte (mixture of triglycerides) is moved from a solid phase (ground soybean) into a liquid phase (organic solvent). Though the term extraction is used commonly and frequently, the mechanism behind it is complex, and is influenced by many factors. Thermodynamics and kinetics are the two main areas that need to be considered when developing a method for separation. Thermodynamics deals with the overall energy change in the system, whereas kinetics concerns the path it takes during the progress of separation.

The second law of thermodynamics says that the position of equilibrium favors the side where entropy (or disorder) is greater. Separation (or purification) is not an entropy-favored process, as the mixing of different compound is when entropy gains. To take care of this, extraction methods are often developed to drive the equilibrium towards separation by changing other factors, like adding work (eg. heat), or choosing the right solvent that has greater affinity to the analyte, etc.^{31, 68}

Kinetics of extraction is less appreciated, but it plays a great role beyond the thermodynamics of separation. The plot of mass extracted versus the extraction progress (**Figure 2.4**) shows an asymptotic curve. The first part of this plot is an equilibrium region, where the mass extracted increases steeply, and the extraction is driven by solubility and partition (or distribution). As the extraction progresses, the second part of the plot is levelled off, and the extraction is driven by solute diffusion.

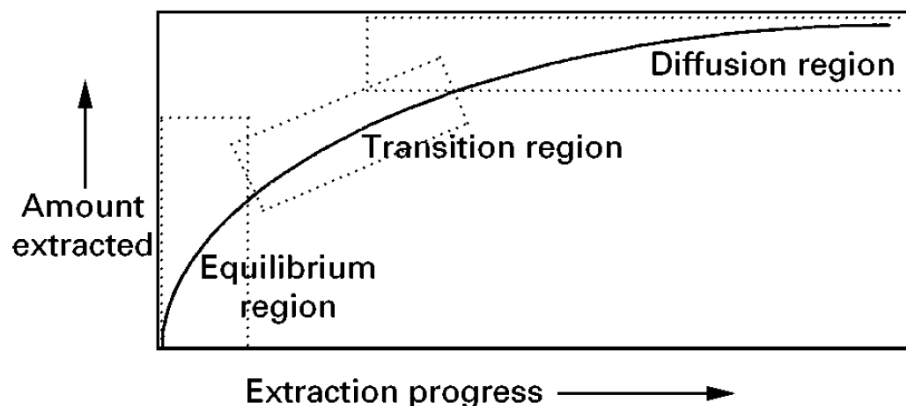


Figure 2.4 The plot defines the three regions i) an equilibrium region dominated by solute partitioning, ii) a diffusion region controlled by solute diffusion, and iii) a transitional region. (Image adapted from Raynie 2000)⁶⁸

Diffusion is a spontaneous and irreversible process of migration of a compound from a higher concentration region to a lower concentration region, which ends in a concentration equilibrium. This is similar to heat energy transfer from hotter region to a cooler region. During the second part of the extraction progress the concentration gradient of analyte between the sample matrix and the solvent causes the mass of analyte transfer into solvent phase. The rate of mass flow per unit area is called diffusion flow (J), and the unit is $\text{g cm}^{-2} \text{s}^{-2}$.

$$J = -D (\Delta c / \Delta x) \quad (\text{Equation 2.1})$$

The Fick's first law of diffusion, above, provides a correlation between the diffusion flow and concentration gradient, where D is diffusion coefficient ($\text{cm}^2 \text{s}^{-1}$), c is concentration (g/cm^3), x is distance (cm), and $(\Delta c / \Delta x)$ is concentration gradient (g cm^{-4}). Diffusion coefficient is independent of solute concentration and is specific for a solute-solvent pair. In some cases, where a steady rate of concentration change is not expected,

the concentration change with time is used, and that is explained by Fick's second law of diffusion.

$$\frac{\Delta c}{Dt} = D \left(\frac{\Delta^2 c}{\Delta x^2} \right) \quad (\text{Equation 2.2})$$

2.1.5 Hot-ball Model of Extraction

In the extraction of solutes from solid samples, it is significant to consider the solute-sample attraction and the ability of solute to diffuse out of the porous sample matrix into the solvent. The diffusion is influenced by the geometry and tortuosity of the porous sample. The diffusion of analyte from a porous solid sample into a liquid solvent resembles transmission of heat energy from a hot body to its environment, as described in the hot-ball model.⁶⁹⁻⁷⁰ This model helps to analyze and validate the results of an extraction process. Typically, in a solid-to-liquid extraction process, most of the solute is extracted in a short period at the beginning, followed by a tailing off of the extraction rate. Hence, to recover 99% of solute, it would take ten times more time than what it needed to extract first 50%.

The hot-ball model is ideal for a perfectly spherical porous solid matrix with a small amount of homogeneously dispersed extractable material (solute or analyte) at the beginning. Also, it is assumed that the initial concentration of solute in the extraction phase (solvent) is always zero, and the solvent is moving fast enough to maintain this zero concentration. As the small quantity of solute is infinitely dilute in the extraction phase (solvent), the extraction is not controlled by solubility but by diffusion. Another assumption is that the movement of solute compounds through the porous sample matrix is similar to the process of diffusion.

The hot-ball model, equation 2.3, defines the rate of extraction in terms of ratio of mass m of analyte remaining in the sample after an extraction time t to the initial mass m_0 of extractable analyte, where, n is integer and D is the diffusion coefficient.

$$\frac{m}{m_0} = \left(\frac{6}{n^2}\right) \sum_{n=1}^{\infty} \frac{1}{n^2} \exp \frac{-n^2 \pi^2 D t}{r^2} \quad (\text{Equation 2.3})$$

Since the extraction time varies for every system depending on various factors like sample type, solute-solvent pair, extraction method, and work applied (temperature, pressure, agitation), there needs to be a simplified or reduced time. To simplify the equation, a reduced time term, t_r is defined in equation 2.4. Reduced time is a function of the diffusion coefficient, extraction time, and particle radius, and is proportional to the extraction time in a real system.

$$t_r = \frac{\pi^2 D t}{r^2} \quad (\text{Equation 2.4})$$

When this equation is simplified to the sum of exponential decay, the plot of $\ln(m/m_0)$ versus extraction time t (or reduced time t_r) will ultimately be linear. This is because at the beginning of the extraction there is a concentration gradient at the outer area of the spherical sample particle, and the mass transfer is faster to reach an equilibrium. This part of the plot is steeper. The second part of the plot is driven by diffusion, when the concentration across the sphere is homogeneous, and the rate of extraction is a simple exponential decay. The extrapolation of the linear diffusion portion of the plot of $\ln(m/m_0)$ versus time can provide valuable information on the length of time an extraction should take to attain quantitative recovery.

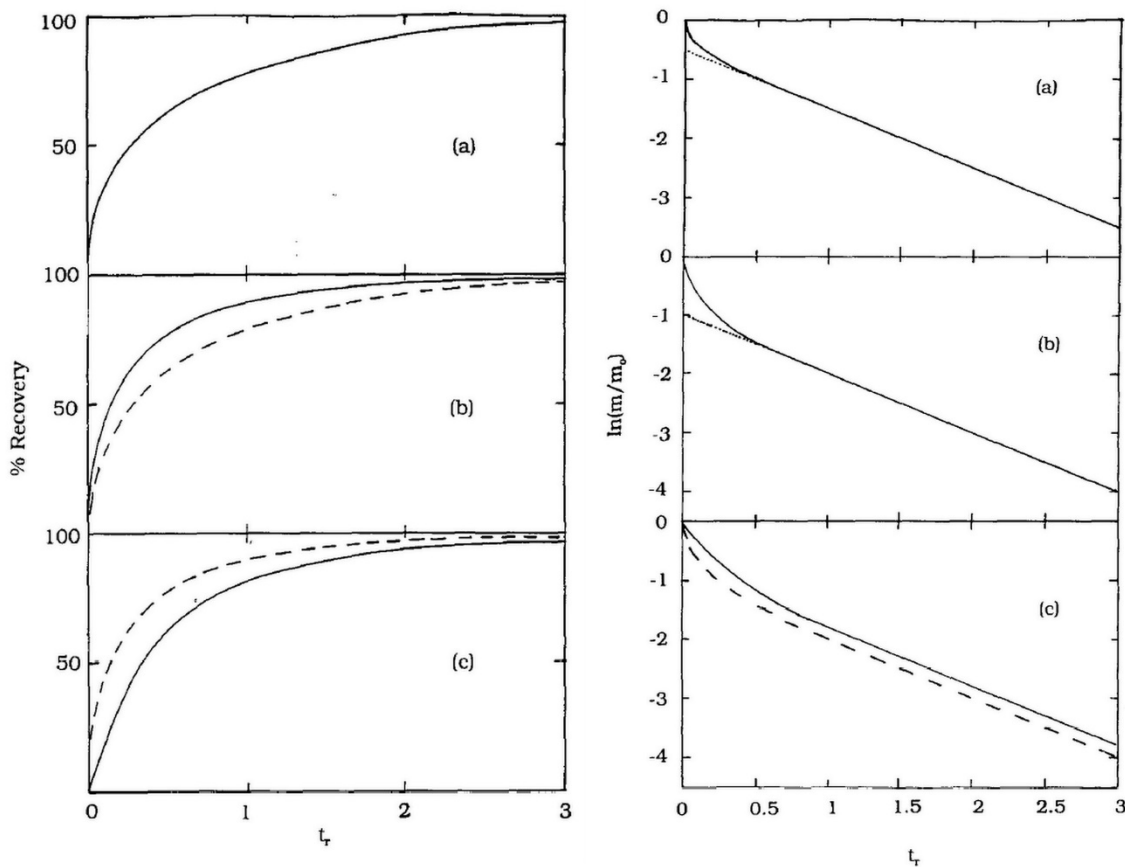


Figure 2.5 Theoretical plots of hot-ball model.

[Left side plots] Percentage recovery vs. scaled time for the hot-ball model and its variations. (a), the basic model; (b), with the effect of particle shape (continuous line) compared with the basic model (dashed line); (c), the effect of solubility limitation (continuous line) compared with little solubility limitation (dashed line); [Right side plots] $\ln(m/m_o)$ vs. scaled time (t_r) for the hot-ball model and its variations (a), the basic model; (b) with the effect of particle shape; (c) with the effect of solubility limitation (continuous line) compared with little solubility limitation (dashed line). – (from ref.69)

Figure 2.5 is plots of the hot-ball model graphs for an ideal extraction process, that correlates the percentage recoveries versus reduced time t_r .⁶⁹ This data was transformed into a straight line using integral calculus, and the plot of natural logarithm of the mass of extractable material remaining as a fraction of the original mass of extractable material, $\ln(m/m_o)$, versus reduced time was shown on the right side in **Figure 2.5**. The basic model is also adapted to the effect of particle shape and solubility

limitation. A steep equilibrium region and a linear diffusion region are seen in every plot. To interpret the plot in words, the change in rate of extraction is high at first until around 60% of the extractable material is recovered, which corresponds to reduced time t_r of 0.5. After an equilibrium in concentration gradient was achieved, the change in rate of extraction becomes small, and the flat region extends until 99% of the extractable material is recovered. The mathematical expression of this plot (equation 2.3) describes the concentration of the extractable material remaining in sample at any given time. The significance of the hot-ball model can be realized when applied to a real extraction system.

In a study of kinetics of extraction, the linear portion of the plot of $\ln(m/m_o)$ versus reduced time t_r is taken into account. That is usually above the reduced time t_r value of 0.5. The extrapolation of this linear diffusion region gives a $\ln(m/m_o)$ intercept that is around -0.5 for spherical particles, however the $\ln(m/m_o)$ intercept of non-spherical particles is more negative than -0.5 .

Application of this hot-ball model to this research study is explained in detail in section 2.2.5. Knowing that ground soybean samples used in this study were not perfectly spherical, our aim is to analyze our results and validate the extraction methods with a close fit to hot-ball model. In this study the hot-ball model equation can be utilized to align the actual extraction times to the reduced time scale. Then with a normalized time scale, the diffusion coefficient of any solute-solvents system can be calculated using equation 2.5. This would give more insight on the efficiency of using green solvents in extraction of soybean oil.

$$D = \frac{t_r r^2}{\pi^2 t} \quad (\text{Equation 2.5})$$

In a comparative study, diffusion coefficient for extraction of fat from coffee was calculated for different extraction techniques. The diffusion coefficient varies based on the temperature used in the techniques. Soxhlet had the slowest diffusion as the temperature was below the boiling point of the solvent. Soxtec had a litter faster diffusion as the temperature was equal to the boiling point of the solvent. The other techniques like accelerated solvent extraction, microwave assisted extraction, and ultrasound extraction had similar fast diffusion as the temperatures were above the boiling point in those techniques.³¹ Driver's outcome precedes the aim of this study that finding diffusion coefficients for different green solvents is significant in order to compare their extraction efficiency.

2.2 Experimental Methods

2.2.1 Materials and Reagents

Soybeans sample was supplied by Prof. Kasiviswanathan Muthukumarappan from the Department of Agricultural & Biosystems Engineering, South Dakota State University. Soybeans were ground using a Thomas Scientific analytical mill (1725/1425 rpm). Care was taken not to expose the ground soybean sample to moisture. The ground soybean samples were dried in an oven at 80 °C overnight and then separated into size fractions using 1400 μm , 1000 μm , 850 μm , 600 μm , 425 μm , 300 μm , 149 μm , 53 μm sieves. The separated particles were stored in an air-tight container. Extractions were performed using pressurized fluid extraction, Dionex™ ASE-350 (Thermo-Fisher, Sunnyvale, CA).

Solvents used:

- *n*-hexane (from Thermo-Fischer Scientific).
- 2-Methyltetrahydrofuran (2-MeTHF) (from Thermo-Fisher Scientific),
- *alpha*-Pinene 97% stabilized with *alpha*-Tocopherol (from Acros Organics),
- Cyclopentyl methyl ether 99+% extra pure stabilized (CPME) (from Acros Organics)
- Ethyl lactate (from Sigma Aldrich)
- *t*-Butyl methyl ether (TBME) (from EMD).

2.2.2 Solubility Study in Computational Method

The computer software, COSMO*quick* version 1.5, a version of COSMO-RS, was used to predict the relative solubility of the triglycerides of major soybean fatty acid, trilinolein, triolein, tripalmitin, and tristearin in different solvents. Briefly, the structures or names of the triglycerides and 21 different solvents were given as inputs to search for

SMILES (Simplified Molecular Input Line Entry Specification) of the compounds. The program then used the SMILES to create charge-density surface (also called σ -surface) for those compounds. The 3D structures and charge density profiles of the compounds were exported. The charge-density profiles of all compounds were plotted to compare the negative and positive charge-densities on a 2D-line graph. The chemical potential (also known as the σ -potential) on the surface was used to see the possibility of intermolecular bonding (hydrogen-bonding donor and acceptor, and non-hydrogen bonding donor and acceptor) characteristic of the solute and solvent compounds. Then solute roles were assigned to the triglycerides (one at a time) and solvent roles were assigned the 21 different solvents. Temperature was defined as 100 °C (the same temperature used for ASE extraction) to predict the relative solubility. The program weighed the highest solubility (mol/mol) of a solute-in-solvent as the baseline and gave a probability percent for solubility of that particular solute in other solvents.

2.2.3 Viscosity Study

Dynamic viscosity of the green solvents was determined by using a viscoanalyzer (ATS Rheosystems, NJ) with respect to change in temperature. The starting temperature was set to 25 °C and ending temperature was determined by the boiling point of the solvents. Equilibrium time was set to 50 s.

2.2.4 Extraction of Soybean oil using Accelerated Solvent Extractor

Extraction was performed using pressurized fluid extraction Dionex™ ASE-350 (Thermo-Fisher, Sunnyvale, CA). Temperature was maintained at 100°C and a pressure of 1500 psi was used.³⁴ Post-extraction solvent flush was set to 60 % and post-extraction

purge time was set to 60 seconds. One gram of ground soybean and two grams of sand (dispersing agent) were accurately weighed and carefully packed between two 30-mm Whatman cellulose filters in a 33-mL stainless steel ASE vessel. The void volume was filled with glass beads and sealed. Then the extraction vessel was placed onto the ASE system. The extraction was conducted using the solvents 2-methyltetrahydrofuran, cyclopentyl methyl ether, ethyl lactate, t-butyl methyl ether, *alpha*-pinene, and *n*-hexane at static extraction times 5, 10, 15, 20 and 30 minutes with 7 minutes preheat time. One extraction cycle was used for each solvent. Three replicates were done for each solvent. The extraction results were studied gravimetrically. Once the extraction is completed, the extract was transferred to pre-weighed collection vials. Then solvent recovery was done in a rotatory evaporator or distillation under low pressure. After the distillation of solvent, the extracted oil was dried under nitrogen flushing. The nitrogen drying and weighing process were repeated until two consecutive weights consistent to within ± 0.0009 grams were obtained. The mass obtained from the triplicate were plotted using Microsoft Excel. Average of the three masses and the standard deviation were calculated. After each experiment, the extraction cells were thoroughly washed, rinsed with acetone, and dried before using for next experiment.

2.2.5 Application of the Hot-ball Model to Extraction Data

The data obtained from the extraction of soybean oil in ASE using different solvents was evaluated in two ways with respect to the hot-ball model. First, it was qualitatively analyzed to see if the experimental plots of percentage recovery versus extraction time, and the $\ln(m/m_0)$ versus extraction time appear to fit the theoretical hot-ball model plots.⁶⁹⁻⁷⁰ Second, it was quantitatively analyzed through the use of the hot-

ball model in calculating the diffusion coefficient of different green solvents for extraction of soybean oil. The diffusion coefficients were then used to compare the extraction efficiency of the green solvents.

The experimental plot of percent extraction versus extraction time was generated separately for each solvent using Microsoft Excel. The average mass of soybean oil extracted was converted into percent extraction using the equation.

$$\text{percent extraction} = \frac{\text{mass of oil extracted}}{\text{initial mass of soybean sample}} \times 100 \quad (\text{Equation 2.6})$$

The percent extraction versus extraction time was plotted for each solvent. The maximum percent extracted during the ASE extraction is 23.24%, and that data was obtained from the 513- μm soybean particles in CPME solvent at 30 min extraction. This mass 0.2324 g was considered as the maximum extractable mass for 1 g of soybean sample. This maximum extractable mass is considered as 99% recovery, and that was used to calculate the original (100%) mass of oil = 0.2347 g present in 1 gram of sample. This mass was used to calculate the percent recovery for each solvent using the equation.

$$\text{percent recovery} = \frac{\text{mass of oil extracted from 1 g of sample}}{\text{total mass of oil present in 1 g of sample}} \times 100 \quad (\text{Equation 2.7})$$

To evaluate the extraction efficiency of each solvent, a plot of percent of oil recovered versus extraction time was graphed and the shape of curve was compared to the theoretical hot-ball model. The equilibrium, and diffusion regions of the asymptotic plot were identified. Once the asymptotic plot was validated for a close fit to the model, then a first-order kinetics plot for each solvent was also graphed and compared to the theoretical model. In the first order kinetic plot, $\ln(m/m_o)$, that is the natural logarithm of

mass of unextracted oil (m) remaining in the sample divided by the original mass of extractable oil (m_o) in 1 gram of sample was plotted against the extraction time.

This first-order kinetics plot was utilized to compare the extraction efficiency of different solvents. The diffusion region of the kinetics plot was identified, which was set to be the data obtained from last three extraction times (15, 20, and 30 min). When the extraction was influenced predominantly by diffusion, the rate of extraction was slower and the plot had become linear. Extrapolation of this diffusion region (the linear portion of the plot) allowed determination of the y-intercept and slope. With the linear regression, r^2 , being optimal the y-intercept and slope were utilized to scale the actual extraction time to the theoretical reduced time, in order to match the theoretical model.

In the hot-ball model a reduced time was used so that the model can be applied to a wide range of extraction methods, irrespective of the extraction technique, size of extraction, solvent-sample system, and length of extraction. To match the experimental data obtained from this study to the theoretical model, reduced time, t_r , was calculated for each solvent extraction data. In the theoretical kinetic plot, the reduced time of one ($t_r = 1$) occurred where the change in slope is one ($m = 1$). Therefore, in the experimental kinetic plot, the slope and y-intercept of the best-fit line were used to calculate the actual extraction time, t , at which the y-value, that is the $\ln(m/m_o)$ value, is one unit different than the y-intercept. In other words, in the slope equation, it was known that $(x_2 - x_1)$ is the difference in t_r , and the $(y_2 - y_1)$ is the difference in $\ln(m/m_o)$. If the denominator, the difference in t_r is 1, then the numerator, the difference in $\ln(m/m_o)$ should also be 1, to obtain the value of 1 for the slope.

$$\text{slope } m = \frac{(y_2 - y_1)}{(x_2 - x_1)} \quad (\text{Equation 2.8})$$

The actual extraction time, t , corresponding to the theoretical reduced time $t_r = 1$ is calculated for each solvent, and a new plot of $\ln(m/m_0)$ versus reduced time was graphed for each solvent. The extraction time, t , correspond to $t_r = 1$, was substituted in the reduced time equation along with the radius, r , of the particle to calculate the diffusion coefficient, D , and the time required for the extraction to be complete. In this calculation, it was assumed that the soybean particles were all spherical with a diameter of 513 μm .

$$D = \frac{t_r r^2}{\pi^2 t} \quad (\text{Equation 2.9})$$

2.2.6 IR Spectroscopy

To confirm the identity of the extracted soybean oil, an IR spectrum for oil extracted using each solvent was acquired. Then it was compared to the IR spectrum of the commercial soybean oil (brand: NutriOli – Pure Soybean Oil). All IR spectra were recorded at room temperature using a Nicolet 380 IR Spectrometer (Thermo Scientific).

2.2.7 Esterification of Extracted Soybean Oil

Around 30 mg of soybean oil sample taken in a vial, 2 mL of *n*-hexane and 2 mL of 10% BF_3 in methanol were added and stirred gently. After the oil was completely dissolved, the mixture was transferred to the 25-mL round bottom flask and refluxed at 60 °C for 60 min in an oil bath. Then the reaction was quenched using 4 mL of DI water and 2 mL of *n*-hexane. After a thorough shaking, the organic layer was separated. The organic layer was washed twice with water. To dry the organic layer, around 1g of

anhydrous sodium sulfate was added and set aside for 10 min. For further drying, the organic phase was passed through a column packed with MgSO₄, sand and cotton. The fatty acid methyl esters (FAME) sample was then filtered through a 0.2- μ m filter before GC-MS characterization. This same procedure was used to derivatize the soybean oil obtained at 30 min from each green solvent extraction.

2.2.8 GC-MS Characterization

The methyl esters of fatty acid obtained from each solvent extraction was analyzed using an Agilent 7890 gas chromatograph (Agilent Technologies, Little Falls, DE) coupled to an Agilent Technologies 5975C mass spectrometer. The instrument was equipped with a 30 m \times 0.25 mm, 0.25- μ m DB-5 column (Agilent Technologies, Little Falls, DE) and the velocity of carrier gas (hydrogen) was kept constant at 1.2 mL/min. The oven-temperature program was initially held at 150 °C for 2 min, then ramped at a rate of 15 °C/min to 250 °C. The temperature was then held at 250 °C for 2 min. Splitless injection (2 μ L) was performed with a HP7673A automatic sampler and an injection port of 250 °C with the transfer line temperature kept at 300 °C. The MS temperatures were ion source 230 °C and quadrupole 150 °C. The scan range was 40-550 U (2.91scans/s).

2.3 Results and Discussion

2.3.1 Experimental Design

This research was focused to study the efficiency of alternative solvents to *n*-hexane for extracting oil from soybeans. As diffusion plays a major role in the kinetics of extraction, comparing the diffusion coefficient of green solvents is the key approach.

Figure 2.6 sketches the experimental design involved in this comparison analysis. The following sections discuss these steps and results in detail. Sample preparation involves grinding of soybeans in analytical mill and separation of different size particles using sieves. Accelerated solvent extraction was then performed for different size particles, using the reference solvent *n*-hexane, to determine the best particle size that offers maximum oil extraction. The best particle size was then used for further analysis with green solvents. Five green solvents were chosen based on their greenness score and solubility predicted in computational method. These five green solvents (2-MeTHF, alpha-pinene, CPME, ethyl lactate, and TBME) were then used in ASE under the optimal operation condition obtained from literature. The extracted oil was then separated from the solvent and the yield was calculated using gravimetric analysis. Quality of the extraction was determined using IR spectroscopy. The fatty acid methyl ester composition of soybean oil was verified using GC-MS analysis of FAME derivatives. The extraction results were evaluated using theoretical (hot-ball) model, and the diffusion coefficient for each green solvent was calculated to compare the efficiency of extracting soybean oil.

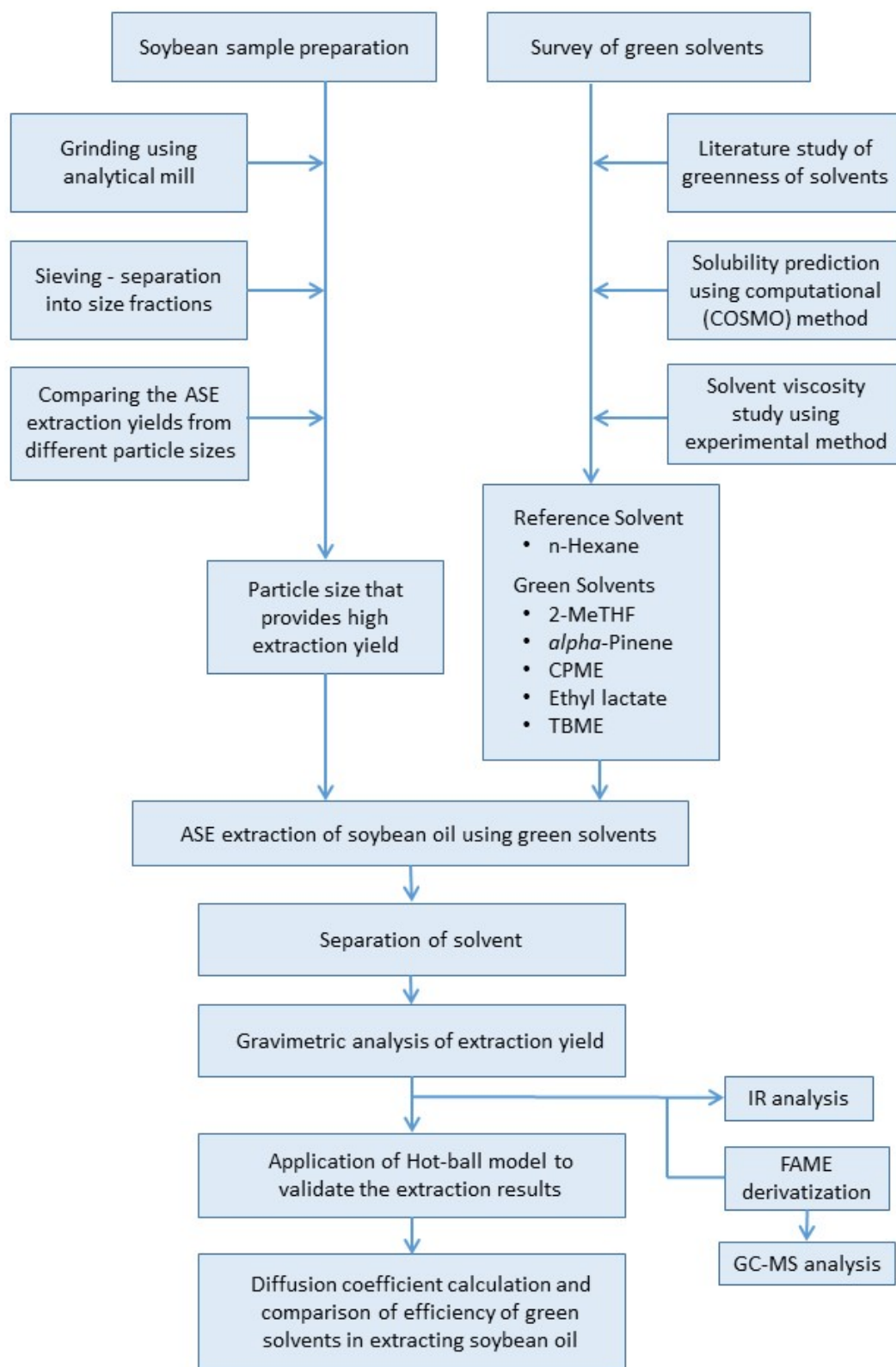


Figure 2.6 Flow chart showing the process involved in the comparison of efficiency of green solvent in ASE extraction of soybean oil.

2.3.2 Sample Pretreatment

Sample pretreatment is an essential step before any extraction process. For a solid-liquid extraction, it is ideal to grind the oilseeds to small particles that have maximum surface area. In this study dry soybeans were ground using an analytical mill. This ground particle can easily absorb atmospheric moisture that would affect the quality of extraction. During the grinding and storing processes, care was taken to expose the particles only to minimal moisture. **Figure 2.7** shows the whole dry soybeans on the left and the ground soybean sample on the right.

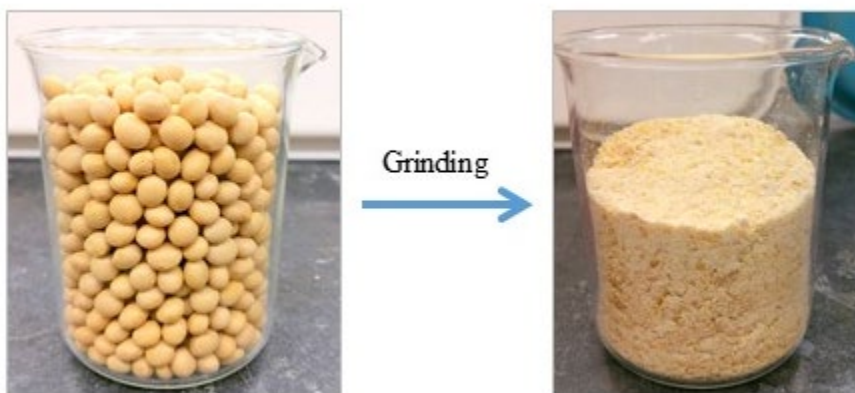


Figure 2.7 Soybeans before and after grinding

The ground soybean sample was dried in oven before taken for sieving. Copper sieves of pore sizes 1400 μm , 1000 μm , 850 μm , 600 μm , 425 μm , 300 μm , 149 μm , and 53 μm were used to sieve the particles into different size fractions, as shown in the **Figure 2.8**. The average size of the particles was determined by taking the average of the pore size of one sieve, and pore size of the next smaller sieve.

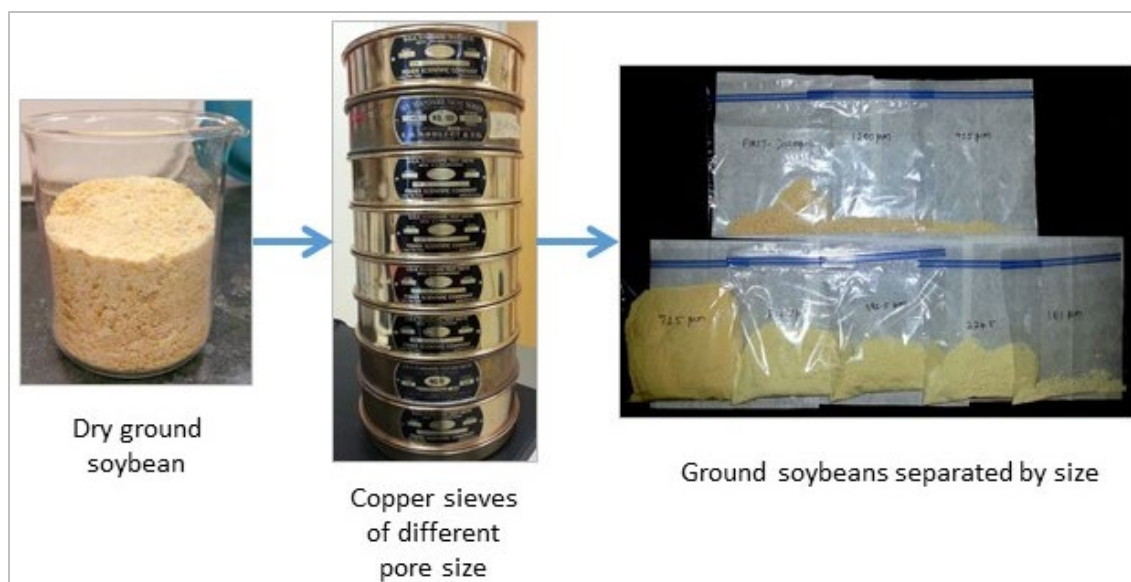


Figure 2.8 Sieving process of ground soybean sample.

The average diameter of the particles after the sieving were 1200, 925, 725, 513, 363, 225, and 101 μm . The percentage of the particle sizes yielded from sieving process was plotted in **Figure 2.9**

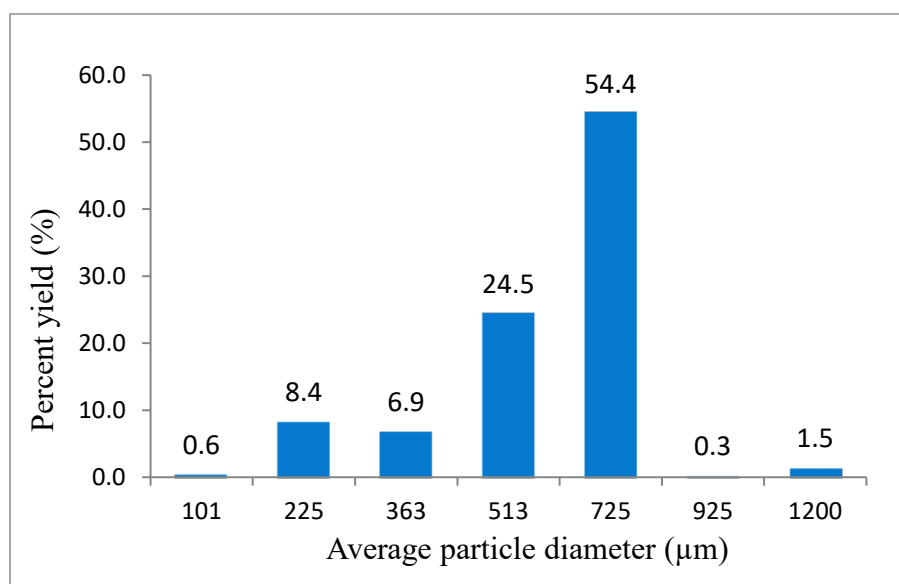


Figure 2.9 The percent yield of different size soybean particles following the sieving process.

It is observed that the grinding of soybean yielded various size particles. The size distribution shows that the majority of the particles passed through the sieve opening size of 850 μm and stopped by the sieve opening size of 600 μm in diameter, therefore the average size of particles were assumed to be 725 μm , and the percent yield in sieving process is 54.4%. The next majority of particles passed through the sieve opening size of 600 μm and stopped by the sieve opening size of 435 μm , therefore the average size of the particles was assumed to be 513 μm in diameter. The percent yield of 513 μm particles in the sieving process is 24.5%. As the percent yield of the ground soybean particles decreases when the size increase or decreases away from the above diameter. Though smaller particles offer overall increased surface area, the amount of particles with uniform particle size is also enough to run a large number of extraction experiments. Therefore, the particle sizes with higher percentage yield were considered more useful for this study.

2.3.3 Effect of Particle Size on Extraction Yield

In order to determine the best soybean particle size for the green-solvent extraction study, an investigation on effect of particle size on extraction yield was carried out first. ASE extraction was performed for the four different particle sizes 513, 725, 925, and 1200 μm using the reference solvent *n*-hexane at 100 $^{\circ}\text{C}$, and 1500 psi. The amount of soybean oil extracted from one gram of different particle sizes were determined gravimetrically. **Table 2.5** shows the extraction results and the **Figure 2.10** shows the percent oil extracted at different times from one-gram soybean samples of different sizes.

Table 2.5 Results of ASE extraction of oil from different size soybean particles using *n*-hexane (temperature is 100 °C).

Particle size (µm)	Extraction time (min)	Average mass of oil extracted per gram of soybean sample (g)	Standard deviation (n=3) (g)	Percent of oil extracted per gram of soybean sample (%)
513	0	0	0	0
	5	0.1702	0.0056	17.02
	10	0.1865	0.0110	18.65
	15	0.1976	0.0155	19.76
	20	0.1990	0.0004	19.90
	30	0.1997	0.0013	19.97
725	0	0	0	0
	5	0.1402	0.0085	14.02
	10	0.1504	0.0039	15.04
	15	0.1570	0.0009	15.70
	20	0.1741	0.0010	17.41
	30	0.1703	0.0010	17.03
925	0	0	0	0
	5	0.1112	0.0008	11.12
	10	0.1221	0.0010	12.21
	15	0.1273	0.0019	12.73
	20	0.1293	0.0024	12.93
	30	0.1312	0.0047	13.12
1200	0	0	0	0
	5	0.0721	0.0024	7.21
	10	0.0865	0.0003	8.65
	15	0.0993	0.0132	9.93
	20	0.1019	0.0009	10.19
	30	0.1043	0.0009	10.43

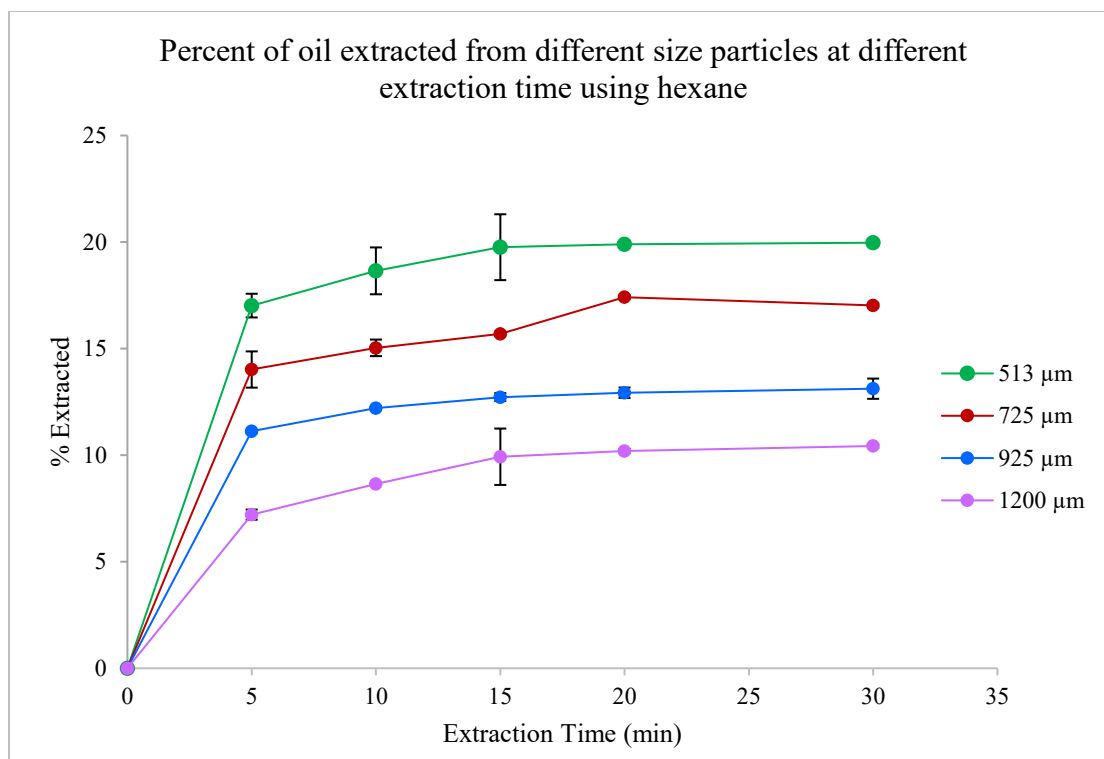


Figure 2.10 Comparison of percent of oil extracted from different size soybean particles in ASE using *n*-hexane.

The rate of extraction was higher at the beginning of extraction for all particle sizes, this can be seen in the steep curve in the percent extracted plot. As the extraction progressed further, the change in rate of extraction flattened. Also, the quantity of oil extracted increased as the particle size decreased. This trend was seen for all extraction times. It is reasonable to consider that the oil from the interior of the seed traverse a shorter path when the seed is crushed to smaller size. The maximum yield obtained for the largest particle size 1200 μm was $10.43 \pm 0.09\%$, which is almost half of the maximum yield obtained for the particle of size 513 μm . This decrease in extraction yield is an effect of the change in internal mass transfer resistance (diffusion path length).

From the results attained for the four different particle sizes, it can be concluded that the internal mass transfer resistance will decrease as particle size decreases. A longer

extraction time would be needed for the larger particles to achieve the same yield as those observed with 513 μm . This trend was found common for other type of samples, as similar effect was observed in previous studies reported for ASE extraction of fats from coffee bean,³¹ extraction of soybean oil using supercritical CO_2 ,⁶² and extraction of wheat germ oil using supercritical CO_2 .⁷¹

On the basis of the above, the best extraction yield of soybean oil by *n*-hexane at 100 °C and 1500 psi was obtained for 513 μm particles. As discussed previously, it was harder to recover the particle sizes smaller than 513 μm in the sieving process of sample preparation. Therefore the 513- μm soybean particles were selected to be used for the green-solvent extraction study.

2.3.4 Solubility of Soybean Oil Components in Green Solvents

Because less polar nature of the triglycerides, the extraction of soybean oil is usually carried out in organic solvents like *n*-hexane. This study is aimed to investigate the performance of greener alternatives to *n*-hexane. The selection of green solvents was initially carried out by a literature survey based on the economic and ecological parameter, and the scores given for impact on health, environment, waste, energy recovery, fire hazard, and life cycle of different solvents (listed in **Table 2.1**). However, when it comes to a large-scale extraction, efficient interaction of a particular solute-solvent system is important. As discussed the first part of the asymptotic plot of any extraction is influenced by thermodynamic factors until an equilibrium in concentration is reached. This initial steep curve referred as equilibrium region is where the effects of solute partition and solubility exist. A low interfacial tension between the solute and extraction phase would facilitate mass transfer across the phase boundary. Therefore, it is

essential to study the solubility. The preliminary requirements of extraction are described⁶⁸: “Prior to choosing an extraction method, knowledge must be gained about the structure (including functional group arrangement), molecular mass, polarity, solubility, pKa, and other physical properties of both the species of interest and potential interfering compounds.” As solubility of solute is one of the fundamental properties, this section of the dissertation discusses the preliminary solubility investigation performed prior to the ASE extraction of soybean oil using different green solvents.

Although an experimental solubility data would be more reliable, it is easier to use a relative solubility scale to meet the purpose of this dissertation study. A computer prediction of the solubility of soybean fatty acid triglycerides in green solvents along with other common solvents was performed. Polarity difference between two phases is the key factor to predict the solubility. Most of the solubility prediction methods characterize the solute-solvent interaction according to the classical “like-dissolve-like” rule.⁶⁸ The underlying concept in the most common solubility parameter, Hansen Solubility Parameter, is based on the total cohesive energy density approximated by the sum of energy density required to overcome the atomic dispersion force (δ_d^2), the polarity (δ_p^2) and the hydrogen-bonding ability (δ_h^2), as given in the following equation.

$$\delta_{total}^2 = \delta_d^2 + \delta_p^2 + \delta_h^2 \quad (\text{Equation 2.10})$$

In this study, a theoretical prediction method called “The Conductor-like Screening Model for Real Solvents” (COSMO-RS), was used to predict the solubility. This computer program uses a statistical thermodynamics approach based on quantum chemical calculations to determine the solubility without experimental data. It is a two-

step process. In the first step, a molecule input was made, and it was converted into SMILES (Simplified Molecular Input Line Entry Specification). Then a virtual conductor environment for the given molecule is simulated, and the induced polarization charge density was mapped on its surface, similar to the electrostatic potential map, that is referred as charge density or σ -surface. A 3D structure was also generated as shown in the **Table 2.6.** and **Table 2.7.** In the second step, the polarization charge density was used for the quantification of the interaction energy. A charge-density profile or σ -profile was calculated for each molecule from their 3D distribution of polarization charges on the surface (**Figure 2.11**). This profile offers detailed data about the molecular polarity distribution. This σ -profile was then used to calculate the chemical potential of the surface, referred as σ -potential that describes the likeliness of the molecule to interact with other molecules via intermolecular forces. In the 2D σ -potential graph shown in **Figure 2.12**, the negative charge was located on the right (H-bond acceptor), and the positive charge is located on the left (H-bond donor) for protic compounds. Also, the negative and positive charges of aprotic compounds were also shown on the graph.

Table 2.6 Structure and σ -surface of the fatty acid triglycerides in soybean oil used for the COSMO solubility calculation.

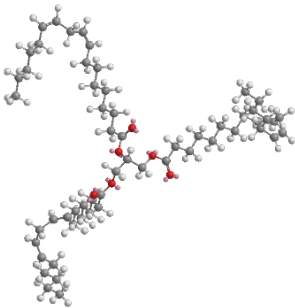
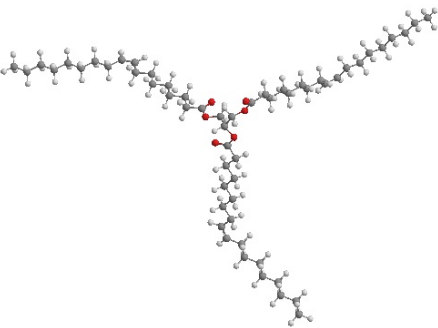
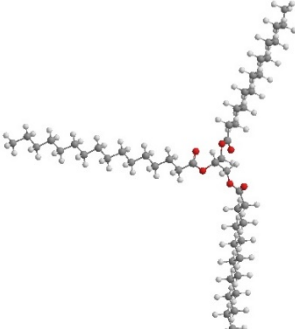
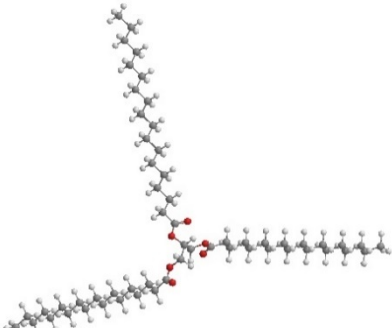
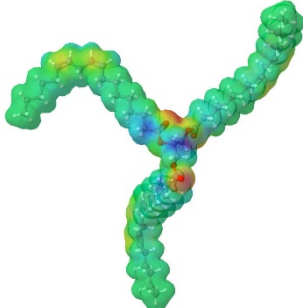
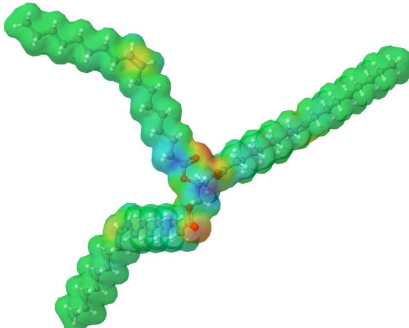
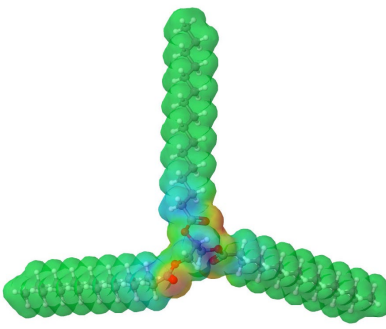
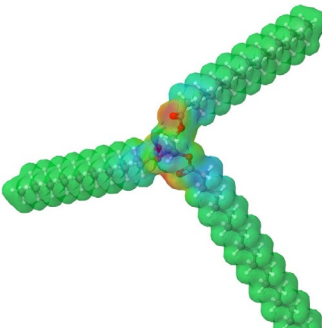
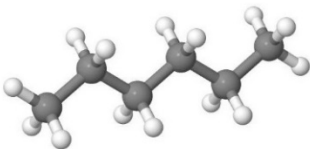
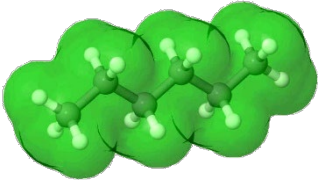
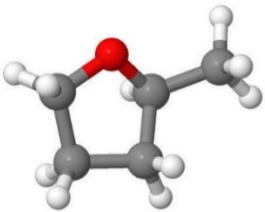
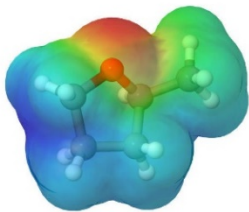
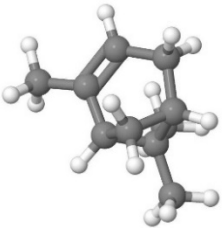
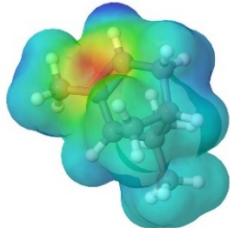
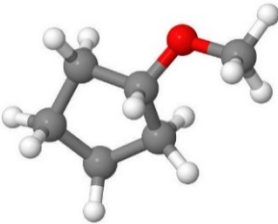
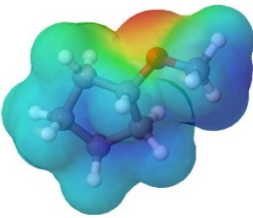
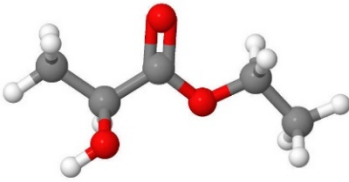
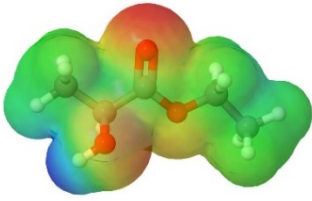
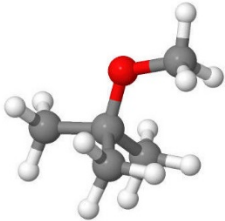
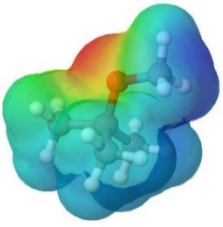
Solute	Ball and stick model (energy minimized)	Calculated σ -Surface
Trilinolein	 A ball and stick model of Trilinolein, showing a central glycerol backbone with three long, flexible, and kinked hydrocarbon chains extending outwards.	
Triolein	 A ball and stick model of Triolein, showing a central glycerol backbone with three long, flexible hydrocarbon chains that have a single kink.	
Tripalmitin	 A ball and stick model of Tripalmitin, showing a central glycerol backbone with three long, relatively straight hydrocarbon chains.	
Tristearin	 A ball and stick model of Tristearin, showing a central glycerol backbone with three long, straight hydrocarbon chains.	
	 A 3D surface representation of Trilinolein, colored by electrostatic potential. The surface shows a Y-shaped structure with a central region of high positive charge (red) and peripheral regions of high negative charge (blue).	
	 A 3D surface representation of Triolein, colored by electrostatic potential. The surface shows a Y-shaped structure with a central region of high positive charge (red) and peripheral regions of high negative charge (blue).	
	 A 3D surface representation of Tripalmitin, colored by electrostatic potential. The surface shows a Y-shaped structure with a central region of high positive charge (red) and peripheral regions of high negative charge (blue).	
	 A 3D surface representation of Tristearin, colored by electrostatic potential. The surface shows a Y-shaped structure with a central region of high positive charge (red) and peripheral regions of high negative charge (blue).	

Table 2.7 Structure and σ -surface of the *n*-hexane and green solvents used for the COSMO solubility calculation.

Solvents	Ball and stick model (energy minimized)	Calculated σ -Surface
<i>n</i> -hexane		
2-MeTHF		
<i>alpha</i> -Pinene		
CPME		
Ethyl lactate		
TBME		

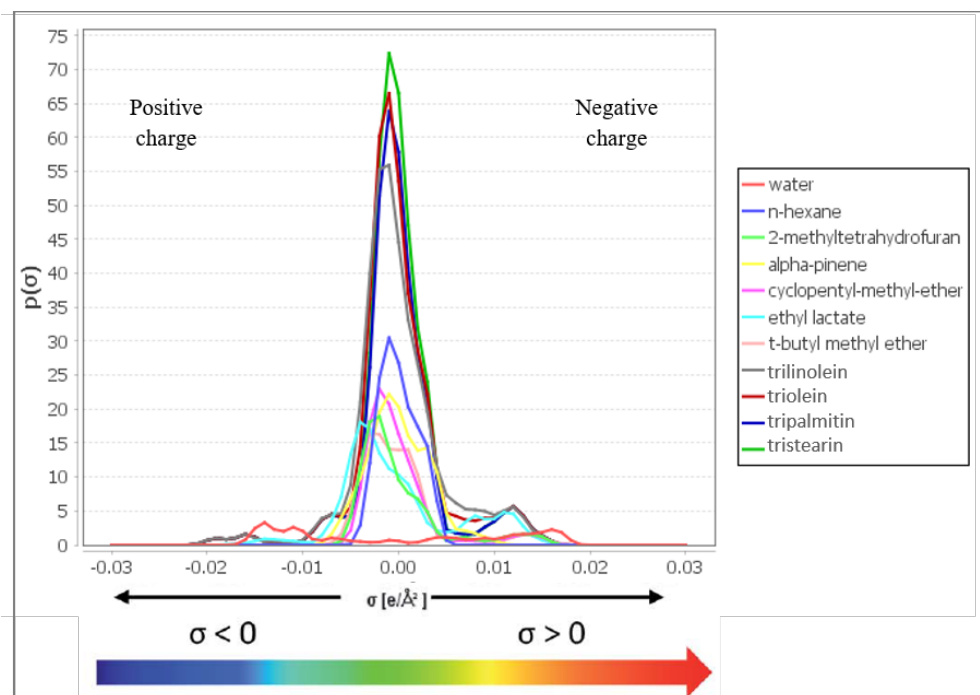


Figure 2.11 Computer predicted σ -profile (charge density profile) of solvents and solute compounds (Generated in COSMO Software). This chart compares the distribution of positive and negative charges on the surface of solvent and solute molecules.

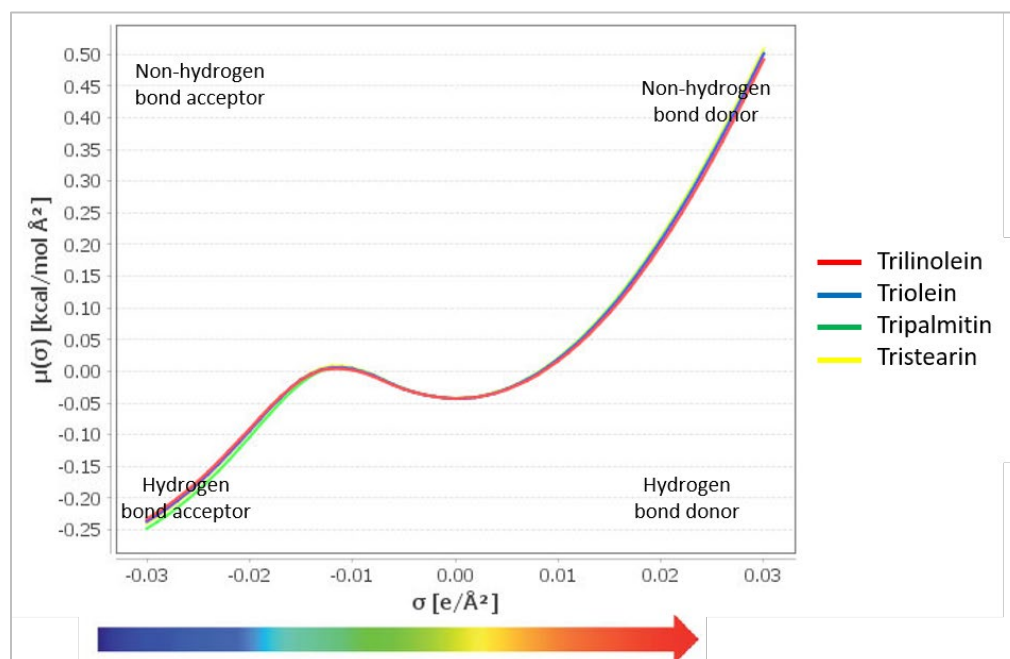


Figure 2.12 Computer predicted σ -potential of soybean triglycerides compounds (Generated in COSMO Software). This chart shows the chemical potential of the four different triglycerides compounds are more or less same.

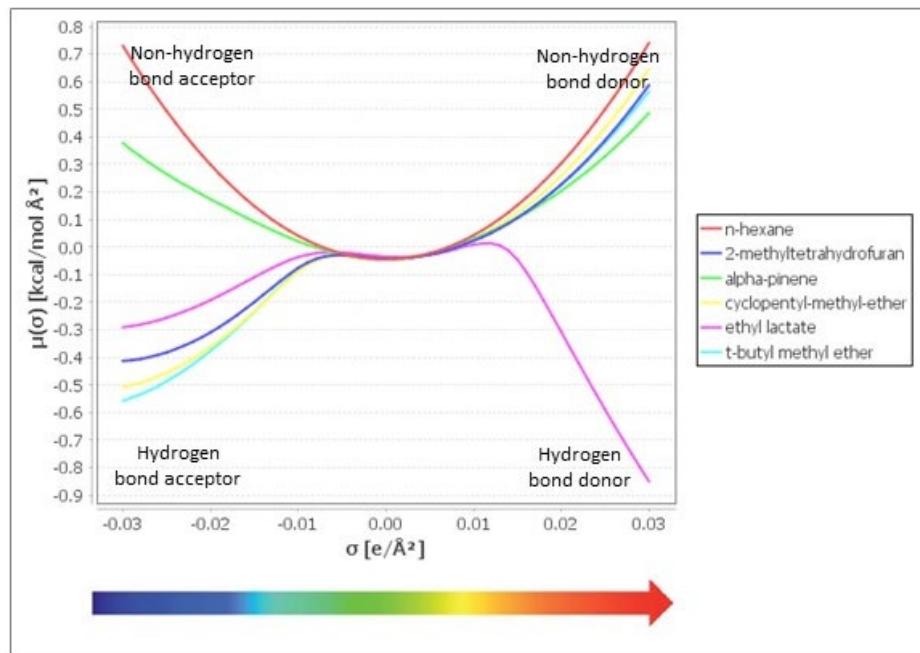


Figure 2.13 Computer predicted σ -potential of soybean hexane and green solvents (Generated in COSMO Software). This chart shows that the chemical potential of the solvents varies with polar, nonpolar, protic and aprotic nature of the compounds.

From the chemical potential of the pure solute μ_i^{pure} and the chemical potential of the solute in solvent at infinite dilution μ_i^{solvent} , and the free energy of fusion $\Delta G_{\text{fus},i}$ the experiment solubility x_i was calculated in *mol/mol* using the equation

$$\Delta G_{\text{fus},i} = \mu_i^{\text{pure}} - \mu_i^{\text{solvent}} - RT \log_{10}(x_i) \quad (\text{Equation 2.11})$$

The predicted value of $\log_{10}x_i$ and the solubility x_i of each major soybean triglycerides in different solvents were listed in **Table 2.8**. The probability of solubility x_i is expressed in percentage that can be visualized as the ratio of amount of solute dissolved in solvent. *(mol of solute / mol of solvent) x 100*.

Presence of long hydrophobic carbon chain and a hydrophilic ester functional group can be seen in the charge density map of the triglycerides of four major fatty acids,

linoleic acid, oleic acid, palmitic acid, and stearic acid. This makes those triglycerides less polar. Therefore, they have a poor solubility in the highly polar solvents like solvents such as water, ethanol, methanol, and acetonitrile. The predicted solubility percentage is less than 20% for those solute-solvents systems. A higher solubility was predicted for the triglycerides in the common non-polar solvents like carbon tetrachloride, benzene, toluene and *n*-hexane.

It is more useful to compare the solubility of the triglycerides of major fatty acids in green solvent to their solubility in *n*-hexane. Looking at the σ -potential curve of the triglycerides of fatty acids in **Figure 2.12**, it can be recognized that all of them have a strong hydrogen bonding acceptor and strong non-hydrogen bond donor character. The solvent that best match with this chemical potential would best dissolve the soybean oil. **Figure 2.13** shows the σ -potential of *n*-hexane and green solvents. It can be visualized that ethyl lactate and *alpha*-pinene have σ -potentials that has poor match with that of the soybean triglycerides. This is because these two solvents are hydrocarbons and do not have any non-carbon electronegative atoms. Although *alpha*-pinene has an unsaturation with small localized charge density that is not enough to match with the polarity of triglycerides. The predictions reveals that ethyl lactate is not the best for solubilizing soybean oil, and that is clearly marked by the solubility probabilities of triglycerides in these that solvent, given in **Table 2.8**. *n*-hexane and other green solvent 2-MeTHF, *alpha*-pinene, CPME, and TBME were predicted to have a high solubility probability for the triglycerides.

Industrial extraction of soybean oil is currently carried out in *n*-hexane, petroleum ether, and ethyl acetate. On the basis of the above predicted solubility, all of the green

solvents in the list are expected to give higher extraction yields, at least in the equilibrium region of the extraction curve, where solubility plays an influential role. Based on the solubility probability given in the above table, the green solvents 2-MeTHF, α -pinene CPME, and TBME should have slightly higher extraction yields than ethyl lactate, at least in the first part of extraction.

Table 2.8 Predicted solubility probability of triglycerides of major soybean fatty acids in different solvents. Green color represents high solubility (100%-60%), yellow color represents moderate solubility (60%-20%), and red color represent low solubility (20%-0%).

Solvents	Trilinolein		Triolein		Tripalmitin		Tristearin	
	$\log_{10}(x_i)$	Solubility Probability (%)	$\log_{10}(x_i)$	Solubility Probability (%)	$\log_{10}(x_i)$	Solubility Probability (%)	$\log_{10}(x_i)$	Solubility Probability (%)
Water	-23.623	0.0	-24.820	0.0	-23.203	0.0	-26.150	0.0
Ethanol	-1.4645	3.4	-1.7542	1.8	-1.7932	1.6	-2.0927	0.8
Methanol	-3.3227	0.0	-3.7839	0.0	-3.7385	0.0	-4.2964	0.0
Ethyl acetate	0.0000	100.0	0.0000	100.0	0.0000	100.0	-0.0326	92.8
Acetone	0.0000	100.0	0.0000	100.0	-0.3046	49.6	-0.4544	35.1
Toluene	0.0000	100.0	0.0000	100.0	0.0000	100.0	0.0000	100.0
Benzene	0.0000	100.0	0.0000	100.0	0.0000	100.0	0.0000	100.0
Diethyl ether	0.0000	100.0	0.0000	100.0	0.0000	100.0	0.0000	100.0
THF	0.0000	100.0	0.0000	100.0	0.0000	100.0	0.0000	100.0
DMF	-0.1423	72.1	-0.6594	21.9	-0.9420	11.4	-1.1875	6.5
Acetonitrile	-5.1739	0.0	-6.1241	0.0	-6.1742	0.0	-7.1162	0.0
CCl ₄	-0.2584	55.2	-0.2510	56.1	-0.3339	46.4	-0.3096	49.0
DCM	0.0000	100.0	0.0000	100.0	0.0000	100.0	0.0000	100.0
Chloroform	0.0000	100.0	0.0000	100.0	0.0000	100.0	0.0000	100.0
<i>n</i> -hexane	0.0000	100.0	0.0000	100.0	0.0000	100.0	0.0000	100.0
2-MeTHF	0.0000	100.0	0.0000	100.0	0.0000	100.0	0.0000	100.0
<i>alpha</i> -Pinene	0.0000	100.0	0.0000	100.0	0.0000	100.0	0.0000	100.0
CPME	0.0000	100.0	0.0000	100.0	0.0000	100.0	0.0000	100.0
Ethyl lactate	0.0000	100.0	-0.3024	49.8	-0.5079	31.1	-0.6517	22.3
TBME	0.0000	100.0	0.0000	100.0	0.0000	100.0	0.0000	100.0

2.3.5 Viscosity of Green Solvents at Different Temperature

For an extraction of a small quantity of solute in a large quantity of solvent, diffusion is the predominant factor that controls the extraction time and yield. As discussed, the rate of extraction in the kinetic region is smaller compared to the thermodynamic region, but still the time required for the maximum extraction is determined by the diffusivity of solute in solvent. The diffusion, in other words the mass transfer of solute from one phase to another, is highly dependent on viscosity (η) of the solvent. Viscosity is informally related to the thickness of a fluid, but formally it is a measure of the fluid's internal flow resistance or resistance to deformation by shear stress or tensile stress. Rate of diffusion increases with decrease in viscosity of the solvent, as the solvent can easily pass through the solid sample matrix with a low interfacial tension.⁶⁸ This highlights the importance of studying the viscosity of the green solvents in comparison with *n*-hexane.

Viscosity of a fluid is related to the molecular structure of the substance and intermolecular links, and is affected by temperature, and pressure.⁷² Viscosity of a fluid decreases with increase in temperature. Although this inverse proportional relation applies to all fluids, the size of influence varies for different substances. Viscosity of some substances are strongly influenced by temperature, with a 1 °C rise in temperature can lower the viscosity by 10%.

In most cases, viscosity of a fluid increases with pressure. When it comes to liquid the effect of pressure on viscosity is very little compared to the effect of temperature. This is because, liquids are almost noncompressible with small changes in pressure. For

most liquids it takes the change in pressure from 0.1 to 30 MPa to cause a considerable change in viscosity that is similar to what a 1 °C temperature change would cause.^{72,73}

Viscosity of green solvent at varying temperature was measured experimentally using ATS Rheosystems viscoanalyzer, and the results are presented in **Figure 2.13**.

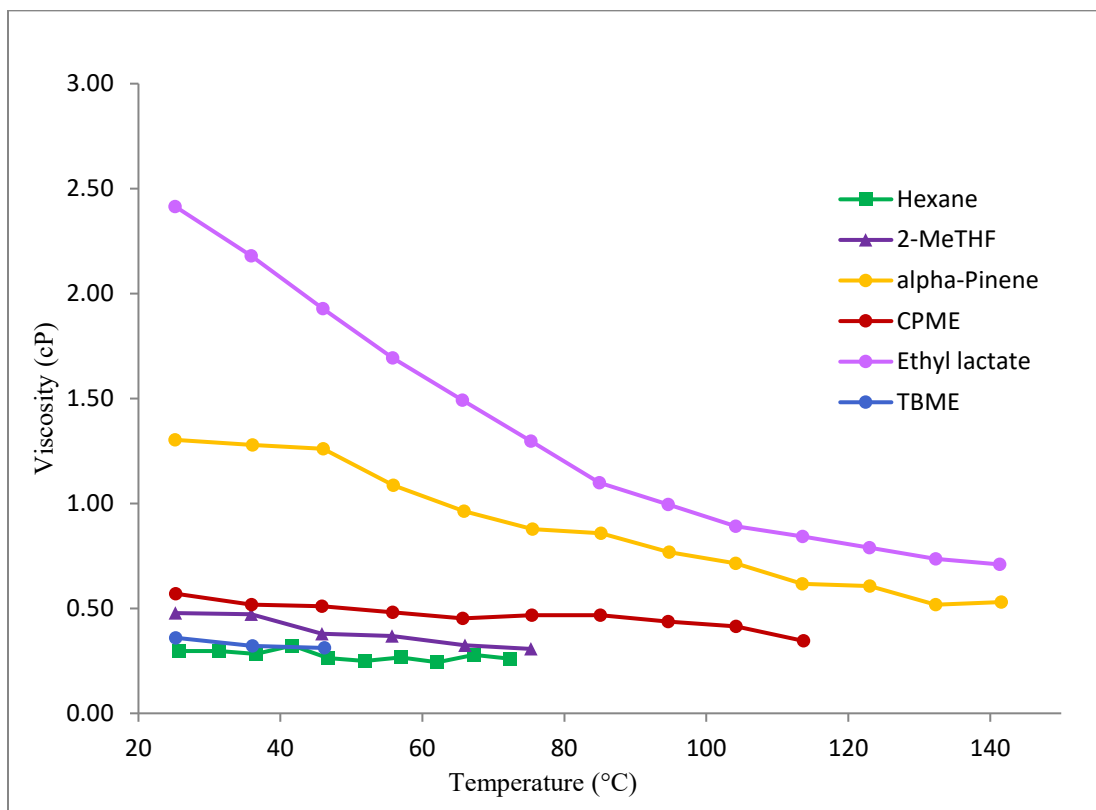


Figure 2.14 Comparison of change in viscosity of solvents at different temperature.

Of the six solvents tested, ethyl lactate has the highest viscosity value of 2.4 cP at room temperature, and it gradually lowers around 0.5 cp for every 10 °C rise in temperature until 100 °C. When the temperature is close the boiling point of ethyl lactate, the change in viscosity is nearly flat. The viscosity of ethyl lactate at 141 °C is 0.7 cP, and this is higher than the room temperature viscosity of a few other green solvents and *n*-hexane. The next higher viscosity is recorded for *alpha*-pinene. At room temperature the viscosity of *alpha*-pinene is 1.3 cP, and it gradually lowers at the rate of 0.1 cP for 10

°C rise in temperature. The viscosity of alpha-pinene at 141 °C is 0.53 cP, again this is greater than the room temperature viscosity of other green solvent and *n*-hexane.

Viscosity of CPME at room temperature is 0.57 cP. CPME, 2-MeTHF and TBME follows *n*-hexane very closely with changing trend of viscosity at different temperatures. For these three solvents the effect of temperature on viscosity is not prominent, and the curve is less steep compared to ethyl lactate and *alpha*-pinene. CPME's viscosity is 0.35 cP near its boiling point. 2-MeTHF's viscosity near its boiling point is 0.30 cP, which slightly lower than the viscosity of CPME. Viscosity of TBME is the lowest of all green solvents. At room temperature, the viscosity of TBME is 0.36 cP and near its boiling point is 0.31 cP. The boiling point of TBME is 55 °C, which is the lowest of all. Hexane is a completely non-polar hydrocarbon, and its viscosity is lowest of all other solvents. At room temperature the viscosity of hexane is 0.29 cP, and that does not change much with the temperature. The viscosity of hexane near boiling point is 0.26 cP.

In ASE extraction of soybean oil, the temperature was maintained at 100 °C, that is higher than the boiling point of TBME, 2-MeTHF, and *n*-hexane, and lower than the boiling point of CPME, *alpha*-pinene, and ethyl lactate. However, to keep all solvents in liquid state, the pressure was maintained at 1500 psi. This is an ideal operating condition for ASE extraction study for a new solute-solvent systems.³⁴ As 100 °C is well below the critical point of all the solvent used for extraction, the solvents were just pressurized to maintain their liquid state.

As pressure does not have a notable effect on viscosity of liquid solvents, the above results and discussion concludes that at 100 °C *n*-hexane, 2-MeTHF, CPME and TBME have lower viscosity, therefore a higher diffusion rate and consequently a higher

mass transfer is expected for those solvents in ASE extraction of soybean oil. On the other hand, a smaller diffusion rate is expected from ethyl lactate and *alpha*-pinene.

2.3.6 Characterization of extracted oil

Soybean oil extracted from ASE method was characterized using GC-MS. Triglycerides can be easily hydrolyzed to form fatty acids, which are polar and can form hydrogen bonds in their free, underivatized form. This may cause adsorption issues during the gas chromatography. Reducing the polarity of carboxylic acids may make them more amenable for GC-MS analysis. For our characterization purpose, the triglycerides in the soybean oil were converted into fatty acid methyl esters (FAME) prior to the GC-MS analysis. The Lewis acid catalyzed esterification reaction scheme shown below was performed to transform the major fatty acids such as palmitic acid, linoleic acid, oleic acid, stearic acid into their respective methyl esters.⁷⁴ Boron trifluoride in this reaction functions as a Lewis acid that catalyze the reaction by increasing the electrophilicity of carbonyl carbons in fatty acids. Methanol in this reaction functions as the nucleophile that attacks the carbonyl carbon to replace hydroxide and produce ester. The reaction mixture was washed with base water to remove any unreacted fatty acid and reagents. The ester products were highly soluble in the organic phase that was collected, and dried using sodium sulfate and magnesium sulfate columns to get rid of trace water. **Figure 2.16** shows the reflux apparatus setup used for the esterification of fatty acids.

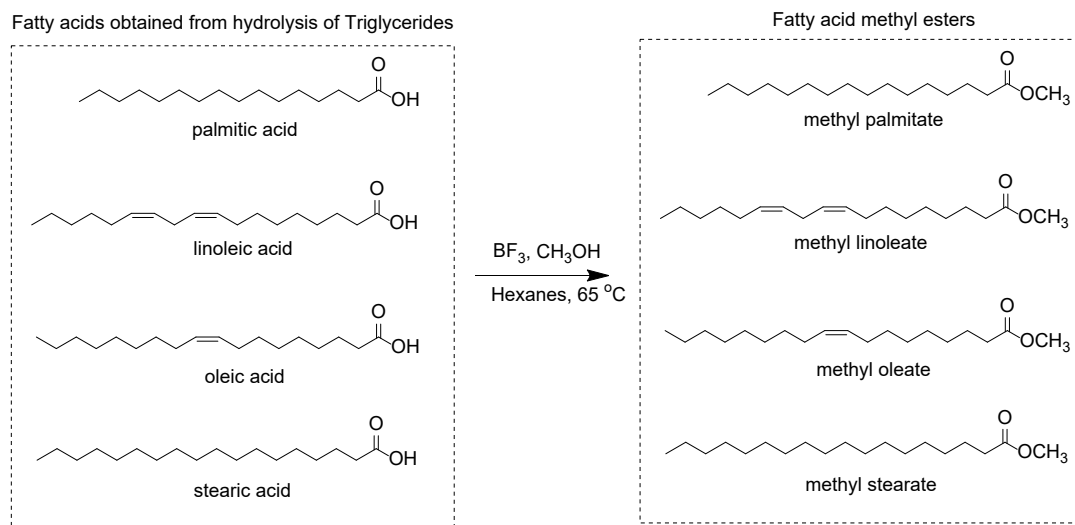


Figure 2.15 Reaction scheme show the conversion of fatty acids (from triglyceride) in the soybean oil into methyl esters using Lewis acid catalyzed esterification.

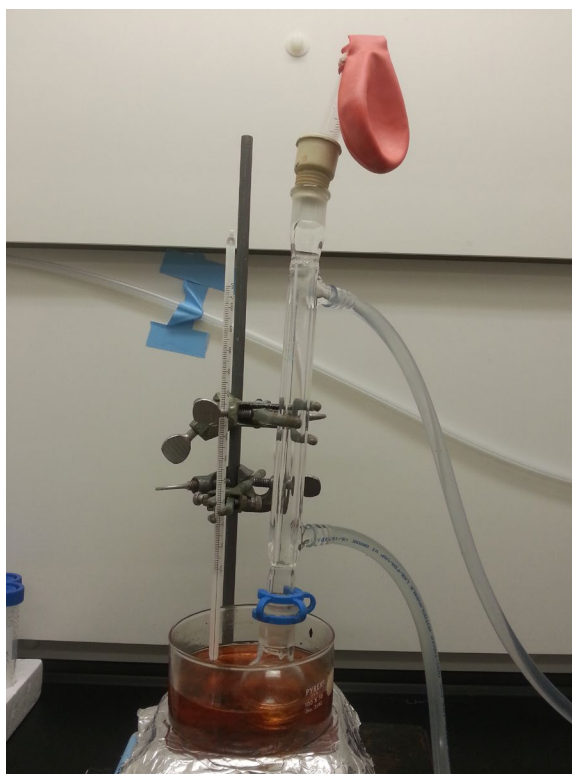


Figure 2.16 Photograph of the reaction setup used for methyl esterification of fatty acids in soybean oil.

2.3.7 ASE Extraction Results and Hot-ball model Comparison

The following sections discuss the results of extraction of soybean oil in accelerated solvent extractor (ASE) using *n*-hexane, the reference hydrocarbon solvent, and these selected green solvents

- 2-Methyl tetrahydrofuran (2-MeTHF)
- Alpha-Pinene
- Cyclopentyl methyl ether (CPME)
- Ethyl lactate
- t-butyl methyl ether (TBME)

All the following ASE extraction results were obtained at 100 °C temperature and 1500 psi pressure. This operating condition of ASE technique that is ideal for studying new solute-solvent system was adopted from the literature.³⁴ This operating condition was also tested and reported to be working well for extraction of fats from coffee.³¹ Thermal degradation point of analyte was also considered while choosing the operating conditions.

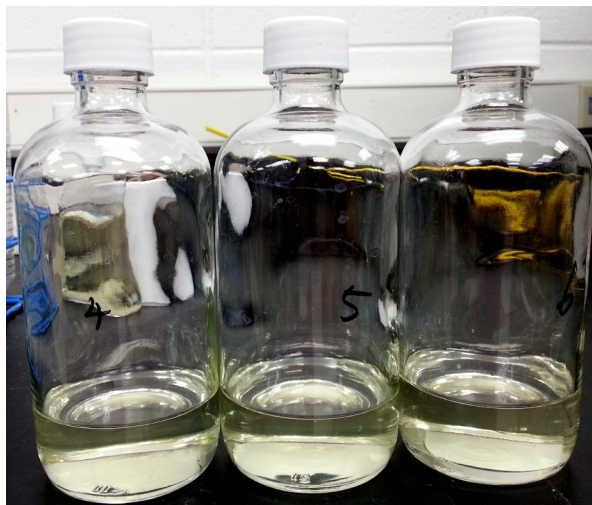


Figure 2.17 Picture of extracts (that contains oil) collected from ASE. As the amount of solvent used is about 30 mL, a concentration and drying process was required after extraction.

The number of cycles, solvent flush volume, purge time, and sample preheat time were determined based on the sample type and volume. Extraction times were set to 5, 10, 15, 20 and 30 min. All extractions were done in triplicate with soybean particle size of 513 μm , and the yields were calculated gravimetrically. The average of the triplicate and the standard deviation were reported for each solvent.

The percentage extracted was calculated for each solvent using equation 2.6. Typically 21% of a soybean is made of oil (**Table 2.3**), however the highest extraction yield obtained in this study was 23.24% (or 0.2324g), which is from CPME. Hence, the amount of maximum extractable (or 100%) analyte per gram of sample was calculated to be 0.2347 g, by assuming the highest experimental yield, that is the yield obtained at 30 min using CPME, as the 99% recovery. Also, it was assumed that the analyte oil was evenly distributed among all soybean particles. Based on this, a percent recovery was calculated for each solvent using the equations 2.6 and 2.7. A plot of percent recovery versus extraction time is shown for each solvent separately, and a qualitative comparison with the hot-ball model was made to validate the experimental results. The main areas of the graph to look for are the initial steep rise in percent recovery (thermodynamics regions), and a later tailed off percent recovery (kinetics region). As shown in **Figure 2.18**, a visual fitting of experimental plot to the theoretical plot is made for each solvent extraction.

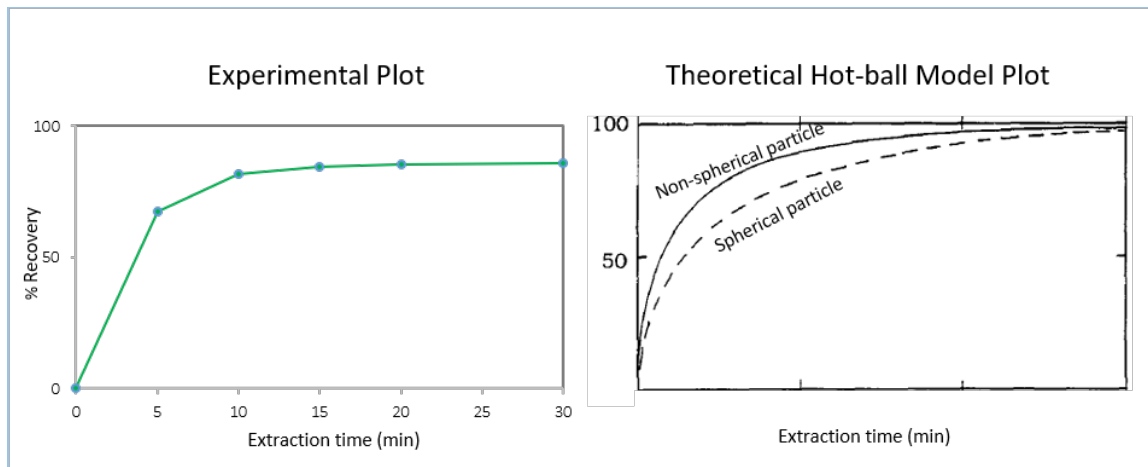


Figure 2.18 Example of qualitative comparison of experimental plot of percent recovery vs. extraction time, obtained from *n*-hexane extraction, with the theoretical hot-ball model plot.

A kinetic plot of $\ln(m/m_0)$ versus extraction time was shown separately for each solvent-extraction for a better qualitative and quantitative analysis. In these kinetics plots, the reduced time $t_r = 1$, is set to match the time in which the linear portion of the curve changes by a value of $\ln(m/m_0) = 1$. A second horizontal axis on the top was added to the same graph that represents the reduced time. Having two axes would help qualitatively visualize how the reduced time is scaled to the actual extraction time. The kinetic plot of each solvent is compared to the theoretical hot-ball model kinetic plot to validate the experimental results. The important areas to look for are initial steep curve, linear diffusion region, the slope of extrapolation of diffusion regions, and the intercept of the extrapolation line at $t=0$ axis. A quantitative comparison is that the $\ln(m/m_0)$ value at the intercept should be more negative than -0.5 in order to validate the experimental results for non-spherical soybean particles, as shown in **Figure 2.19**. The $\ln(m/m_0)$ value at the intercept and the slope of the diffusion region would be quantitatively used to calculate the diffusion coefficient, and the time required to extract a desired amount of

soybean oil. Application of hot-ball model to qualitatively validate the extraction results, and quantitatively calculate the diffusion coefficient was reported for each solvent. IR and GC-MS spectra were given to confirm the purity of the extracted oil. A comparison of extraction efficiency of all solvents was made at the end.

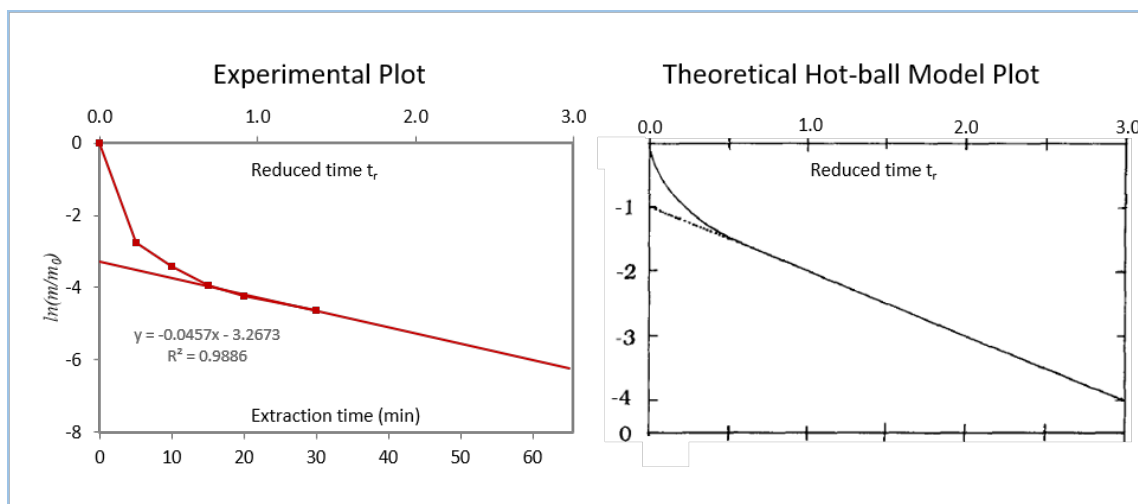


Figure 2.19 Example of qualitative and quantitative comparison of experimental plot of $\ln(m/m_0)$ vs. reduced time, obtained from CPME solvent extraction, with the theoretical hot-ball model plot.

2.3.8 *n*-Hexane Extraction and Hot-ball Model Results

(a) *Qualitative comparison to the hot-ball model*

The percent recovery of soybean oil using *n*-hexane is plotted against extraction time in **Figure 2.20**. A fast initial rate of extraction is observed as predicted by the hot-ball model. In the graph it appears as a steep rise in percent recovery between 0 – 15 min. As listed in **Table 2.9** an average of $67.62 \pm 1.14\%$ of the total extractable mass of soybean oil is recovered in five minutes. The first part, that is the 0 – 15 min, is considered as the equilibrium region, where the solute partitioning, and thus solubility of the solute-solvent system, plays a dominant role. As presented previously in **Table 2.8**, the predicted relative solubility of triglycerides of the major fatty acids of soybean oil in *n*-hexane is high. As the extraction progressed, the rate of extraction becomes smaller, and that is indicated by a flattening of the recovery curve. After 15 min, the rate of extraction turns out to not change much. This agrees with the prediction of hot-ball model. The maximum recovery of $85.85 \pm 0.66\%$ is observed at 30 min.

The diffusion region of the recovery graph starts at 15 min and after that a slow exponential decay of extraction rate was observed. As most of the oil has already been extracted, the mass transfer of the remaining oil is drawn by the concentration gradient through diffusion. Viscosity of solvent should be the predominant factor in this diffusion region. A quantitative approach with respect to hot-ball model is needed to analyze this region.

Table 2.9 Results of accelerated solvent extraction (ASE) of soybean oil using *n*-hexane as solvent (particle size is 513 μm , temperature is 100 $^{\circ}\text{C}$).

Extraction time (min)	Average mass of oil extracted per gram of soybean sample (g)	Percent of oil extracted per gram of soybean sample (%)	Percent Recovery (where $m_o = 0.2347$ g) (%)	Standard deviation for % recovery (n=3) (%)
0	0	0	0	0
5	0.1587	15.87	67.62	1.14
10	0.1918	19.18	81.72	3.54
15	0.1985	19.85	84.58	1.83
20	0.2006	20.06	85.46	2.08
30	0.2015	20.15	85.85	0.66

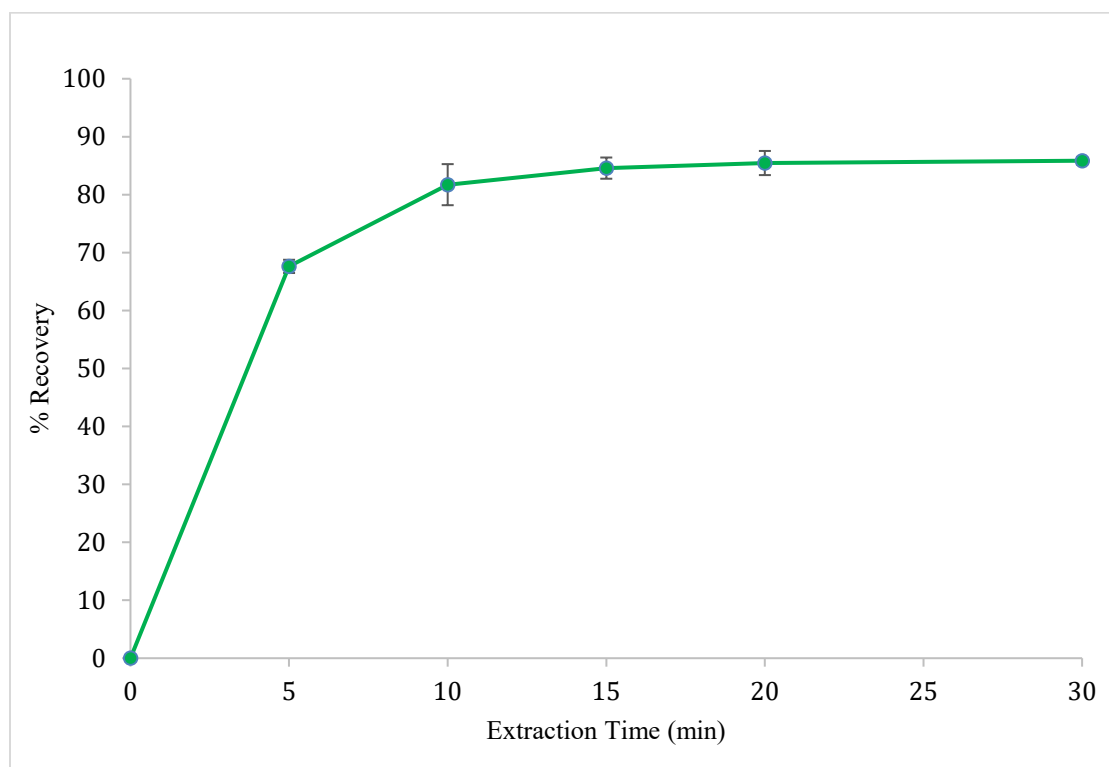


Figure 2.20 Percent of oil recovered out of total extractable oil in soybean sample using *n*-hexane at different extraction times. Particle size is 513 μm .

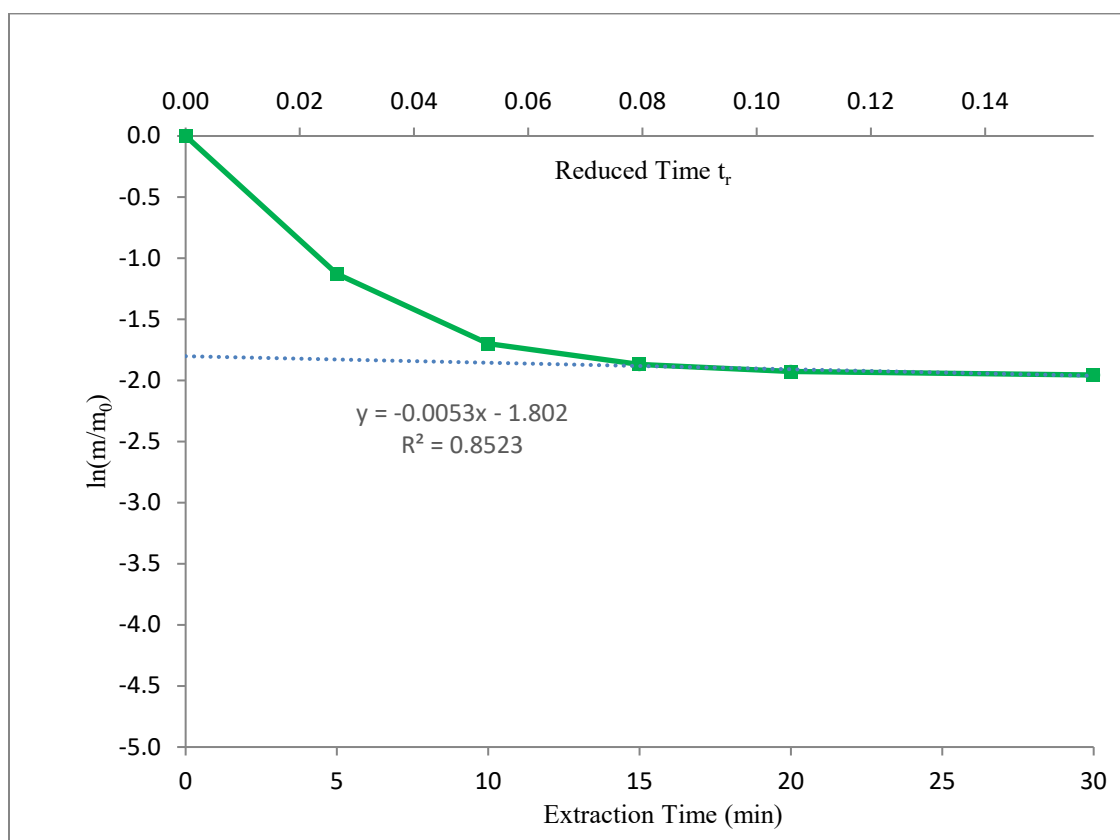
(b) Calculation of diffusion coefficient using hot-ball model

The characteristic of experimental data of soybean extraction using *n*-hexane is matched to the hot-ball model. The extraction kinetics is plotted using the natural logarithm of ratio of mass of unextracted oil to the original mass of extractable oil, $\ln(m/m_o)$ versus extraction time, as shown in **Figure 2.21**. To match with the theoretical model, this extraction time is simplified to the reduced time, t_r . The extraction time (horizontal axis on the bottom) is quantitatively scaled to the reduced time (horizontal axis on the top) in the same graph. The numerical values are given in the **Table 2.10**. The actual extraction time equivalent to reduced time $t_r = 1$, for *n*-hexane is calculated to be 189 min. The kinetic curve initially falls infinitely steeply. Even though this is a small portion of the curve, it represents the loss of majority of extractable material from the particle ($84.58 \pm 1.83\%$) within 15 min. But after the extraction time of 15 min, which corresponds to the t_r of around 0.08, the rate of fall tails off and the curve become almost linear.

At first the concentration at the surface of the sample particle diffuse out quickly, and as the extraction progresses, the surface concentration drops significantly. This leads to a large concentration gradient near the surface, which makes the solute from core of the particle to diffuse out. Eventually, when the concentration gradient thins out, a smoother profile is established, and the loss of solute concentration is turns out to be a simple exponential decay.

Table 2.10 Hot-ball model results for the ASE extraction of soybean oil using *n*-hexane.

Extraction time (min)	Average mass of analyte oil extracted per gram of soybean sample (g)	Average mass (m) of analyte unextracted per gram of soybean sample (if $m_0 = 0.2347$ g) (g)	m/m_0	$\ln(m/m_0)$	Reduced time t_r
0	0	0.2347	1.0000	0	0
5	0.1587	0.0760	0.3238	-1.1276	0.027
10	0.1918	0.0429	0.1828	-1.6994	0.053
15	0.1985	0.0362	0.1542	-1.8692	0.080
20	0.2006	0.0341	0.1453	-1.9290	0.106
30	0.2015	0.0332	0.1415	-1.9558	0.159

**Figure 2.21** Plot of $\ln(m/m_0)$ vs. extraction time for *n*-hexane scaled to the reduced time (t_r) to compare with the hot-ball model.

Extrapolation of the linear portion of the curve to $t = 0$ axis provides an intercept of $\ln(m/m_0) = -1.802$. This aligns to the hot-ball model with the effect of non-spherical particle shape that was given in **Figure 2.5**. The close fit of experimental y-intercept with the y-intercept of hot-ball model endorses the experimental data obtained from *n*-hexane extraction to be valid, as the 513 μm ground soybean particle were not spherical.

The linear regression of the trend line is 0.8523 and the slope of the line -0.0053. The intercept on $t = 0$ axis is -1.802. From this data, the diffusion coefficient of *n*-hexane is calculated to be $5.9 \times 10^{-9} \text{ cm}^2\text{s}^{-1}$. Also, the time required for the recovery of 99% of oil using *n*-hexane is 531 min, which is relatively higher than other solvents. The experimental viscosity of *n*-hexane is relatively low compared to the other solvent.

The identity of soybean oil extracted in ASE using *n*-hexane is confirmed by IR spectroscopy. **Figure 2.22** shows that the IR peaks for the stretching frequencies of C=O at 1743 cm^{-1} , $\text{sp}^3 \text{ C-H}$ at 2853 cm^{-1} and 2923 cm^{-1} , $\text{sp}^2 \text{ C-H}$ at 3009 cm^{-1} , and C-O at 1159 cm^{-1} for the triglycerides in the extracted soybean oil perfectly match with the IR peaks of commercial soybean oil.

The GC-MS chromatogram also confirms the identity of fatty acid methyl esters in the *n*-hexane extracted soybean oil (**Figure 2.23**). For four major fatty acid methyl esters in the extracted oil have a relative abundance that matches with the theoretical relative ratio of the four fatty acids soybean sample.

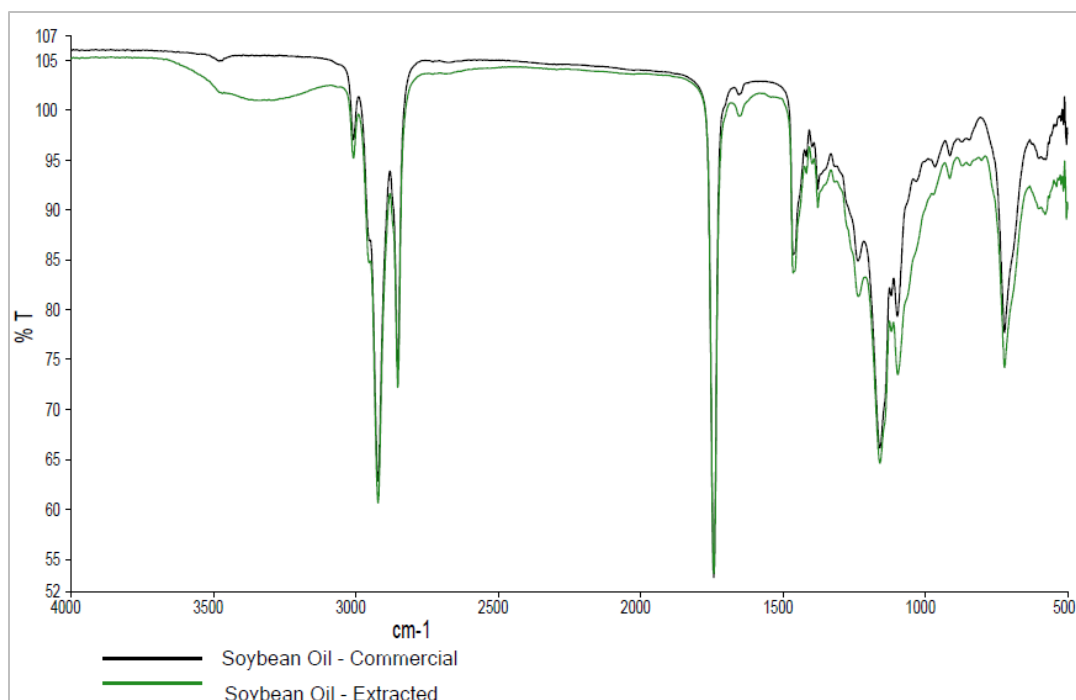


Figure 2.22 Comparison of IR spectra of commercial soybean oil and soybean oil extracted in ASE using *n*-hexane.

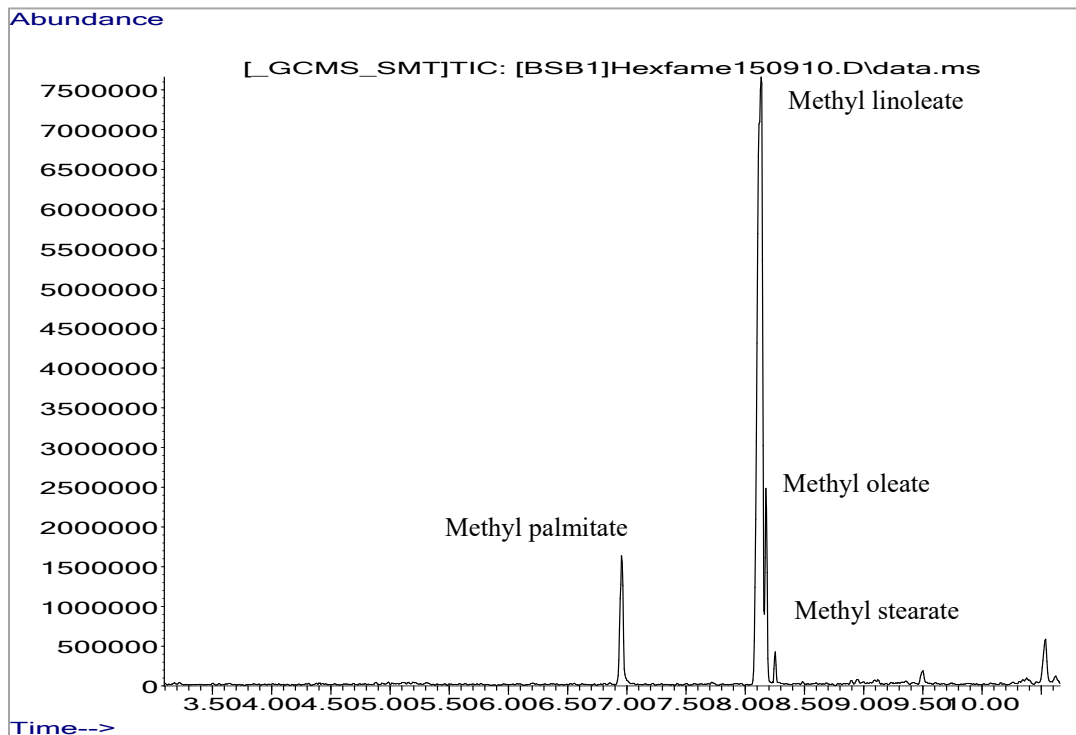


Figure 2.23 Gas chromatogram shows the presence of fatty acid methyl ester derivatives from soybean oil extracted in ASE using *n*-hexane.

2.3.9 2-MeTHF Extraction and Hot-ball Model Results

(a) Qualitative comparison to the hot-ball model

The percent recovery of soybean oil using 2-MeTHF is plotted against extraction time in **Figure 2.24**. As was seen for *n*-hexane, 2-MeTHF also has a fast initial rate of extraction as predicted by hot-ball model. In the graph it appears as a steep rise in percent recovery between 0 – 15 min. This is steeper than *n*-hexane initial rate of extraction. As given in the **Table 2.11**, results of accelerated solvent extraction (ASE) of soybean oil using 2-MeTHF as solvent (particle size is 513 μm , temperature is 100 $^{\circ}\text{C}$). an average of $89.69 \pm 0.19\%$ of the total extractable mass of soybean oil is recovered in five minutes. This is relatively high compared to that of the reference solvent *n*-hexane. As the extraction progressed, the rate of extraction becomes smaller, indicated by a flattening of the recovery curve. After 15 min, the rate of extraction turns out to not change much. This agrees with the prediction of hot-ball model. The maximum recovery of oil using 2-MeTHF is $95.88 \pm 1.36\%$ that is observed at 30 min.

The initial steep rise in rate of extraction can be related to the predicted high solubility for the triglycerides of soybean oil in 2-MeTHF at 100 $^{\circ}\text{C}$ (**Table 2.8**). The diffusion region of recovery graph starts from 15 min where a slow exponential decay of extraction rate was observed. Viscosity of solvent should be the controlling factor in this region. A quantitative approach with respect to hot-ball model is discussed below to analyze this region.

Table 2.11 Results of accelerated solvent extraction (ASE) of soybean oil using 2-MeTHF as solvent (particle size is 513 μm , temperature is 100 $^{\circ}\text{C}$).

Extraction time (min)	Average mass of oil extracted per gram of soybean sample (g)	Percent of oil extracted per gram of soybean sample (%)	Percent Recovery (where $m_o = 0.2347$ g) (%)	Standard deviation for % recovery (n=3) (%)
0	0	0	0	0
5	0.2105	21.05	89.69	0.19
10	0.2158	21.58	91.93	0.18
15	0.2220	22.20	94.57	0.37
20	0.2239	22.39	95.40	0.65
30	0.2250	22.50	95.88	1.36

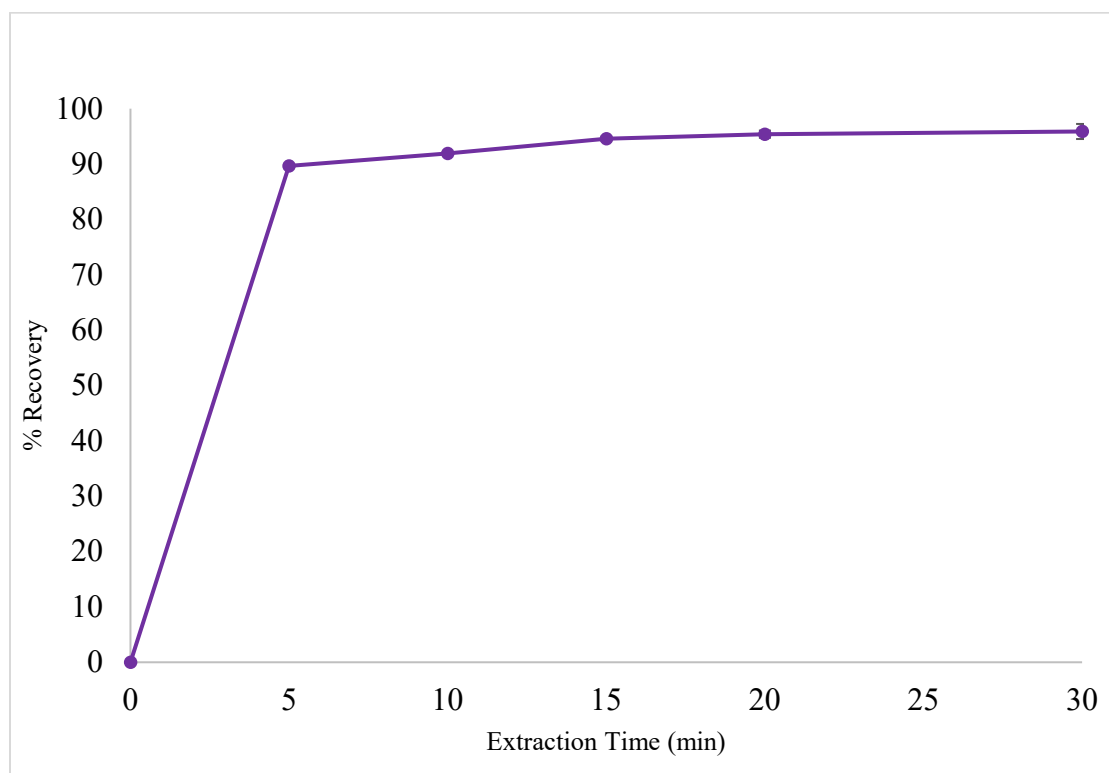


Figure 2.24 Percent of oil recovered out of total extractable oil in soybean sample using 2-MeTHF at different extraction times. Particle size is 513 μm .

(b) Calculation of diffusion coefficient using hot-ball model

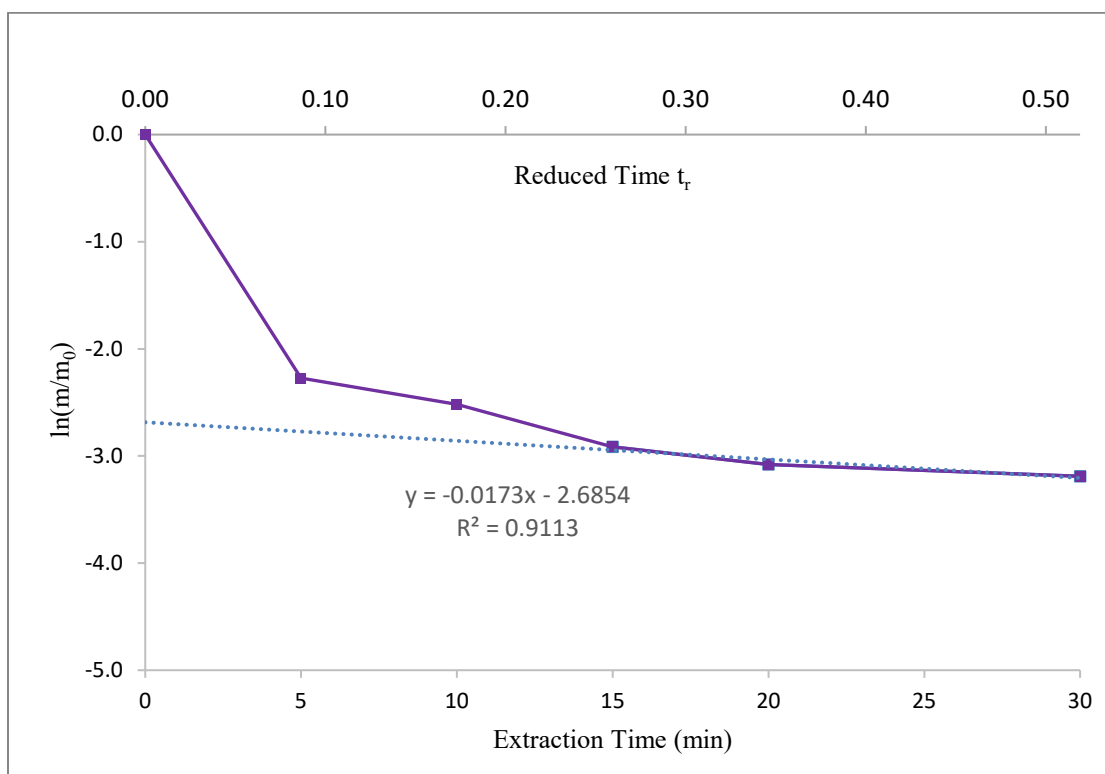
The shape of experimental kinetic plot of extraction of soybean oil using the green solvent 2-MeTHF fits with the hot-ball model. The extraction kinetics is plotted using the natural logarithm of ratio of mass of unextracted oil to the original mass of extractable oil, $\ln(m/m_o)$, versus extraction time, as shown in **Figure 2.25**. The extraction time (horizontal axis on the bottom) is quantitatively scaled to the reduced time (horizontal axis on the top) in the graph, as previously explained for *n*-hexane. The values are given in the **Table 2.12**. The actual extraction time at $t_r = 1$, for 2-MeTHF is calculated to be 58 min. The curve initially falls infinitely steeply, and it represents the loss of majority of extractable material from the particle ($94.57 \pm 0.37\%$) within 15 min. But after of 15 min, which corresponds to the t_r of around 0.26, the rate of fall drops off and the curve become linear similar to what is seen for *n*-hexane.

The linear regression of the trend line is 0.9113, the slope is -0.0173, and the intercept on $t = 0$ axis is at the value of $\ln(m/m_o) = -2.6854$. From this data, the diffusion coefficient of 2-MeTHF is calculated to be $1.9 \times 10^{-8} \text{ cm}^2\text{s}^{-1}$. This is significantly high compared *n*-hexane. The actual time required to recover 99% of the oil is calculated to be 112 min. This increased diffusion coefficient and thus the short extraction time for 2-MeTHF are related to the viscosity of the pressurized liquid 2-MeTHF solvent at 100°C.

The identity of soybean oil extracted in ASE using 2-MeTHF is confirmed by IR spectroscopy. **Figure 2.26** shows that the IR peaks for C=O, sp^3 C-H, sp^2 C-H, C=C, and C-O stretching frequencies of triglycerides in extracted soybean oil perfectly match with the IR peaks of commercial soybean oil. In **Figure 2.27** GC-MS chromatogram shows the presence of four major fatty acid methyl esters in the extracted soybean sample.

Table 2.12 Hot-ball model results for the ASE extraction of soybean oil using 2-MeTHF

Extraction time (min)	Average mass of analyte oil extracted per gram of soybean sample (g)	Average mass (m) of analyte unextracted per gram of soybean sample (if $m_0 = 0.2347$ g) (g)	m/m_0	$\ln(m/m_0)$	Reduced time t_r
0	0	0.2347	1.0000	0	0
5	0.2105	0.0242	0.1031	-2.2720	0.087
10	0.2158	0.0189	0.0807	-2.5174	0.173
15	0.2220	0.0127	0.0543	-2.9141	0.260
20	0.2239	0.0108	0.0460	-3.0788	0.346
30	0.2250	0.0097	0.0412	-3.1896	0.519

**Figure 2.25** Plot of $\ln(m/m_0)$ vs. extraction time for 2-MeTHF scaled to the reduced time (t_r) to compare with the hot-ball model.

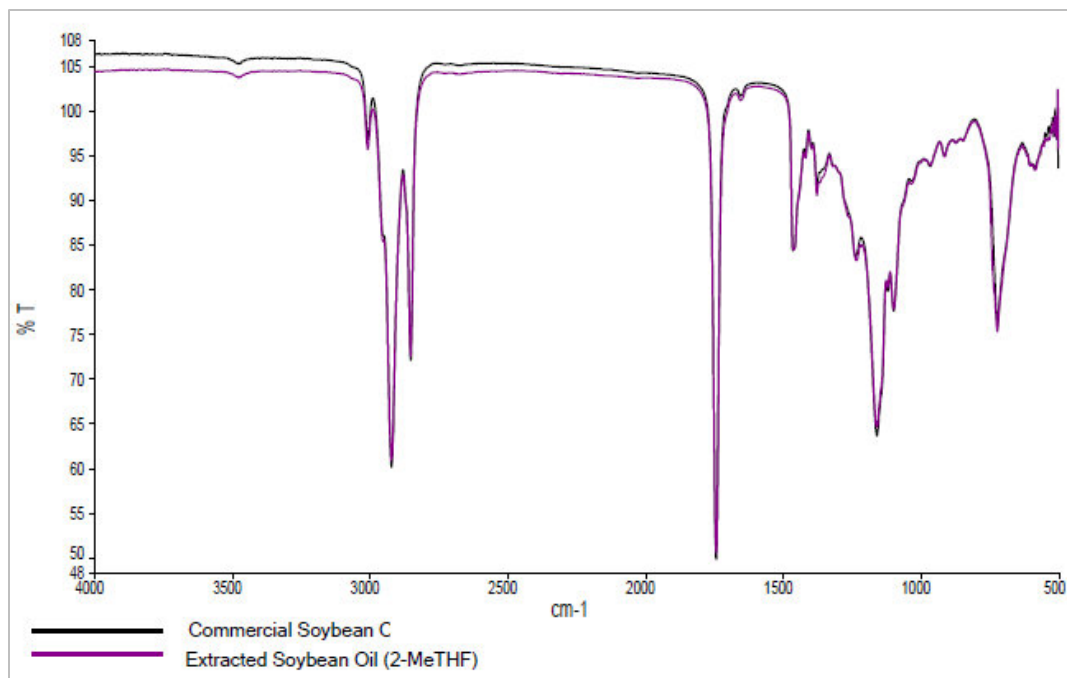


Figure 2.26 Comparison of IR spectra of commercial soybean oil and soybean oil extracted in ASE using 2-MeTHF.

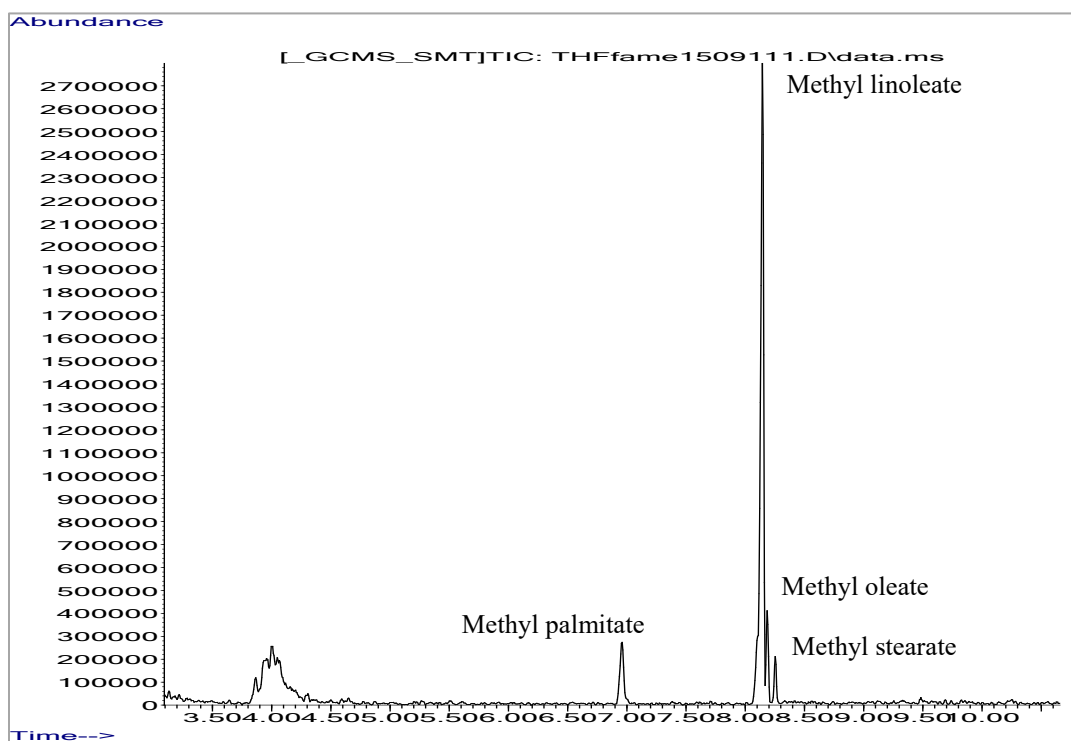


Figure 2.27 Gas chromatogram shows the presence of fatty acid methyl ester derivatives from soybean oil extracted in ASE using the green solvent 2-MeTHF.

2.3.10 *alpha*-Pinene Extraction and Hot-ball Model Results

(a) *Qualitative comparison to the hot-ball model*

The percent recovery of soybean oil using *alpha*-pinene is plotted against extraction time in **Figure 2.28**. A fast initial rate of extraction as predicted by hot-ball model is observed for *alpha*-pinene, as a steep rise in percent recovery between 0 – 15 min. The percent recovery for *alpha*-pinene at 5 min is greater than *n*-hexane, but smaller than all other solvents. As given in the **Table 2.13** an average of $84.31 \pm 0.72\%$ of the total extractable mass of soybean oil is recovered in first five minutes. This is relatively high compared to that of the reference solvent *n*-hexane. As the extraction progressed, the rate of extraction becomes smaller, indicated by a flattening of the recovery curve. After 15 min, the rate of extraction tailed off. This agrees with the prediction of hot-ball model. The maximum recovery of oil using *alpha*-pinene is $92.96 \pm 2.93\%$ that is observed at 30 min. This is smaller than observed for most of the other green solvents at 30 min.

The predicted relative solubility of triglycerides in *alpha*-pinene at 100 °C is high around 100%. (**Table 2.8**). This is reflected in the higher percent recovery at the beginning of the extraction, where solubility plays major role. Like the previous two solvents the diffusion region of percent recovery graph start from 15 min where a slow exponential decay of extraction rate was observed. Viscosity of solvent should be the controlling factor in this region. A quantitative approach with respect to hot-ball model is discussed below to analyze this region.

Table 2.13 Results of accelerated solvent extraction (ASE) of soybean oil using *alpha*-pinene as solvent (particle size is 513 μm , temperature is 100 $^{\circ}\text{C}$).

Extraction time (min)	Average mass of oil extracted per gram of soybean sample (g)	Percent of oil extracted per gram of soybean sample (%)	Percent Recovery (where $m_o = 0.2347$ g) (%)	Standard deviation for % recovery (n=3) (%)
0	0	0	0	0
5	0.1979	19.79	84.31	0.72
10	0.2147	21.47	91.46	0.33
15	0.2176	21.76	92.70	0.63
20	0.2180	21.80	92.88	0.08
30	0.2182	21.82	92.96	2.93

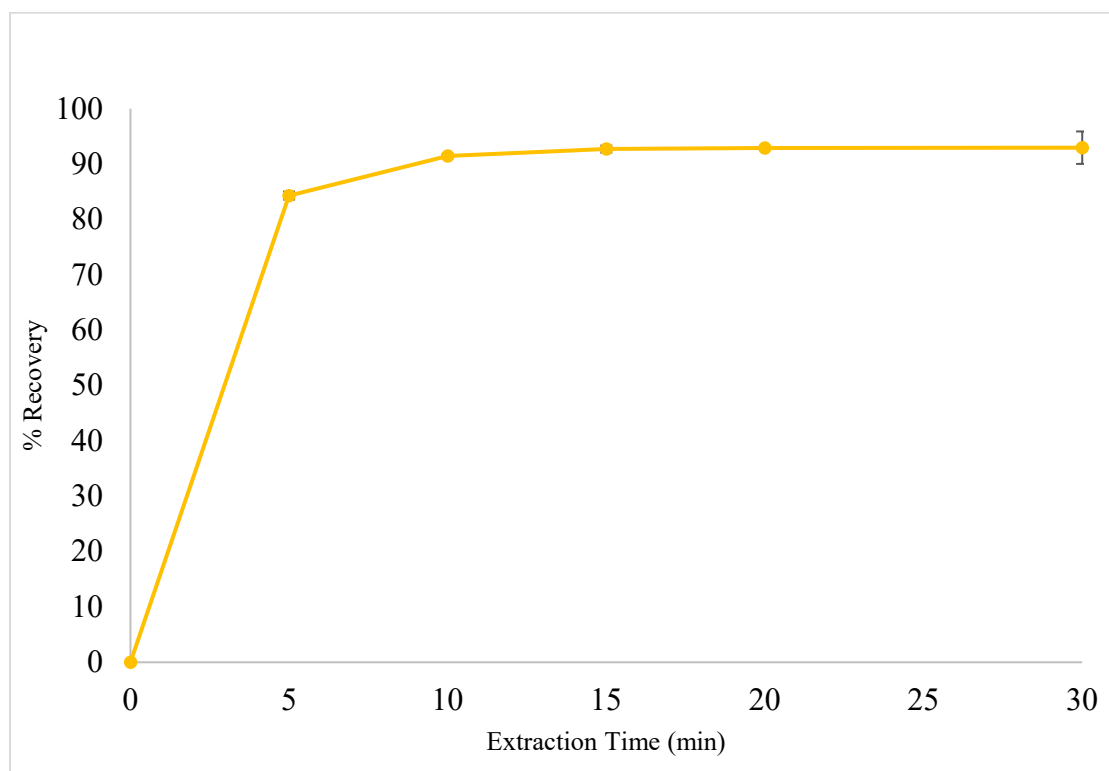


Figure 2.28 Percent of oil recovered out of total extractable oil in soybean sample using *alpha*-pinene at different extraction times.

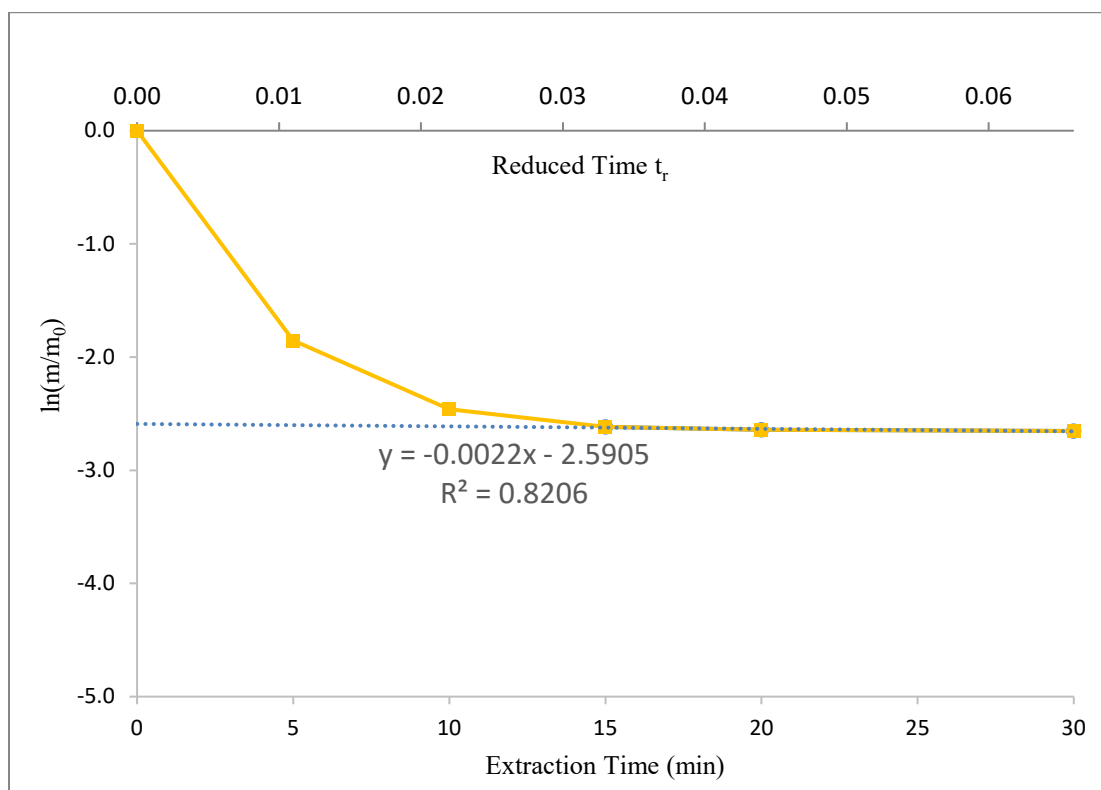
(b) Calculation of diffusion coefficient using hot-ball model

Qualitatively the appearance of experimental kinetic plot of extraction of soybean oil for *alpha*-pinene fits with the hot-ball model. The extraction kinetics is plotted using the natural logarithm of ratio of mass of unextracted oil to the original mass of extractable oil, $\ln(m/m_o)$ versus extraction time, as shown in **Figure 2.29**. The extraction time (horizontal axis on the bottom) is quantitatively scaled to the reduced time (horizontal axis on the top) in the graph, as previously explained for *n*-hexane and 2-MeTHF. The values are given in the following Table 2.15. The actual extraction time at $t_r = 1$, for *alpha*-pinene is calculated to be 455 min. The curve initially falls infinitely steeply like any other solvents, and this represents the loss of majority of extractable material from the particle ($92.70 \pm 0.63\%$) within 15 min. But after the extraction time of 15 min, which corresponds to the t_r of around 0.033, the rate of fall drops off and the curve become almost linear similar to what is seen for *n*-hexane and 2-MeTHF.

The linear regression of the trend line is 0.8206, the slope is -0.0022, and the intercept on $t = 0$ axis is at the value of $\ln(m/m_o) = -2.5905$. From this data, the diffusion coefficient of *alpha*-pinene is calculated to be $2.4 \times 10^{-9} \text{ cm}^2\text{s}^{-1}$. This is significantly low compared to *n*-hexane and other green solvents. The actual time required to recover 99% of the oil is calculated to be 920 min. Compared to other solvents this decreased diffusion coefficient and the extended extraction time for *alpha*-pinene are related to the higher viscosity of the pressurized liquid *alpha*-pinene solvent at 100 °C. The identity of soybean oil extracted in ASE using *alpha*-pinene is confirmed by IR spectroscopy and GC-MS chromatography in **Figure 2.30** and **Figure 2.31**.

Table 2.14 Hot-ball model results for the ASE extraction of soybean oil using α -pinene.

Extraction time (min)	Average mass of analyte oil extracted per gram of soybean sample (g)	Average mass (m) of analyte unextracted per gram of soybean sample (if $m_0 = 0.2347$ g) (g)	m/m_0	$\ln(m/m_0)$	Reduced time t_r
0	0	0.2347	1.0000	0	0
5	0.1979	0.0368	0.1569	-1.8519	0.011
10	0.2147	0.0200	0.0854	-2.4609	0.022
15	0.2176	0.0171	0.0730	-2.6173	0.033
20	0.2180	0.0167	0.0712	-2.6429	0.044
30	0.2182	0.0165	0.0704	-2.6529	0.066

**Figure 2.29** Plot of $\ln(m/m_0)$ vs. extraction time for α -pinene scaled to the reduced time (t_r) to compare with the hot-ball model.

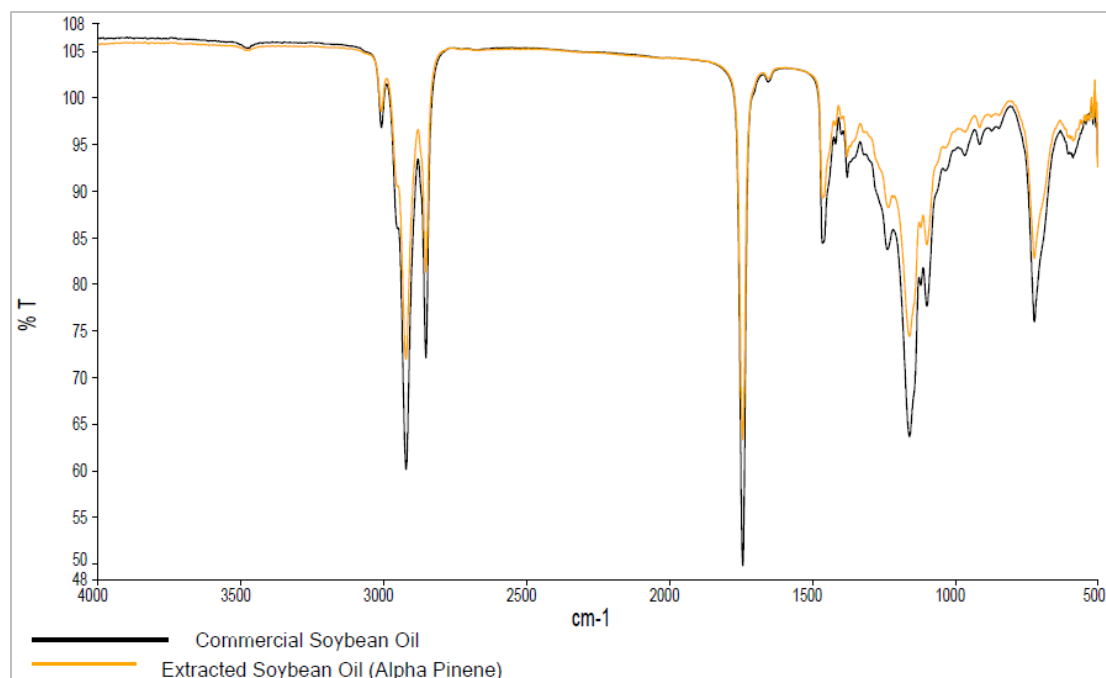


Figure 2.30 Comparison of IR spectra of commercial soybean oil and soybean oil extracted in ASE using *alpha*-pinene.

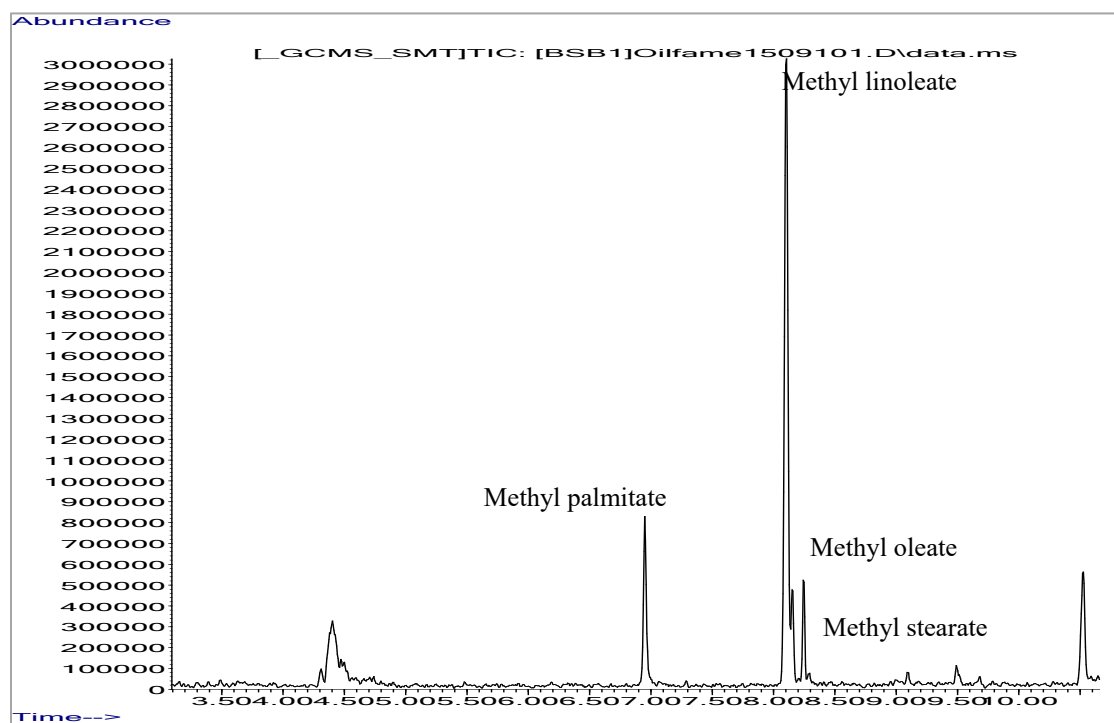


Figure 2.31 Gas chromatogram shows the presence of fatty acid methyl ester derivatives from soybean oil extracted in ASE using the green solvent *alpha*-pinene.

2.3.11 CPME Extraction and Hot-ball Model Results

(a) Qualitative comparison to the hot-ball model

The percent recovery of soybean oil using CPME is plotted against extraction time in **Figure 2.32**. A fast-initial rate of extraction as predicted by hot-ball model is observed for CPME, as a steep rise in percent recovery between 0 – 15 min. The percent recovery for CPME at 5 min is greater than previous solvents. As given in **Table 2.13** an average of $93.59 \pm 1.30\%$ of the total extractable mass of soybean oil is recovered in first five minutes. This is relatively high compared to that of the reference solvent *n*-hexane and all other green solvents. As the extraction progresses, the rate of extraction becomes smaller, indicated by a flattening of the recovery curve. After 15 min, the rate of extraction tailed off. This agrees with the prediction of the hot-ball model. The maximum recovery of oil using CPME is $99.02 \pm 0.16\%$ that is observed at 30 min. This is the highest of all solvents tested in this study and considered for the calculation of 100% extractable mass.

The predicted relative solubility of triglycerides in CPME at 100 °C is high (**Table 2.8**). This is reflected in the higher percent recovery at the beginning of the extraction, where solubility plays major role. Like the previous solvents the diffusion region of percent recovery graph start from 15 min where a slow exponential decay of extraction rate was observed. Viscosity of solvent should be the controlling factor in this region. A quantitative approach with respect to hot-ball model is discussed below to analyze this region.

Table 2.15 Results of accelerated solvent extraction (ASE) of soybean oil using CPME as solvent (particle size is 513 μm , temperature is 100 $^{\circ}\text{C}$).

Extraction time (min)	Average mass of oil extracted per gram of soybean sample (g)	Percent of oil extracted per gram of soybean sample (%)	Percent Recovery (where $m_o = 0.2347$ g) (%)	Standard deviation for % recovery (n=3) (%)
0	0	0	0	0.00
5	0.2197	21.97	93.59	1.30
10	0.2269	22.69	96.68	1.77
15	0.2301	23.01	98.03	0.05
20	0.2313	23.13	98.54	0.05
30	0.2324	23.24	99.00	0.16

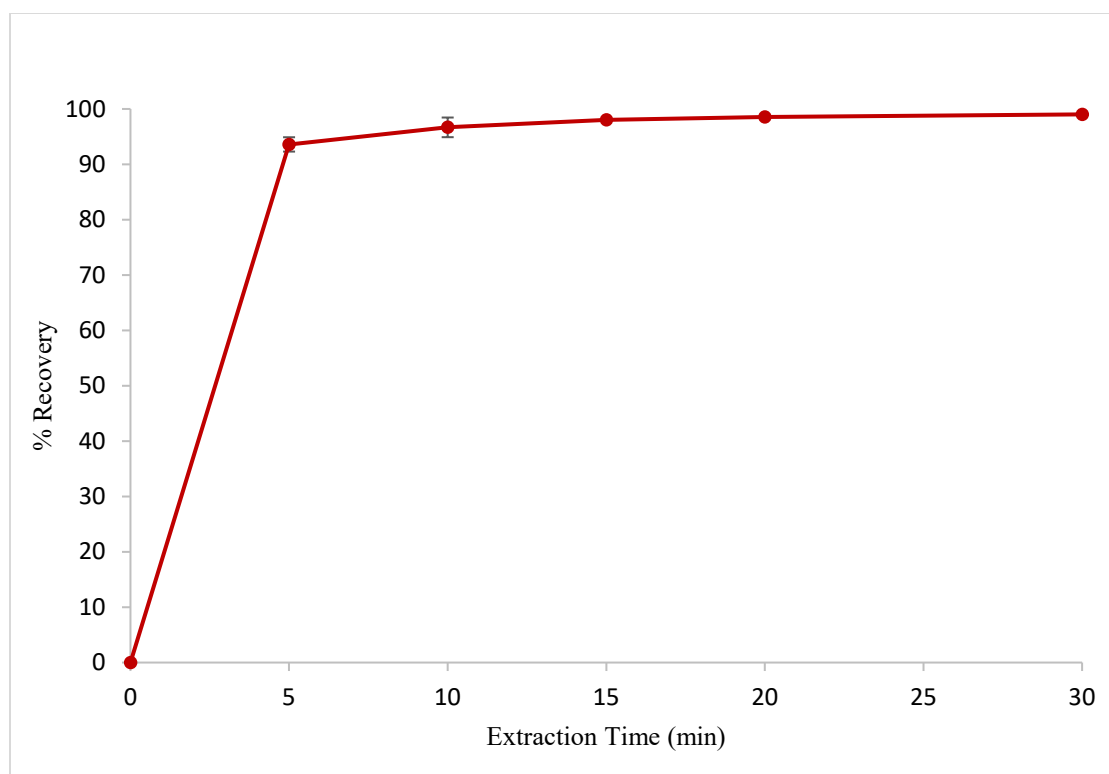


Figure 2.32 Percent of oil recovered out of total extractable oil in soybean sample using CPME at different extraction times.

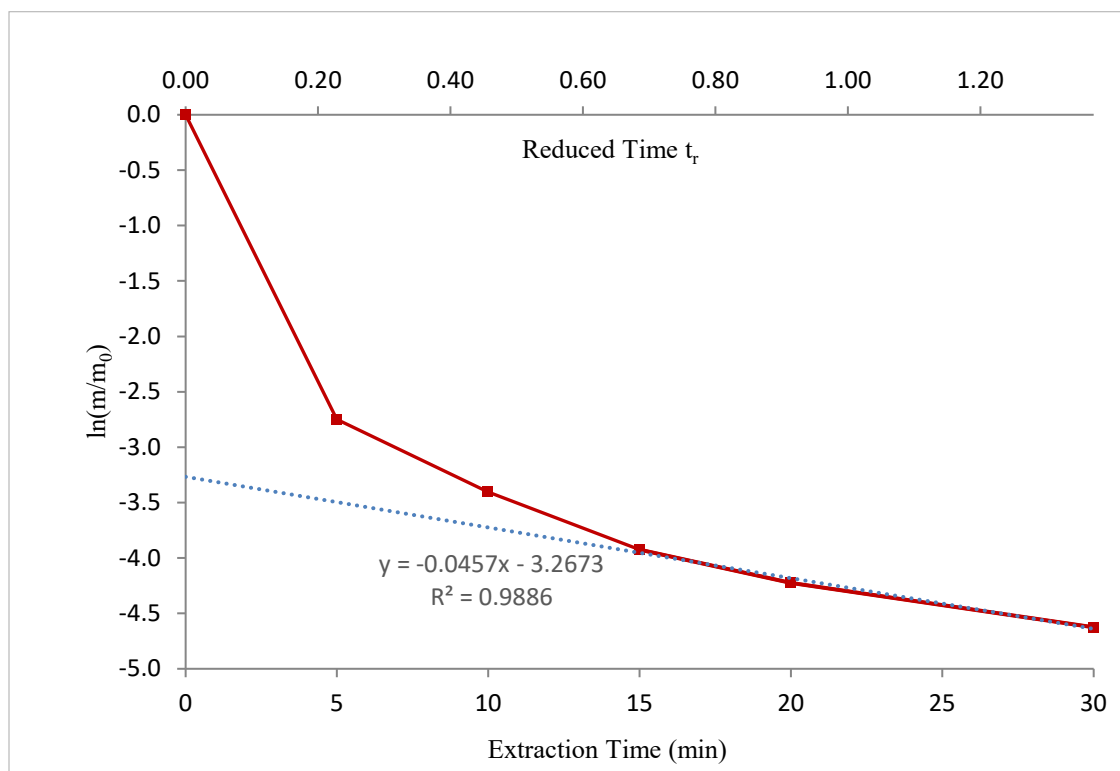
(b) Calculation of diffusion coefficient using hot-ball model

The appearance of the experimental kinetic plot of extraction of soybean oil using CPME fits with the hot-ball model. The extraction kinetics is plotted, $\ln(m/m_o)$, versus extraction time, as shown in **Figure 2.33**. The extraction time (horizontal axis on the bottom) is quantitatively scaled to the reduced time (horizontal axis on the top) in the graph. The values are given in the **Figure 2.33**. The actual extraction time at $t_r = 1$, for CPME is calculated to be 22 min, which is the smallest of all solvents. The curve initially falls infinitely steeply like any other solvents, and this represents the loss of majority of extractable material from the particle ($98.03 \pm 0.05\%$) within 15 min. But after 15 min, which corresponds to the t_r of around 0.686, the rate of fall drops off and the curve become almost linear similar to what is seen for other solvents.

The linear regression of the trend line is 0.9886, the slope is -0.0457, and the intercept on $t = 0$ axis is at the value of $\ln(m/m_o) = -3.2673$. From this data, the diffusion coefficient of CPME is calculated to be $5.1 \times 10^{-8} \text{ cm}^2\text{s}^{-1}$. This is the highest value compared all other solvents tested. The actual time required to recover 99% of the oil is calculated to be 30 min. The highest diffusion coefficient and the shortest extraction time for CPME are related to the low viscosity of the pressurized liquid CPME solvent at 100 °C. The identity of soybean oil extracted in ASE using CPME is confirmed by IR spectroscopy. **Figure 2.34** shows that the IR peaks for C=O, sp^3 C-H, sp^2 C-H, C=C, and C-O stretching frequencies of triglycerides in extracted soybean oil perfectly match with the IR peaks of commercial soybean oil. GC-MS chromatogram (**Figure 2.35**) also shows the presence of four major fatty acid methyl ester with a relative abundance that matches with the theoretical ratio of the four fatty acids soybean sample.

Table 2.16 Hot-ball model results for the ASE extraction of soybean oil using CPME

Extraction time (min)	Average mass of analyte oil extracted per gram of soybean sample (g)	Average mass (m) of analyte unextracted per gram of soybean sample (if $m_0 = 0.2347$ g) (g)	m/m_0	$\ln(m/m_0)$	Reduced time t_r
0	0	0.2347	1.0000	0	0
5	0.2197	0.0150	0.0641	-2.7480	0.229
10	0.2269	0.0078	0.0332	-3.4042	0.457
15	0.2301	0.0046	0.0197	-3.9250	0.686
20	0.2313	0.0034	0.0146	-4.2248	0.914
30	0.2324	0.0023	0.0098	-4.6254	1.371

**Figure 2.33** Plot of $\ln(m/m_0)$ vs. extraction time for CPME solvent was scaled to the reduced time (t_r) to compare with the hot-ball model.

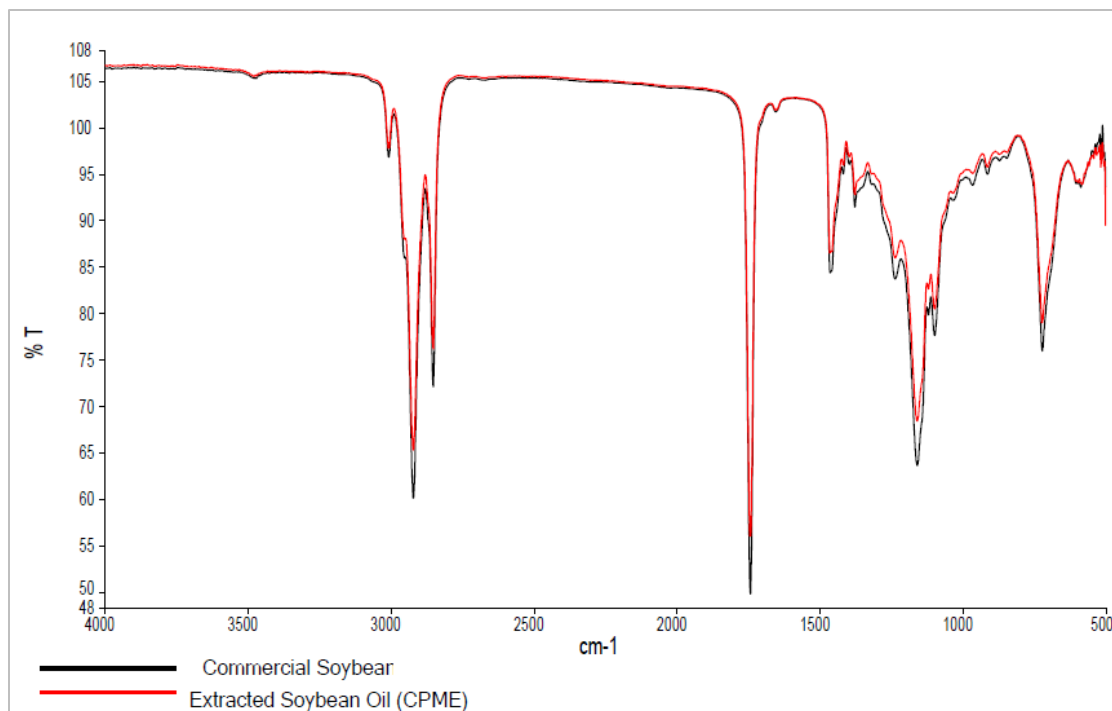


Figure 2.34 Comparison of IR spectra of commercial soybean oil and soybean oil extracted in ASE using CPME solvent

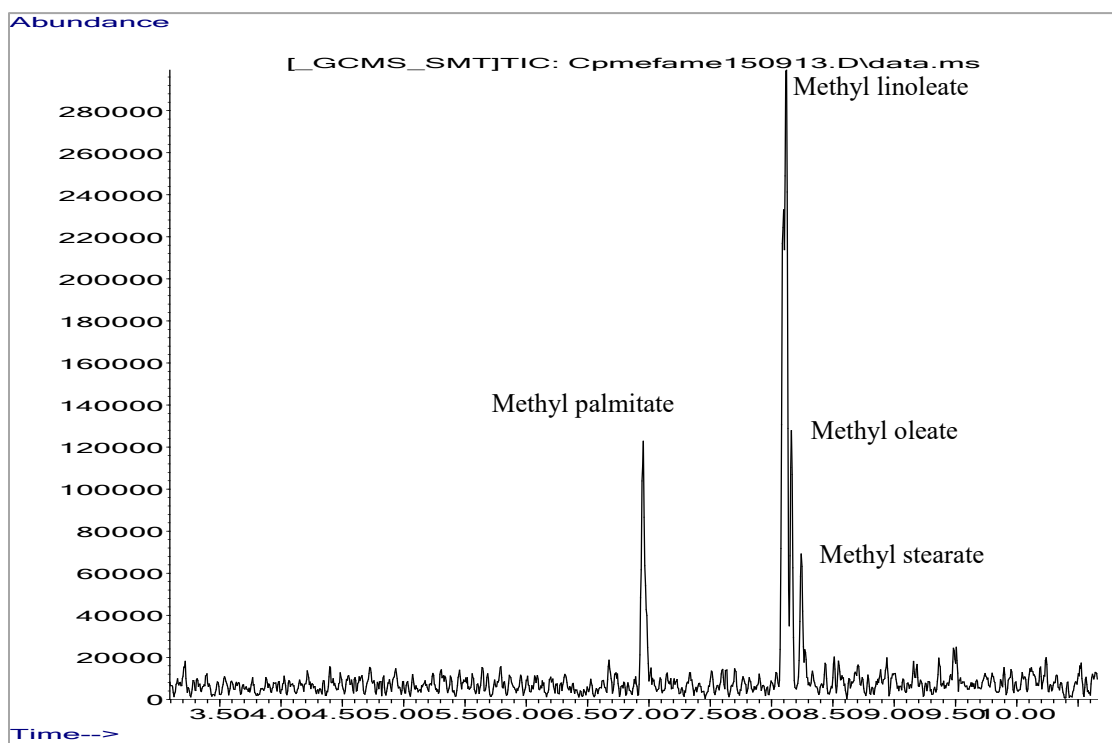


Figure 2.35 Gas chromatogram shows the presence of fatty acid methyl ester derivatives from soybean oil extracted in ASE using the green solvent CPME.

2.3.12 Ethyl Lactate Extraction and Hot-ball Model Results

(a) Qualitative comparison to the hot-ball model

The percent recovery of soybean oil using ethyl lactate is plotted against extraction time in **Figure 2.36**. A fast-initial rate of extraction was seen as predicted by hot-ball model. In the graph it appears as a steep rise in percent recovery between 0 – 5 min. As given in the **Table 2.17** an average of $94.36 \pm 0.13\%$ of the total extractable mass of soybean oil is recovered in five minutes. This is relatively high compared to that of the reference solvent *n*-hexane and other green solvents. As the extraction progressed, the rate of extraction becomes smaller, indicated by a flattening of the recovery curve. After 15 min, the rate of extraction turns out to not change much. This agrees with the prediction of the hot-ball model. The maximum recovery of oil using ethyl lactate is $96.09 \pm 0.29\%$, that is observed at 30 min.

The initial steep rise in rate of extraction can be related to the predicted solubility of the triglycerides of soybean oil in ethyl lactate at 100 °C (**Table 2.8**). The diffusion region of the recovery graph starts from 15 min where a very slow exponential decay of extraction rate was observed. A high viscosity of ethyl lactate should be the controlling factor in this region. A quantitative approach with respect to hot-ball model is discussed below to analyze this region.

(b) Calculation of diffusion coefficient using hot-ball model

Qualitatively the appearance of the experimental kinetic plot of extraction of soybean oil for ethyl lactate fits with the hot-ball model. The extraction kinetics is plotted using the natural logarithm of ratio of mass of unextracted oil to the original mass of extractable oil, $\ln(m/m_o)$, versus extraction time, as shown in **Figure 2.37**.

Table 2.17 Results of accelerated solvent extraction (ASE) of soybean oil using ethyl lactate as solvent (particle size is 513 μm , temperature is 100 $^{\circ}\text{C}$).

Extraction time (min)	Average mass of oil extracted per gram of soybean sample (g)	Percent of oil extracted per gram of soybean sample (%)	Percent Recovery (where $m_o = 0.2347$ g) (%)	Standard deviation for % recovery (n=3) (%)
0	0	0	0	0.00
5	0.2215	22.15	94.36	0.13
10	0.2241	22.41	95.48	0.16
15	0.2251	22.51	95.91	0.18
20	0.2251	22.51	95.91	0.33
30	0.2255	22.55	96.09	0.29

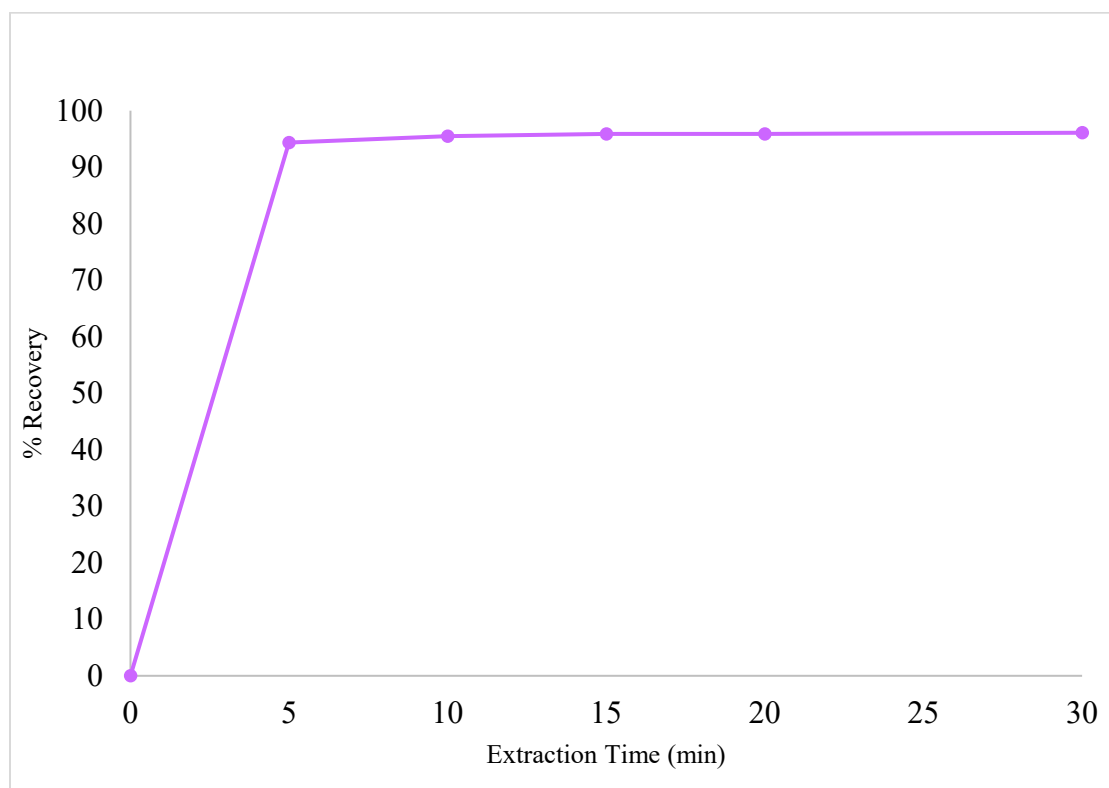


Figure 2.36 Percent of oil recovered out of total extractable oil in soybean sample using ethyl lactate at different extraction times.

The extraction time is quantitatively scaled to the reduced time in the graph and the values are given in the **Table 2.18**. The actual extraction time at $t_r = 1$ for ethyl lactate is calculated to be 303 min. The curve initially falls infinitely steeply like any other solvents, and this represents the loss of majority of extractable material from the particle ($95.91 \pm 0.18\%$) within 15 min. But after the extraction time of 15 min, which corresponds to the t_r of around 0.050, the rate of fall drops off and the curve become almost linear.

The linear regression of the trend line is 0.8929, the slope is -0.0033, and the intercept on $t = 0$ axis is at the value of $\ln(m/m_o) = -3.1405$. From this data, the diffusion coefficient of ethyl lactate is calculated to be $3.7 \times 10^{-9} \text{ cm}^2\text{s}^{-1}$. This is higher compared *n*-hexane, and *alpha*-pinene, but lower than CPME, 2-MeTHF, and TBME. The actual time required to recover 99% of the oil is calculated to be 447 min. The lower diffusion coefficient and the extended extraction time for ethyl lactate are related to the highest viscosity of the pressurized liquid ethyl lactate solvent at 100 °C. The identity of soybean oil extracted in ASE using ethyl lactate is confirmed by IR spectroscopy. **Figure 2.38** shows that the IR peaks for C=O, $\text{sp}^3\text{C-H}$, $\text{sp}^2\text{C-H}$, C=C, and C-O stretching frequencies of triglycerides in extracted soybean oil match with the IR peaks of commercial soybean oil. The GC-MS chromatogram, **Figure 2.39**, shows the presence of the four major fatty acid methyl esters in the extracted soybean sample. Interestingly, the relative abundance of methyl oleate, methyl palmitate and methyl stearate, with respect to methyl linoleate were lower than what was seen for other solvents. This agrees with the lower predicted solubility of oleic acid (49.8%), palmitic acid (31.1%), and stearic acid (22.3%) in ethyl lactate, compared to their solubility in other solvents (100%).

Table 2.18 Hot-ball model results for the ASE extraction of soybean oil using ethyl lactate

Extraction time (min)	Average mass of analyte oil extracted per gram of soybean sample (g)	Average mass (m) of analyte unextracted per gram of soybean sample (if $m_0 = 0.2347$ g) (g)	m/m_0	$\ln(m/m_0)$	Reduced time t_r
0	0	0.2347	1.0000	0	0
5	0.2215	0.0132	0.0564	-2.8756	0.017
10	0.2241	0.0106	0.0452	-3.0975	0.033
15	0.2251	0.0096	0.0409	-3.1965	0.050
20	0.2251	0.0096	0.0409	-3.1965	0.066
30	0.2255	0.0092	0.0391	-3.2427	0.099

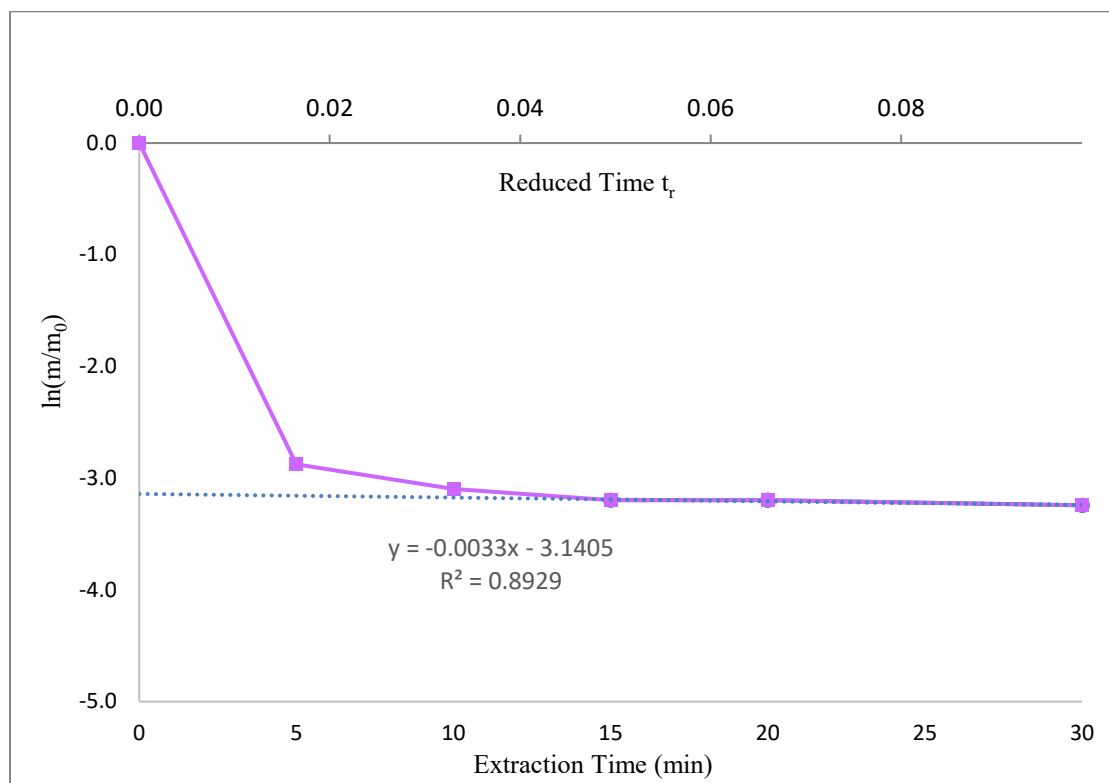


Figure 2.37 Plot of $\ln(m/m_0)$ vs. extraction time for ethyl lactate was scaled to the reduced time (t_r) to compare with the hot-ball model.

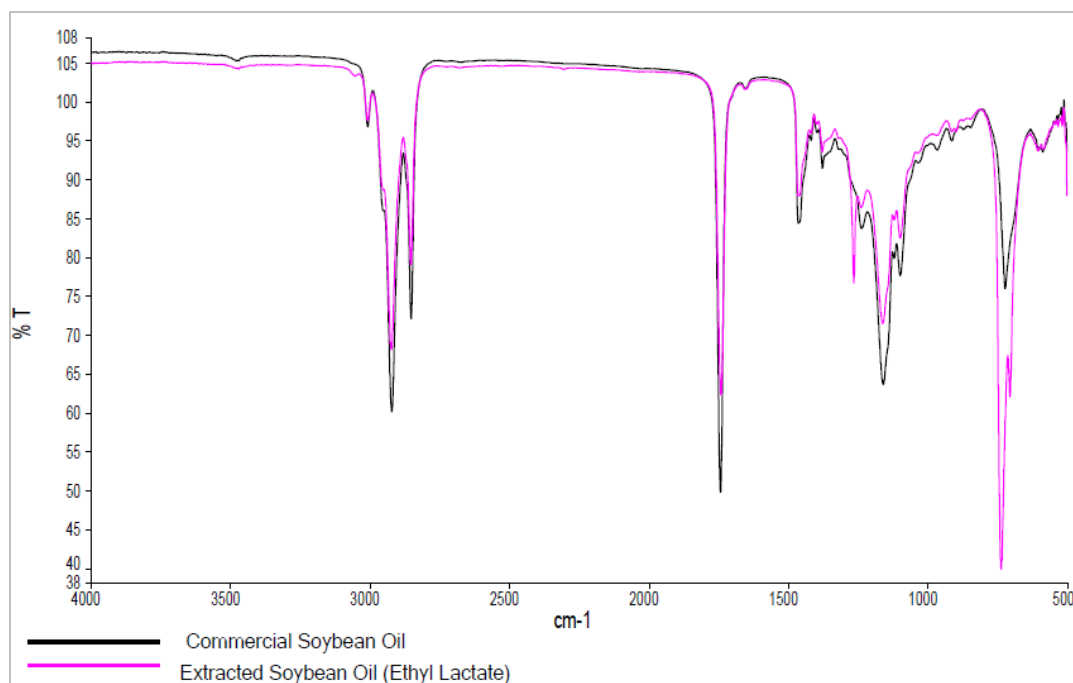


Figure 2.38 Comparison of IR spectra of commercial soybean oil and soybean oil extracted in ASE using ethyl lactate.

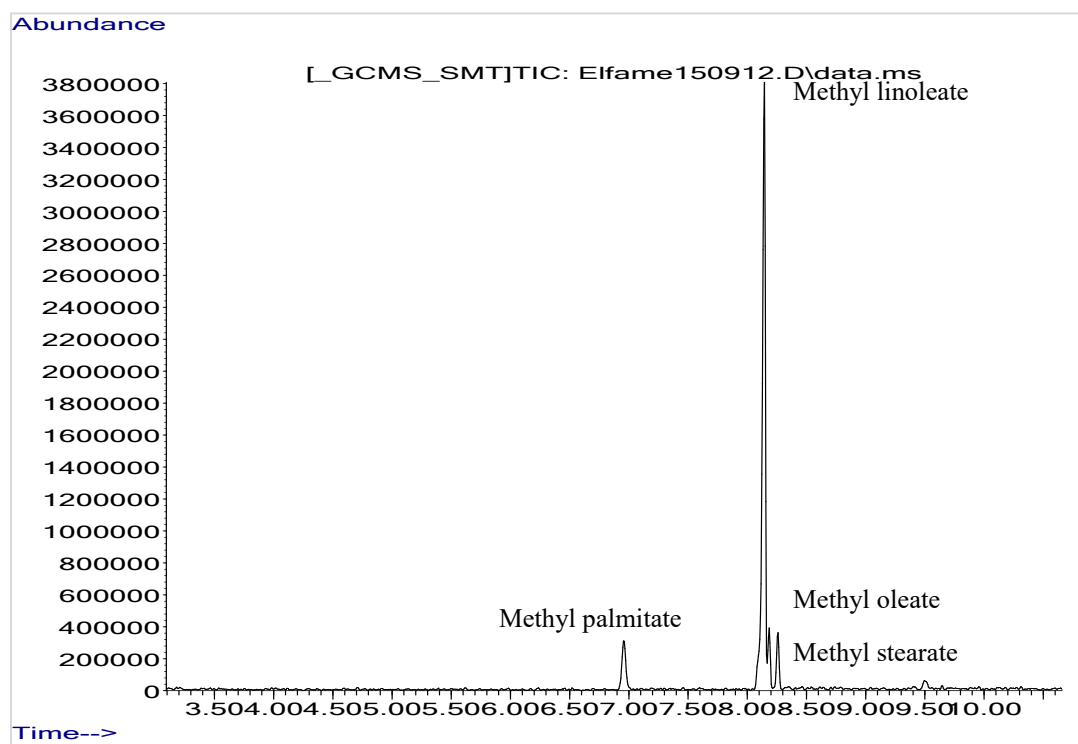


Figure 2.39 Gas chromatogram shows the presence of fatty acid methyl ester derivatives from soybean oil extracted in ASE using the green solvent ethyl lactate.

2.3.13 TBME Extraction and Hot-ball Model Results

(a) *Qualitative comparison to the hot-ball model*

The percent recovery of soybean oil using TBME is plotted against extraction time in **Figure 2.40**. A fast-initial rate of extraction was seen as predicted by the hot-ball model. In the graph it appears as a steep rise in percent recovery between 0 – 10 min. As given in the **Table 2.19** an average of $85.09 \pm 1.21\%$ of the total extractable mass of soybean oil is recovered in five minutes. This is relatively high compared to that of the reference solvent *n*-hexane and *alpha*-pinene, but lower than CPME, 2-MeTHF, and ethyl lactate. As the extraction progressed, the rate of extraction becomes smaller, indicated by a flattening of the recovery curve. After 15 min, the rate of extraction becomes to not change much. This agrees with the prediction of the hot-ball model. The maximum recovery of oil using TBME is $92.87 \pm 0.12\%$, which is observed at 30 min.

The initial steep rise in rate of extraction can be related to the predicted solubility of 100% for the triglycerides of soybean oil in TBME at 100 °C (**Table 2.8**). The diffusion region of recovery graph starts from 15 min where a very slow exponential decay of the extraction rate was observed. A low viscosity of TBME should be the controlling factor in this region. A quantitative approach with respect to the hot-ball model is discussed below to analyze this region.

Table 2.19 Results of accelerated solvent extraction (ASE) of soybean oil using TBME as solvent (particle size is 513 μm , temperature is 100 $^{\circ}\text{C}$).

Extraction time (min)	Average mass of oil extracted per gram of soybean sample (g)	Percent of oil extracted per gram of soybean sample (%)	Percent Recovery (where $m_o = 0.2347$ g) (%)	Standard deviation for % recovery (n=3) (%)
0	0	0	0	0.00
5	0.1997	19.97	85.09	1.21
10	0.2118	21.18	90.26	1.25
15	0.2153	21.53	91.75	0.56
20	0.2169	21.69	92.42	0.05
30	0.2180	21.80	92.87	0.12

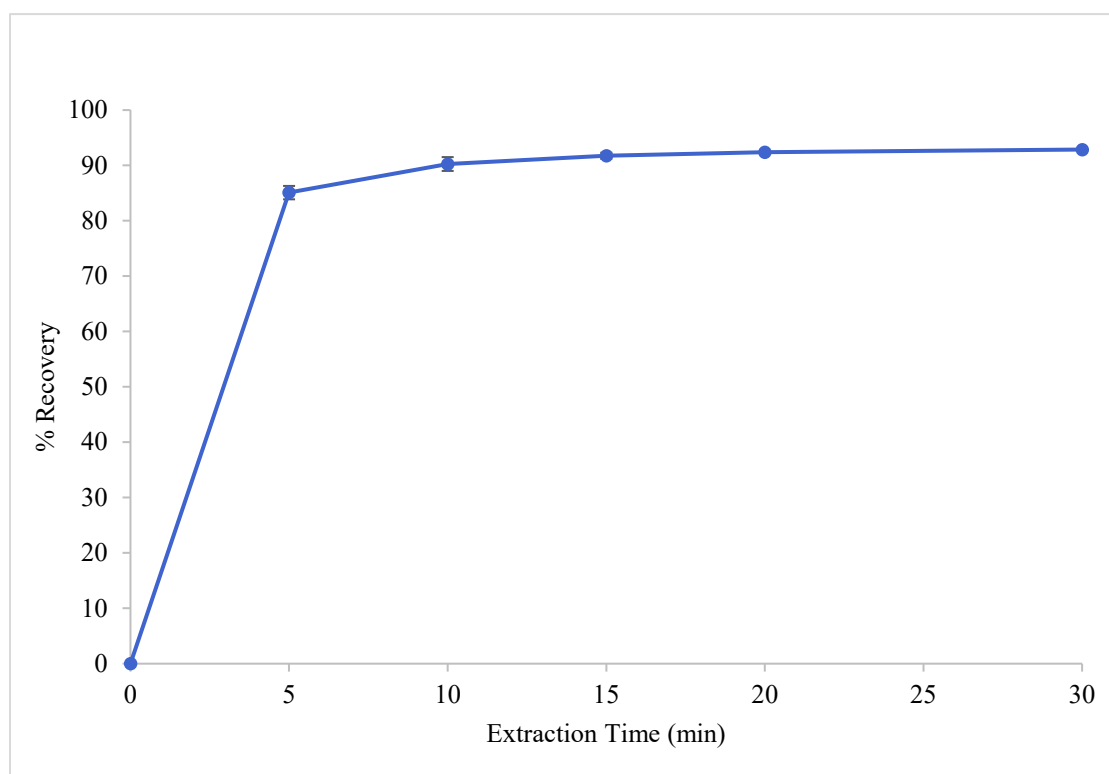


Figure 2.40 Percent of oil recovered out of total extractable oil in soybean sample using TBME at different extraction times.

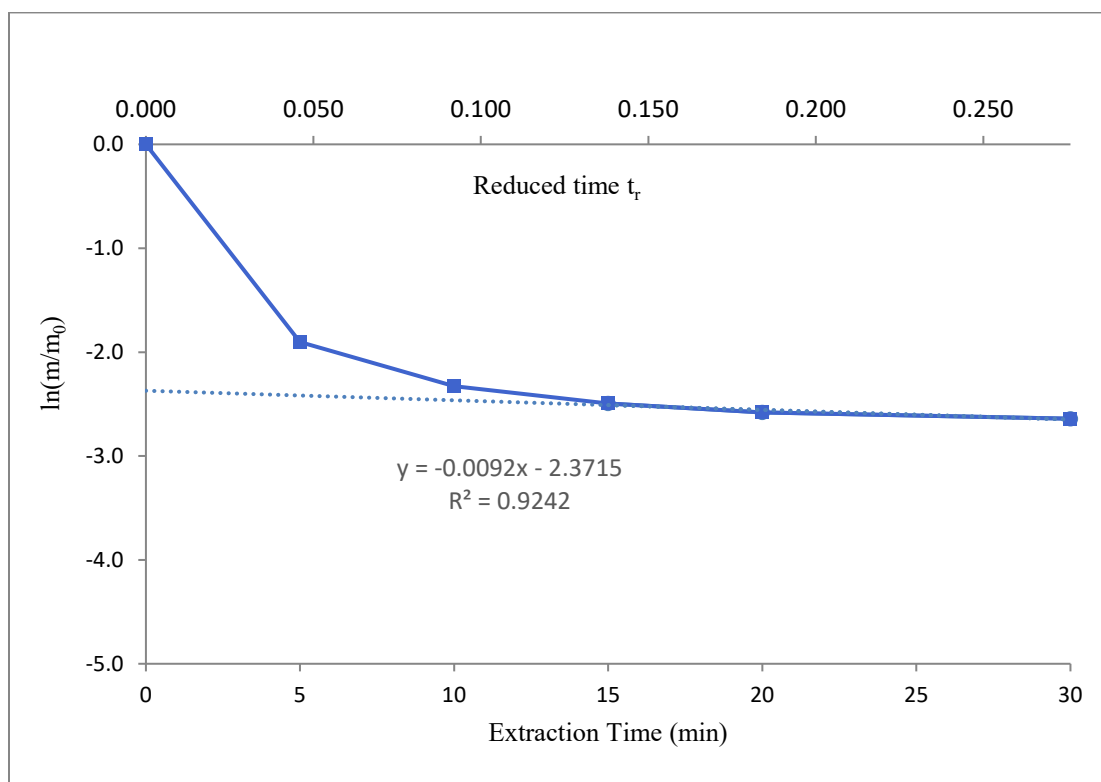
(b) Calculation of diffusion coefficient using hot-ball model

Qualitatively the appearance of the experimental kinetic plot of extraction for TBME fits with the hot-ball model. The extraction kinetics is plotted using the natural logarithm of ratio of mass of unextracted oil to the original mass of extractable oil, $\ln(m/m_o)$, versus extraction time, as shown in **Figure 2.41**. The extraction time is quantitatively scaled to the reduced time in the graph, as previously explained. The values are given in the **Table 2.20**. The actual extraction time at $t_r = 1$ for TBME is calculated to be 109 min. The curve initially falls infinitely steeply like other solvents, and this represents the loss of a majority of extractable material from the particle ($91.75 \pm 0.56\%$) within 15 min. But after 15 min, which corresponds to t_r of around 0.138, the rate drops off and the curve becomes almost linear.

The linear regression of the trend line is 0.9242, the slope is -0.0092, and the intercept is at the value of $\ln(m/m_o) = -2.3715$. From this data, the diffusion coefficient of TBME is calculated to be $1.0 \times 10^{-8} \text{ cm}^2\text{s}^{-1}$. This is higher compared with *n*-hexane, *alpha*-pinene, and ethyl lactate, but lower than CPME and 2-MeTHF. The actual time required to recover 99% of the oil is calculated to be 244 min. The identity of soybean oil extracted in ASE using TBME is confirmed by IR spectroscopy. **Figure 2.43** shows that the IR peaks for C=O, $\text{sp}^3\text{C-H}$, $\text{sp}^2\text{C-H}$, C=C, and C-O stretching frequencies of triglycerides in extracted soybean oil match with the IR peaks of commercial soybean oil. GC-MS chromatogram (**Figure 2.43**) also shows the presence of four major fatty acid methyl esters in the extracted oil with a relative abundance that matches with the theoretical relative ratio of the four fatty acids soybean sample.

Table 2.20 Hot-ball model results for the ASE extraction of soybean oil using TBME

Extraction time (min)	Average mass of analyte oil extracted per gram of soybean sample (g)	Average mass (m) of analyte unextracted per gram of soybean sample (if $m_0 = 0.2347$ g) (g)	m/m_0	$\ln(m/m_0)$	Reduced time t_r
0	0	0.2347	1.0000	0	0
5	0.1997	0.0350	0.1491	-1.9030	0.046
10	0.2118	0.0229	0.0974	-2.3286	0.092
15	0.2153	0.0194	0.0825	-2.4948	0.138
20	0.2169	0.0178	0.0758	-2.5791	0.184
30	0.2180	0.0167	0.0713	-2.6409	0.276

**Figure 2.41** Plot of $\ln(m/m_0)$ vs. extraction time for TBME solvent was scaled to the reduced time (t_r) to compare with the hot-ball model.

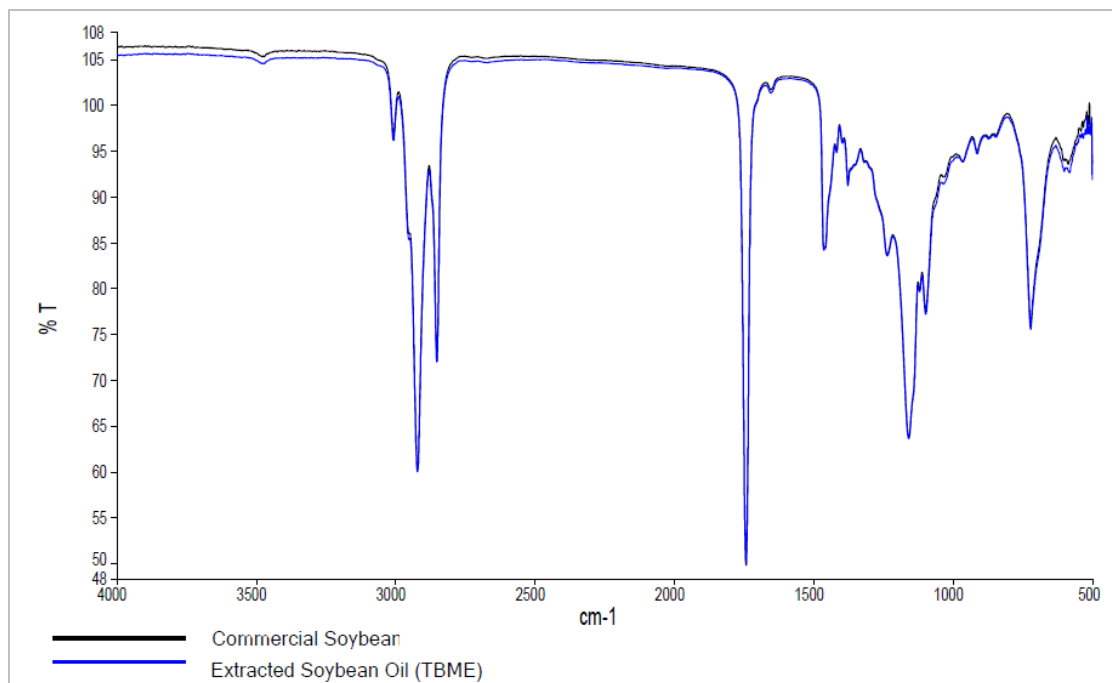


Figure 2.42 Comparison of IR spectra of commercial soybean oil and soybean oil extracted in ASE using TBME solvent.

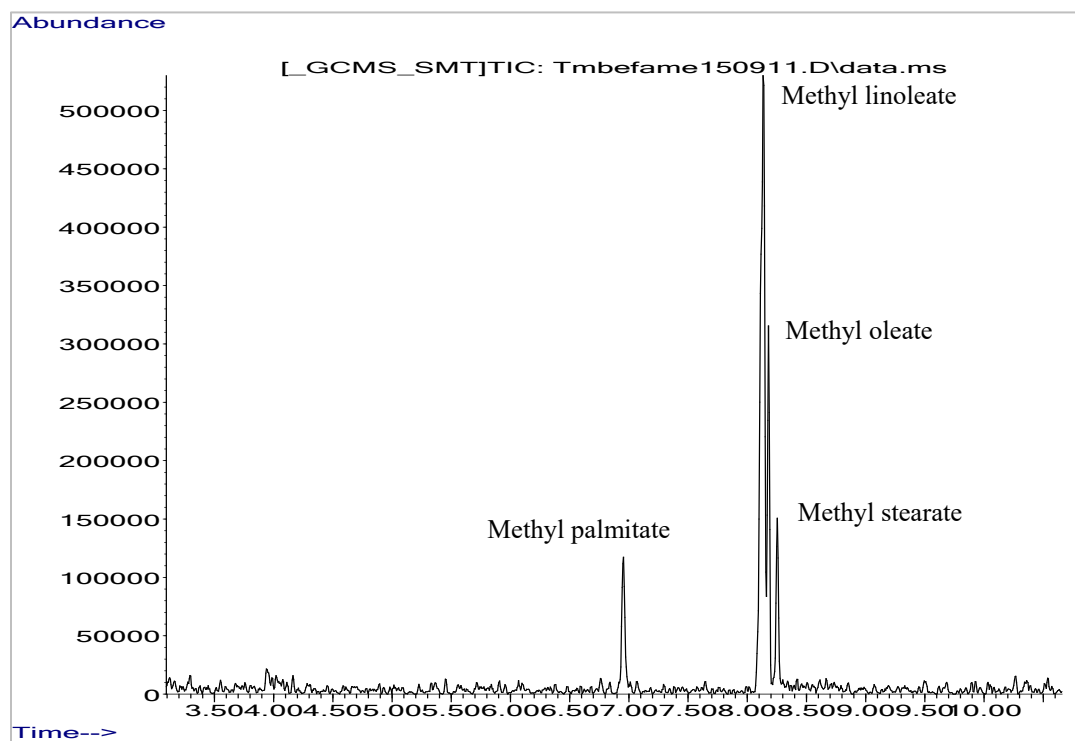


Figure 2.43 Gas chromatogram shows the presence of fatty acid methyl ester derivatives from soybean oil extracted in ASE using the green solvent TBME.

2.3.14 Comparison of Extraction Efficiency of Green Solvents

Typically, soybeans are made of 21% of oil, but this may vary based on geographical location, climate, and cultivation method. The comparison of extraction using green solvents should provide informative results, as there is no published literature found for a direct comparison of the diffusion and extraction efficiency using these solvents. Also, the application of the theoretical hot-ball model would offer a validation for the experimental data. As discussed in the previous sections, all of the experimental extraction results fit perfectly with the hot-ball model including the effect of non-spherical particle shape.

The highest extraction percentage quantified in this study is 23.24% by weight of the soybean sample. This is acquired from the 30 min ASE extraction using CPME solvent at 100 °C and 1500 psi. The operation condition was maintained constant for all solvent extractions. The percentage extractions values obtained from all solvents are compiled in **Table 2.21**. The chart shown in **Figure 2.44** compares the percent of oil extracted using different solvents at various times. The mass of the above highest extraction yield is considered as 99% recovery. Based on this, the maximum (100%) extractable mass is calculated to be 23.47%. The relative percent recoveries for all solvents at various times are compiled in **Table 2.22**, and the chart shown in **Figure 2.45** compared the percent recoveries for all solvent at various times.

Table 2.21 Comparison of percent of soybean oil extracted in ASE using different solvents at different times.

Percent of soybean oil extracted in ASE using different solvents (%)						
Extraction time (min)	0	5	10	15	20	30
Hexane	0	15.87	19.18	19.85	20.06	20.15
2-MeTHF	0	21.05	21.58	22.20	22.39	22.50
alpha-Pinene	0	19.79	21.47	21.76	21.80	21.82
CPME	0	21.97	22.69	23.01	23.13	23.24
Ethyl lactate	0	22.15	22.41	22.51	22.51	22.55
TBME	0	19.97	21.18	21.53	21.69	21.80

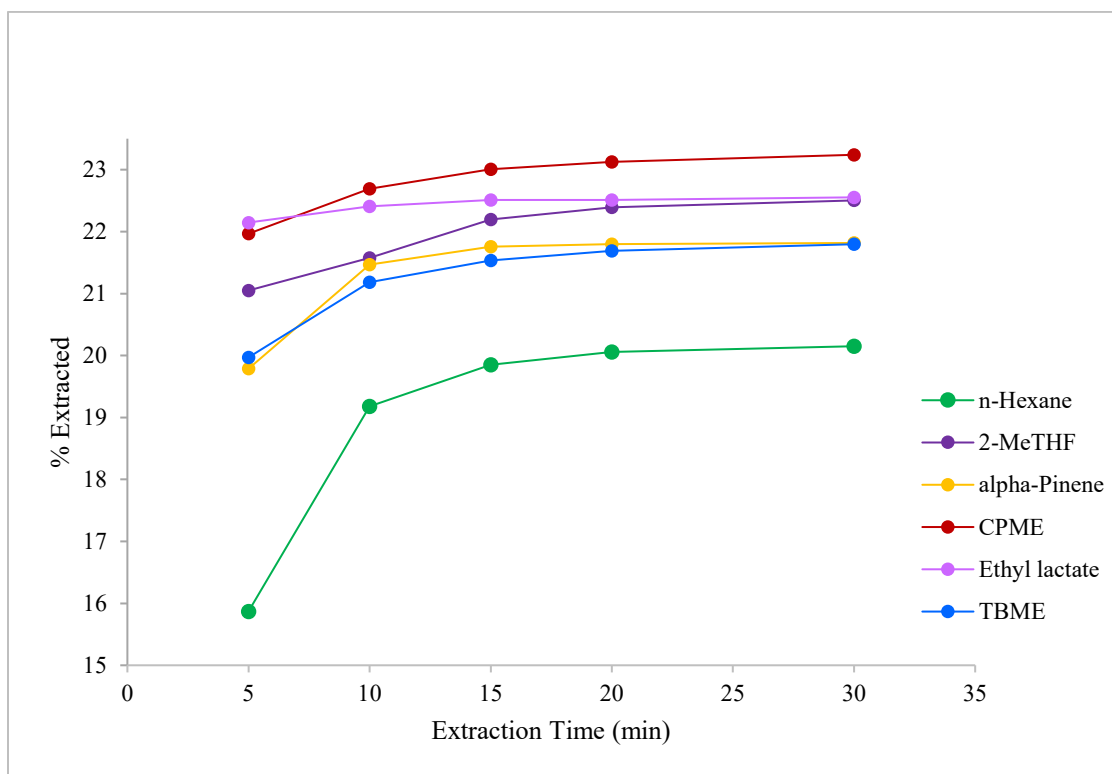


Figure 2.44 Percent of oil extracted from soybean using different solvents at different extraction times. As the y-axis is an extended % extraction, zero intercept is not shown.

Table 2.22 Comparison of percent of soybean oil recovered in ASE using different solvents at different times.

Percent of soybean oil recovered in ASE using different solvents (%)						
Extraction time (min)	0	5	10	15	20	30
Hexane	0	67.62	81.72	84.58	85.46	85.85
2-MeTHF	0	89.69	91.93	94.57	95.40	95.88
alpha-Pinene	0	84.31	91.46	92.70	92.88	92.96
CPME	0	93.59	96.68	98.03	98.54	99.00
Ethyl lactate	0	94.36	95.48	95.91	95.91	96.09
TBME	0	85.09	90.26	91.75	92.42	92.87

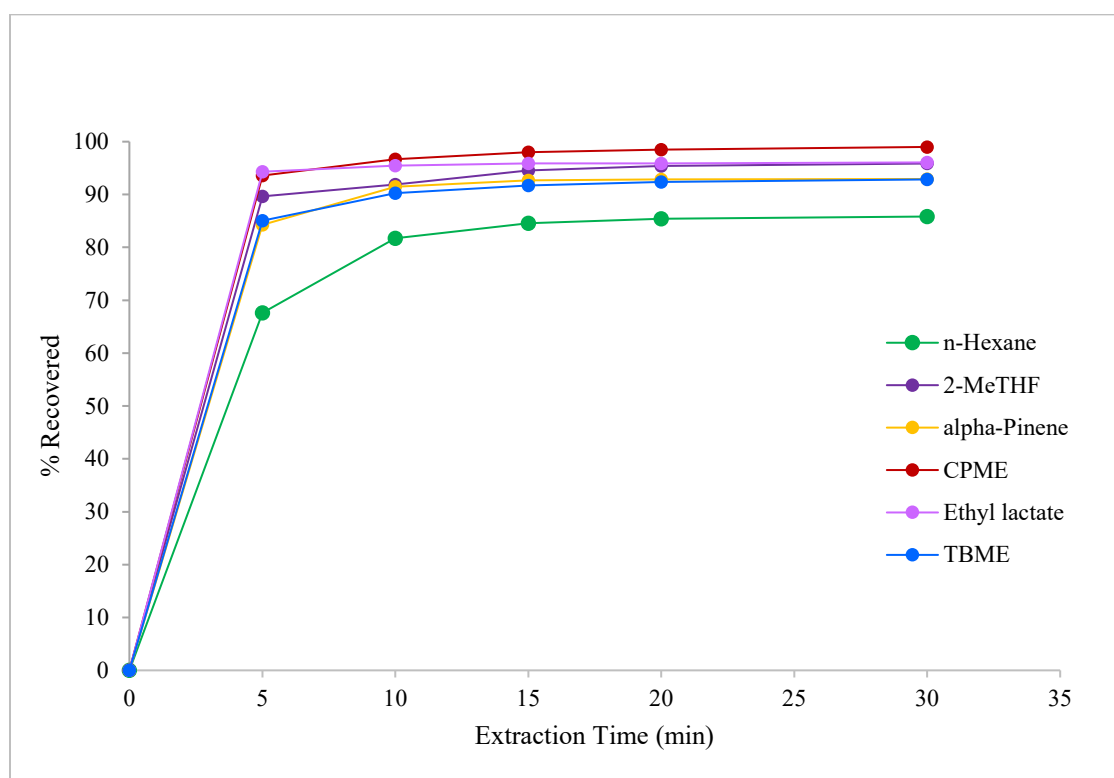


Figure 2.45 Percent of oil recovered from soybean using different solvents at different extraction times.

The $\ln(m/m_o)$ versus extraction time plot of all solvents are compared in a single chart given in **Figure 2.46**, and the linear regression values for the extrapolation of diffusion regions of solvent is compiled in **Table 2.23**. The fit for trend line for each of the solvents is good with linear regressions greater than 0.82, as shown in the table. Also, the $t = 0$ intercepts for all solvents are more negative than -0.5, the theoretical intercept proposed in the hot-ball model. The difference in intercept is expected since the 513- μm ground soybean particles are not spherical as indicated by the $t = 0$ intercept. This matches with the effect of non-spherical particle shape on the original hot-ball model.

For the irregular shaped soybean sample, the concentration of the oil at the beginning of extraction is transferred quickly due to the solubility. In general, for non-spherical particles the intercept on the $t = 0$ axis is greater negative than -0.5, as the surface-to-volume ratio is greater than that of spheres. This effect would be larger for more irregular particles. Also, since the soybean particles are irregular in shape, the initial part of the logarithmic plot is a more rapid curve, and extraction tail doesn't perfectly superimpose on hot-ball model. Therefore, it is expected that the time needed to recover 99% of oil, is a greater multiple of the time required to extract the first 50%, than the original hot-ball model.

The reference solvent *n*-hexane yields the lowest percent recovery of all solvents at any extraction times tested. The values listed in the **Table 2.21** indicates that the maximum oil recovered using *n*-hexane is $85.85 \pm 0.66\%$ at 30 min. This is in fact lower than the percent of oil recovered at 5 min for all other solvents. The justification for this poor performance of *n*-hexane should originate from the slow diffusion of oil into *n*-hexane. The diffusion coefficient of *n*-hexane is 10 time smaller than CPME. At 5 min *n*-

hexane can extract only $67.62 \pm 1.14\%$, and this slow start impacts the transition region and diffusion region of the extraction.

However if the diffusion region of the $\ln(m/m_o)$ versus extraction time plot of *n*-hexane is extrapolated, it gives a slope of -0.0053 and an intercept of $t = 0$ axis at -1.8026 (**Table 2.23**). The slope of *n*-hexane is steeper than that of *alpha*-pinene (-0.0022) and ethyl lactate (-0.0033). As this linear portion of first order kinetic line is steeper than that of *alpha*-pinene and ethyl lactate (**Figure 2.46**), *n*-hexane has a faster diffusion rate than the other two. The reason for this may arise from the viscosity of *n*-hexane, which is significantly lower than the viscosity of the *alpha*-pinene, and ethyl lactate. As a result, the diffusion coefficient of the two green solvents *alpha*-pinene ($2.4 \times 10^{-9} \text{ cm}^2\text{s}^{-1}$) and ethyl lactate ($3.7 \times 10^{-9} \text{ cm}^2\text{s}^{-1}$) for the solute is notably lower than the diffusion coefficient of *n*-hexane ($5.9 \times 10^{-9} \text{ cm}^2\text{s}^{-1}$).

Table 2.23 Linear regression analysis for the plot of $\ln(m/m_0)$ vs. extraction time for different solvents.

Solvent	$\ln(m/m_0)$ intercept at $t=0$	Slope	R^2
Hexane	-1.8020	-0.0053	0.8523
2-MeTHF	-2.6854	-0.0173	0.9113
Alpha Pinene	-2.5905	-0.0022	0.8206
CPME	-3.2673	-0.0457	0.9886
Ethyl Lactate	-3.1405	-0.0033	0.8929
TBME	-2.3715	-0.0092	0.9242

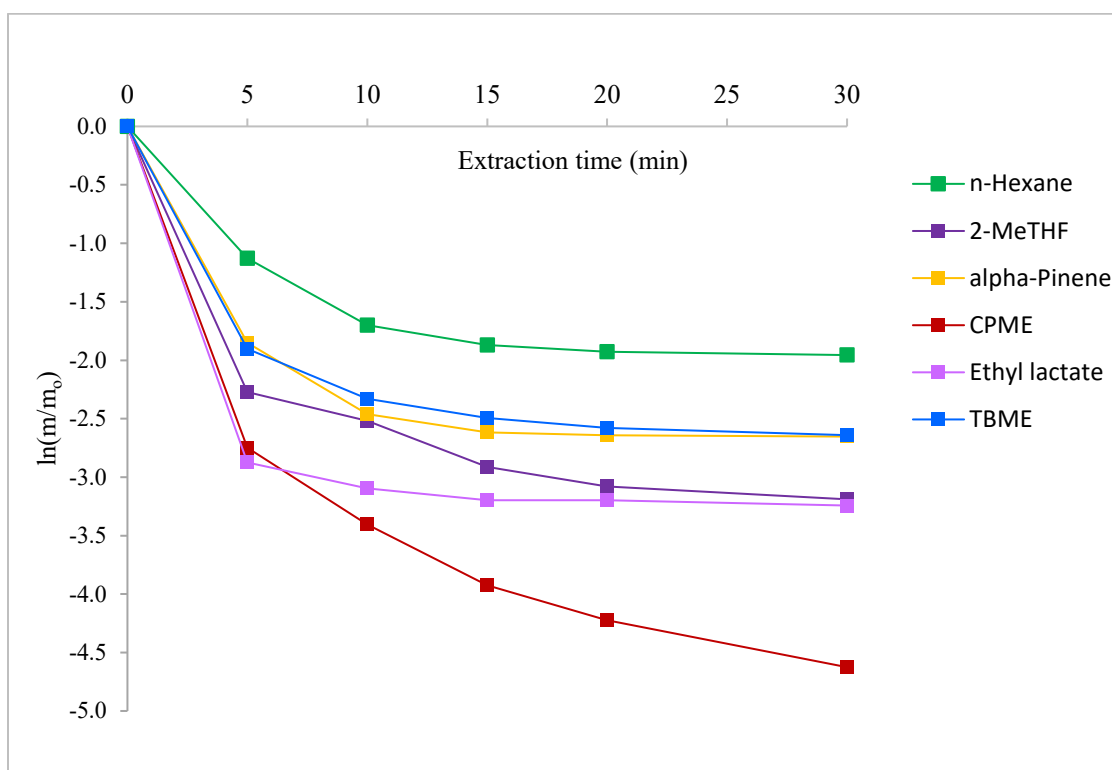


Figure 2.46 Comparison of $\ln(m/m_0)$ vs extraction time of different solvents

However, when it comes to the total time a solvent takes to recover the maximum (99%) solute, there are two effects, solubility and diffusion, that need to be considered. Given in the **Table 2.24**, the calculated time required for 99% soybean oil recovery is 531 min for *n*-hexane, which is significantly shorter than the 920 min for *alpha*-pinene. This longer extraction time can be justified by high viscosity of *alpha*-pinene. But for ethyl lactate, although the diffusion coefficient is smaller than *n*-hexane, the total time required for 99% recovery is 447 min, shorter than *n*-hexane.

Interestingly, the other three green solvents, CPME, 2-MeTHF, and TBME, are more efficient in extracting soybean oil. They all have higher rate of extraction in both the initial equilibrium region and in the final diffusion region. As given in the **Table 2.22**, the percent recovery at 5 min for CPME, 2-MeTHF, and TBME are 93.58 ± 1.30 , 89.69 ± 0.19 , and $85.09 \pm 1.21\%$ respectively, that are significantly higher than *n*-hexane's 67.6%.

The percent recovery at 30 min for CPME, 2-MeTHF, and TBME are respectively 99.00 ± 0.16 , 95.88 ± 1.36 , and $92.87 \pm 0.12\%$ and are significantly higher than *n*-hexane $85.85 \pm 0.66\%$. Also, the extrapolation of the diffusion region yields a steeper slope for these three green solvents compared to that of *n*-hexane. This may be because, the viscosity of CPME, 2-Me-THF, and TBME are very close to the viscosity of *n*-hexane. The higher solubility effect in equilibrium region, and the lower viscosity effect in the diffusion region are cumulatively reflected on the diffusion coefficients of these solvents. As given in the **Figure 2.47**, CPME stands out with a highest diffusion coefficient of $5.1 \times 10^{-8} \text{ cm}^2\text{s}^{-1}$ of all solvents, which is ten times more than that of *n*-hexane. The diffusion coefficients of 2-MeTHF ($1.9 \times 10^{-8} \text{ cm}^2\text{s}^{-1}$) and TBME ($1.0 \times 10^{-8} \text{ cm}^2\text{s}^{-1}$) are also higher

than *n*-hexane. The calculated time required for maximum (99%) recovery is 6.5×10^2 min that is extremely shorter extraction period compared to that of *n*-hexane's 1.0×10^5 min.

Although, these values are determined in ASE at 100 °C and 1500 psi, the trend in diffusion coefficient and the time required for maximum extraction time would not change much in other extraction methods at the same temperature. This comparison study offers a strong qualitative and quantitative result that can be interpreted into the following ranking. This ranking compares the overall efficiency of the solvents based on their total time required for 99% of soybean oil recovery (**Figure 2.48**).

- 1) CPME (best)
- 2) 2-MeTHF
- 3) TBME
- 4) Ethyl lactate
- 5) *n*-hexane
- 6) *alpha*-Pinene

Table 2.24 Calculated extraction time equivalent to $t_r = 1$ and diffusion coefficient for ASE extraction of soybean oil using different solvents (particle size = 513 μm).

Solvent	Extraction time equivalent to $t_r = 1$ (min)	Diffusion coefficient D (cm^2s^{-1})	Predicted time required to recover 99% of oil (min)
Hexane	189	5.9×10^{-9}	531
2-MeTHF	58	1.9×10^{-8}	112
Alpha Pinene	455	2.4×10^{-9}	920
CPME	22	5.1×10^{-8}	30
Ethyl Lactate	303	3.7×10^{-9}	447
TBME	109	1.0×10^{-8}	244

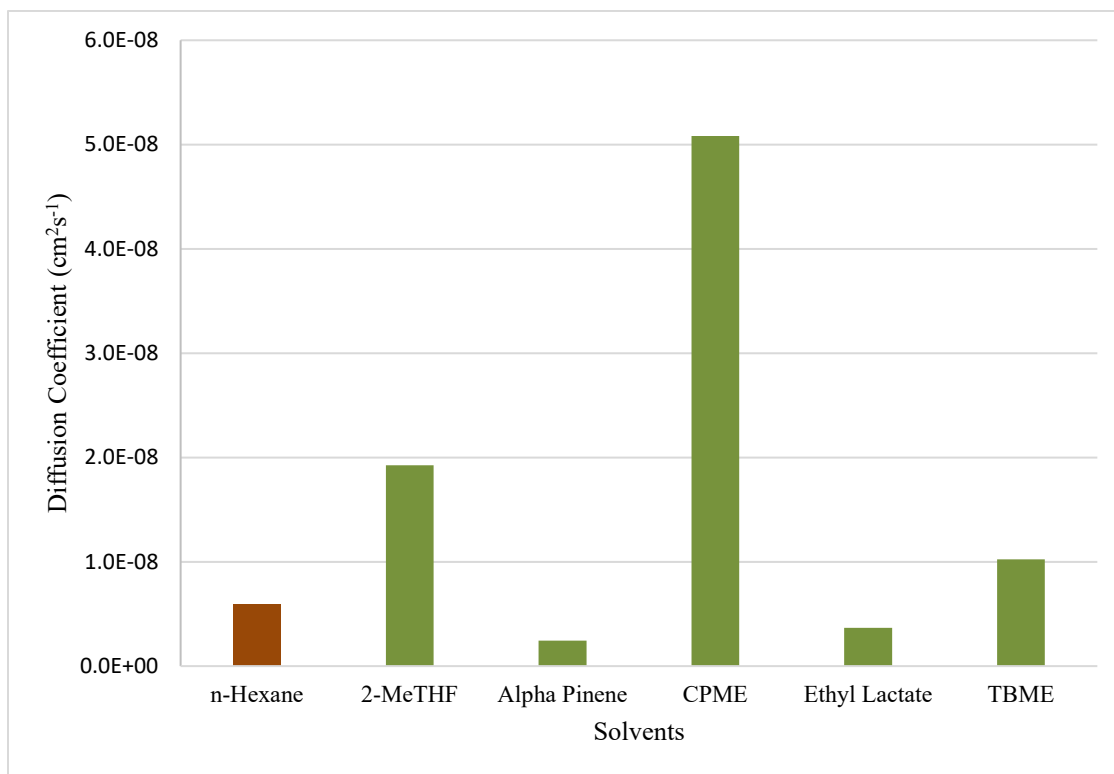


Figure 2.47 Comparison of diffusion coefficients of green solvents with *n*-hexane.

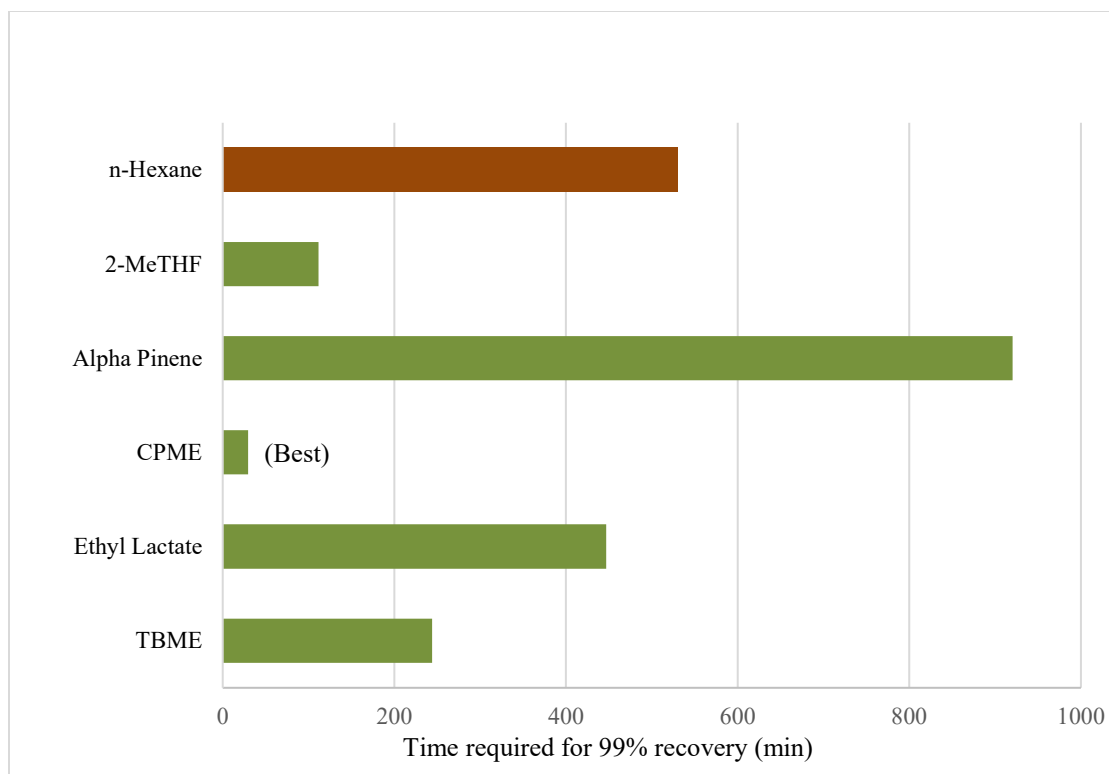


Figure 2.48 Comparison of the overall efficiency of green solvents based on the time required for 99% oil recovery.

2.4 Summary and Conclusions

Five green solvents, namely 2-methyltetrahydrofuran (2-MeTHF), *alpha*-pinene, cyclopentyl methyl ether (CPME), ethyl lactate, and t-butyl methyl ether (TBME), and a petroleum-based reference solvent *n*-hexane were tested in accelerated solvent extraction (ASE). The experiments were designed with an emphasis on comparing the efficiency of green solvents based on their diffusion coefficient and the time required for maximum oil extraction.

Soybean sample preparation was carried out with grinding of dry soybeans, sieving the particles into different size fractions, and drying the particles before extraction. To study the effect of particle size on the extraction yield, ASE extraction was carried out for four different particle sizes using *n*-hexane. Results of this study showed that the extraction yield increases as the particle size decreases. A maximum of only 10% oil was extracted from the largest size 1200 μm diameter particles. Whereas a maximum of 20% oil was obtained from the 513- μm diameter particles. This concludes that the extraction yield was doubled when the particle size was reduced to half.

The five green solvents were selected based on a literature survey of the ecological and economic impacts of solvents. A solvent scoring system was adopted to roughly compare the relative impact of the solvents on waste, health, environment, fire hazard, reactivity, and lifecycle. After this preliminary screening of green solvents, solubility of the triglycerides of major soybean fatty acids (linoleic acid, oleic acid, palmitic acid, and stearic acid) in the green solvents were theoretically predicted and compared to the other common solvents. The COSMO program predicted solubility data revealed that all the five green solvents possess a high solubility as *n*-hexane for the

triglycerides. Except ethyl lactate, all other green solvents were predicted to have high relative solubility for the triglycerides of soybean fatty acids. This theoretical solubility data was later used to evaluate and justify the trends seen in extraction results.

Viscosities of the green solvents at different temperature were experimentally acquired and compared to the viscosity of the reference solvent *n*-hexane. Except ethyl lactate and *alpha*-pinene, whose viscosities at 100 °C are 0.9 and 0.7 cP respectively, all other green solvents possess low viscosity, close to *n*-hexane. This viscosity data was also used to evaluate and justify the trends seen in extraction results.

The experimental extraction results were analyzed using the theoretical hot-ball model. This model illustrates any extraction process using a plot of percent recovery versus time or plot of $\ln(m/m_o)$ versus time. The structure of the plots consists of an initial solubility-controlled equilibrium region, followed by a viscosity-dominated diffusion region. The plots obtained from the experimental results were qualitatively compared to structure of the hot-ball model plots for non-spherical particles. Also, the experimental results were quantitatively analyzed to calculate the diffusion coefficient and the time required for maximum extraction.

Each of green solvents studied in this dissertation showed a best-fit to the hot-ball model despite of the irregular shape of the solute particles. The initial rapid rate of the extraction followed by a development of a liner portion at around the reduced time, $t_r = 0.5$ validated the experimental data to be reliable. The extrapolation of the linear portion of the logarithmic curves of all solvents gave intercepts on $t = 0$ axis that are always more negative than the value of -0.5 for a theoretical spherical sample particle. This was related to the fact that the tested 513- μm soybean particles were mostly non-spherical and

irregular shapes. The mass transfer out of the solid matrix is not a perfect diffusion within homogeneous medium, but more likely a migration of mass from one adsorption site to another, as the extraction fluid replaces the solute molecules at the adsorption site.

Among the green solvents tested, cyclopentyl methyl ether (CPME) demonstrated an excellent overall performance in both solubility-controlled and diffusion-controlled extraction regions. The diffusion coefficient of CPME ($5.1 \times 10^{-8} \text{ cm}^2\text{s}^{-1}$) was the highest of all solvents and it was remarkably almost ten times greater than that of the conventional petroleum-based solvent *n*-hexane ($5.9 \times 10^{-9} \text{ cm}^2\text{s}^{-1}$). The time required to recover 99% of the soybean oil, was calculated to be 30 min for CPME. The next highest efficient alternate solvents were 2-MeTHF with 112 min, TBME with 244 min, and ethyl acetate with 447 min time required for 99% oil recovery. These above highly efficient solvents could be the potential green alternatives for *n*-hexane. The time required for *n*-hexane for 99% soybean oil recovery is 531 min. *alpha*-Pinene takes 920 min for that, hence it is less efficient than *n*-hexane.

The long linear tails in the kinetic plots of green solvents involve a mass transfer of only minority of solute, but still this diffusion region is significant in industrial extraction processes to calculate the time it takes to complete an extraction.

3 EXTRACTION OF SOYBEAN OIL USING A PROTOTYPE AUTOMATED EXTRACTOR

3.1 Introduction

This chapter focuses on examining a new green extraction technique. The prototype extractor from CEM is a crossover between automated Soxhlet extraction and energized solvent extraction. The results from extraction of soybean oil using *n*-hexane were validated using the hot-ball model and compared to the results from ASE.

3.1.1 Automated Soxhlet Extraction

Soxhlet extraction is the process of extracting analyte from a solid matrix to the liquid phase using a Soxhlet extractor. This old solid-liquid extraction technique is used widely in analysis of food and agricultural products. The apparatus invented by Franz Von Soxhlet in 1879 has three components, a percolator flask that heats and circulates the solvent, a sample chamber that holds the filter paper thimble with solid sample, and a siphon arm drains the solvent back into the flask of boiling solvent.⁷⁵ The heated and refluxed solvent is introduced into the extraction chamber where the partially soluble analyte are slowly transferred to the warm fresh solvent through a dispersion mechanism. The disadvantage of the Soxhlet extraction is that it is time consuming (6-24 hours) and it requires a large volume of samples (150-800mL). The alternate extraction methods were developed to minimize the extraction time and solvent usage.⁷⁶⁻⁷⁹ Partial or fully automated Soxhlet techniques were developed to improve the simplicity, ease of handling and adaptability of this traditional technique.⁸⁰

The general mechanism of a solid-liquid extraction technique is that the analyte disperses from a more concentration region (solid matrix) to a less concentration region

(solvent) until an equilibrium is reached.⁸¹ Applying heat energy and adding fresh solvent in this mechanism increases the recovery. The solid matrix is stopped at the filter paper thimble while the extracted analyte passes along with the solvent.

There are several automated Soxhlet extraction systems available in market, such as Soxtec (by Foss Analytics), Soxtherm (by OI Analytics), and Ankom XT10 (by Ankom Technology). They generally use sophisticated technology for controlling extraction time, solvent volume, and temperature while maintaining a better yield. We previously investigated the efficiency of the Soxtec Extractor (Tecator Soxtec System HT6 1043 Extraction Unit, by Foss Analytics, Edina, MN) in extracting lipids from coffee beans.³¹ In this instrument the sample loaded in a cellulose thimble was soaked in 10-15 mL boiling solvent for about 40-50 minutes. The diffusion coefficient in Soxtec is ten times greater than that of Soxhlet. This higher extraction efficiency of Soxtec is due to the constant contact between the sample and boiling solvent, as opposed to the Soxhlet.⁸² On the other hand, Driver reported that the diffusion coefficient of Soxtec is 5 times lower than that of ASE.

3.1.2 Prototype Automated Extractor from CEM

In this work CEM Corporation's prototype automated extractor, named Energized Dispersive Guided Extractor (EDGE), was used to extract oil from soybean. This instrument is more automated than Soxhlet and simpler than pressurized fluid extractor (PFE or ASE). This prototype extractor handles one sample cell at a time. An upgraded version of EDGE is available on the market that can handle 12 samples at a time. This extractor can be used to isolate fat from food, pesticides from produce, semi-volatile

organic compounds from soil, phthalates from plastic, air pollutants from XAD resin, or absorbed pollutants (polychlorinated biphenyls) from polyurethane foam (PUF) plugs.⁸³

The prototype automated extractor from CEM, shown in **Figure 3.1**, consists of an extraction chamber that can be moved in and out of a heating block. Temperature of the heating block can be adjusted on the instrument. Pressure can be controlled and monitored with a gauge on the instrument. On this prototype instrument the volume of solvent is manually measured and pumped into the system. A cellulose thimble loaded with solid sample is placed into the extraction chamber. In this static extraction process the sample would have a constant contact with the solvent. After extraction the solid matrix are stopped at the thimble, while the extract pass through the thimble to collection vial. This relatively simple process would take about 30 minutes to complete, and the volume of solvent is much less than the traditional Soxhlet technique.

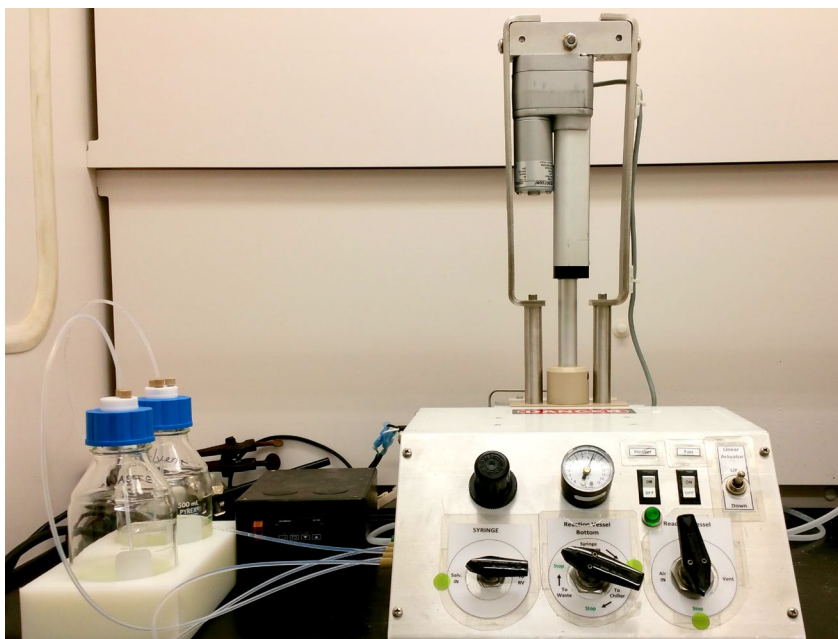


Figure 3.1 The prototype energized dispersive extraction from CEM Corporation.

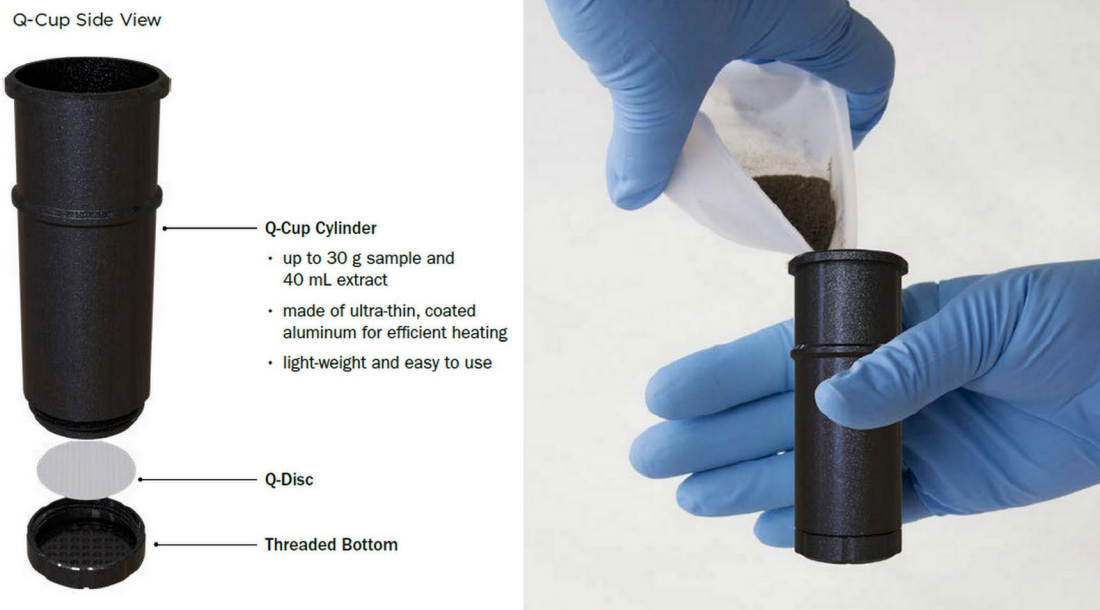


Figure 3.2 The sample holder (Q-cup) used in CEM EDGE. (Image obtained from CEM.)

An alternate to the cellulose thimble is the Q-cup that is made of ultra-thin coated aluminum (for efficient heating) and a cellulose membrane for filtration. The parts are shown in the **Figure 3.2**. After inserting the cellulose filter, the bottom of the aluminum cell is screwed. A sample up to 30 g can be loaded into the cell. This packed aluminum cell is placed into the heating chamber. A pressure cap is placed to create a pressurized seal on the top of the cell.

A rapid extraction and filtration are promoted by the dispersive effect created in the chamber. A solvent is first introduced from the bottom to fill the gap between the chamber and the cell. This small volume of solvent initiates the heat transfer to the solvent and sample matrix. Then, more solvent is added from the top to completely soak the sample. As the chamber walls are heated, the solvent pressure in the gap between cell

and chamber increases. This overcomes the pressure inside the cell, forcing the solvent to disperse into the sample. Once the sample reaches the desired temperature, the instrument maintains the temperature for a set time. Then the solvent filters through the cellulose membrane and passes through a cooling coil to the collection vial. This mechanism is shown in the **Figure 3.3**.

An upgraded version of the automated extractor (EDGE) is shown in **Figure 3.4**. This instrument is lot cheaper than other extraction techniques such as microwave, QuEChERs, pressurized fluid extraction (PFE), Soxhlet, automated soxhlet, and ultrasonic techniques. EDGE can extract up to 30 g in 5 minutes that includes filtering and cooling cycles. Although, CEM claims that EDGE is 6 times faster than PFE the extraction efficiency needs to be considered. The amount of solvent required in EDGE and PFE is almost same.

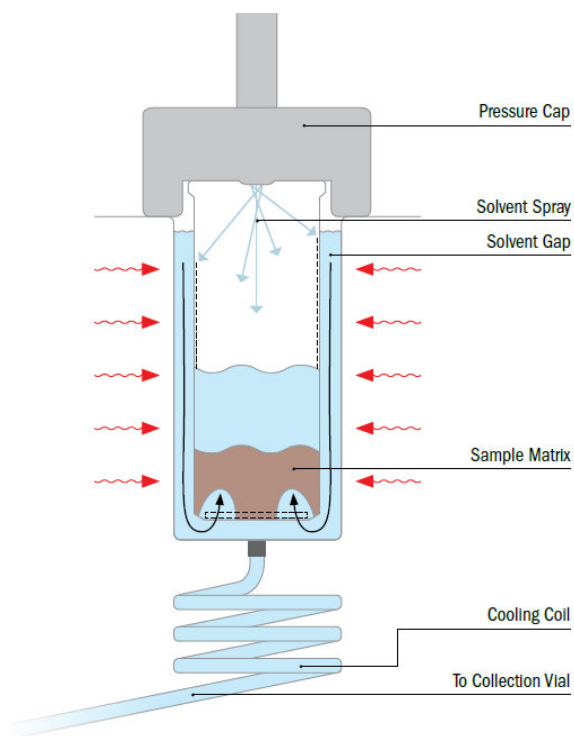


Figure 3.3 The energized dispersive extraction process in CEM prototype extractor. (Image obtained from CEM)

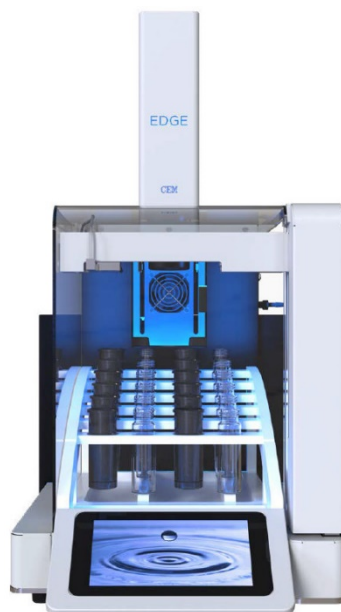


Figure 3.4 An upgraded version of automated energized dispersive extraction EDGE from CEM. (Image obtained from CEM)

3.2 Experimental Methods

3.2.1 Materials and Reagents

Soybeans sample was supplied by the Department of Agricultural & Biosystems Engineering, South Dakota State University. The sample preparation described in section 2.3.2 was followed and an average particle size of 513 μm was used in this study.

Extraction was performed using the prototype automated extraction system named Energized Dispersive Guided Extractor (EDGE) from CEM Corporation (Matthews, NC). *n*-Hexane was purchased from Thermo-Fischer Scientific.

3.2.2 Extraction of Soybean Oil Using CEM's Prototype Extractor

The CEM's prototype automated extractor uses a Soxhlet-like technique to extract, for example, the oil from soybean. In a cellulose thimble, 1 g of ground soybean with average particle size of 513 μm was added along with 2 g of sand (dispersive agent). The thimble was then placed into an extraction chamber that can be sealed and lowered into a heating block using the linear actuator switch. The temperature was maintained at 100 °C and the pressure at 6 psi. The extraction was conducted with 30 mL of *n*-hexane manually pumped using the syringe. Turning on a switch sent the solvent to the extraction chamber in two stages and initiated the extraction process, as explained in section 3.1.2. This prototype extractor can handle only one extraction at a time. Experiments were performed at various extraction times (5, 10, 15, 20 and 30 minutes) with triplicate samples for each time. Once the extraction was completed, the extracts were collected in a pre-weighed glass vial. Then solvent recovery was done in rotatory evaporator or distillation under low pressure. After the distillation of solvent, the extracted oil was dried under nitrogen flushing. The nitrogen drying and weighing

process were repeated until two consecutive weights consistent to within ± 0.0009 grams were obtained. The mass obtained from the triplicate were plotted using Microsoft Excel. Average of the three masses, and the standard deviation were calculated.

The extraction results were validated using the hot-ball model as explained in Section 2.2.5. IR spectral analysis, esterification and GC-MS characterization were conducted as described in Sections 2.2.6, 2.2.7, and 2.2.8.

3.3 Results and Discussion

3.3.1 Validating the CEM Extractor using the Hot-Ball Model

In this section the results of extraction of soybean oil using *n*-hexane in CEM's prototype extractor are evaluated by comparing to the theoretical hot-ball model. The extraction was carried at 100 °C and 6 psi. Extraction times were set to 5, 10, 15, 20 and 30 min. All extractions were done in triplicate with soybean particle size of 513 μm , and the yields were calculated gravimetrically. The average for the replicates and the standard deviation were reported. The amount of maximum extractable (0.2347 g) analyte per gram of sample was calculated based on the results from previous ASE extraction. It is assumed that the oil was evenly distributed throughout the soybean particles. The percent recoveries were calculated using equations 2.6 and 2.7.

(a) Qualitative comparison to the hot-ball model

First, a visual fitting of the experimental plot to the theoretical plot was made. The percent recovery of soybean oil using *n*-hexane in the CEM prototype extractor is plotted against the extraction time in **Figure 3.5**. Like in ASE, a fast initial rate of extraction is observed. In the graph it appears as a steep rise in percent recovery between 0 – 15 min. As listed in the **Table 3.1** an average of $43.46 \pm 0.75\%$ of the total extractable mass of soybean oil is recovered in five minutes. The first 15 min is considered the equilibrium region. As the extraction progressed, the rate of extraction becomes smaller, and that is indicated by a flattening of the recovery curve. After 15 min, the rate of extraction turns out to not change much. This agrees with the prediction of the hot-ball model. The maximum recovery of $61.94 \pm 2.07\%$ is observed at 30 min. The diffusion region of the

recovery graph starts at 15 min, and after that a slow exponential decay of extraction rate was observed.

Table 3.1 Results of soybean oil extraction using *n*-hexane in the CEM prototype extractor (particle size is 513 μm , temperature is 100 $^{\circ}\text{C}$).

Extraction time (min)	Average mass of oil extracted per gram of soybean sample (g)	Percent of oil extracted per gram of soybean sample (%)	Percent Recovery (where $m_o = 0.2347$ g) (%)	Standard deviation for % recovery (n=3) (%)
0	0	0	0	0.00
5	0.1020	10.20	43.46	0.75
10	0.1291	12.91	54.99	1.95
15	0.1360	13.60	57.94	2.19
20	0.1399	13.99	59.62	1.57
30	0.1454	14.54	61.94	2.07

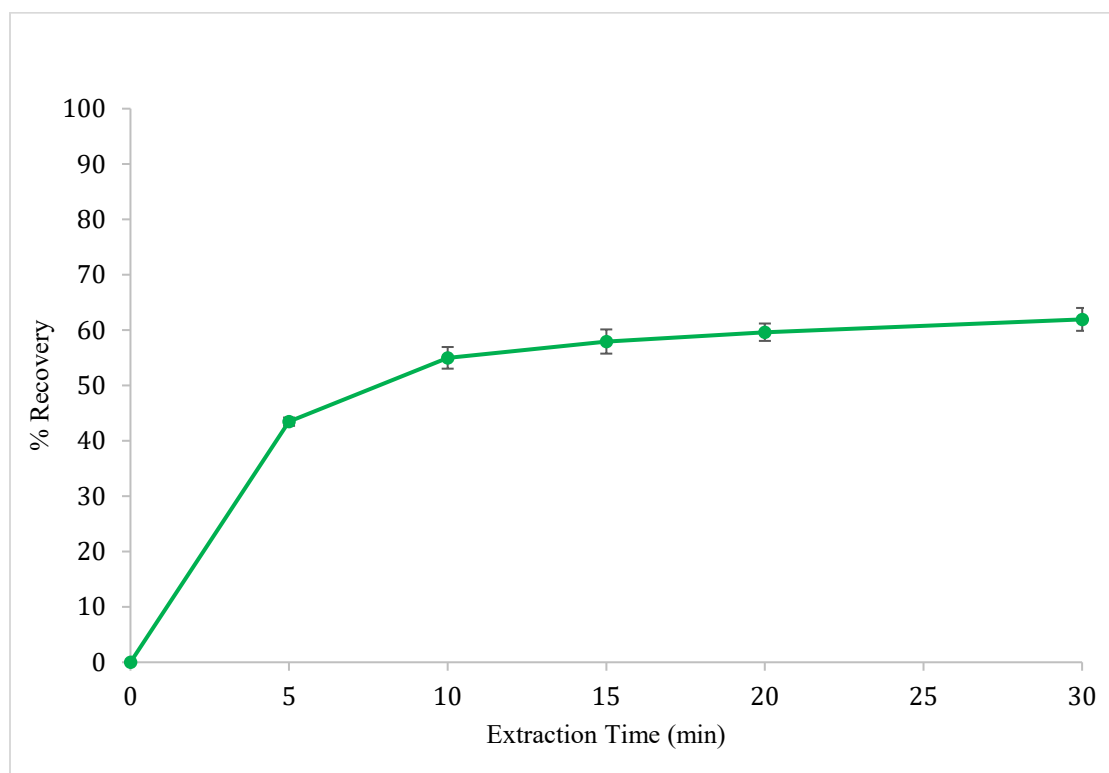


Figure 3.5 Percent oil recovered from the soybean sample using *n*-hexane at different extraction times in the CEM prototype extractor. The average particle size is 513 μm .

(b) Calculation of diffusion coefficient using the hot-ball model

The characteristics of experimental data of soybean extraction using *n*-hexane in the CEM prototype extractor is matched to the hot-ball model. The extraction kinetics is plotted using the natural logarithm of ratio of mass of unextracted oil to the original mass of extractable oil, $\ln(m/m_o)$, versus extraction time, as shown in **Figure 3.6**. The extraction time is quantitatively scaled to the reduced time in the graph, as previously explained. The numerical values are given in the **Table 3.2**. The actual extraction time equivalent to reduced time $t_r = 1$, for *n*-hexane is calculated to be 151 min. Like in ASE extraction, the kinetic curve initially falls infinitely steeply. Even though this is a small portion of the curve, it represents the loss of majority of extractable material from the particle within 15 min. But after 15 min, which corresponds to the t_r of around 0.066, the rate of fall tails off and the curve become almost linear.

Extrapolation of the linear portion of the curve to $t = 0$ provides an intercept of $\ln(m/m_o) = -0.771$. This aligns to the hot-ball model with the effect of nonspherical particles shape that was given in the **Figure 2.5**. The close fit of experimental y-intercept with the y-intercept of hot-ball model endorses the experimental data obtained from the prototype extractor to be valid, as the 513- μm ground soybean particle were not spherical.

Table 3.2 Hot-ball model results for soybean oil extraction using *n*-hexane in the CEM prototype extractor.

Extraction time (min)	Average mass of analyte oil extracted per gram of soybean sample (g)	Average mass (m) of analyte unextracted per gram of soybean sample (if $m_o = 0.2347$ g) (g)	m/m_o	$\ln(m/m_o)$	Reduced time t_r
0	0	0.2347	1.0000	0.0000	0
5	0.1020	0.1327	0.5654	-0.5702	0.033
10	0.1291	0.1056	0.4501	-0.7983	0.066
15	0.1360	0.0987	0.4206	-0.8661	0.099
20	0.1399	0.0948	0.4038	-0.9069	0.132
30	0.1454	0.0893	0.3806	-0.9659	0.198

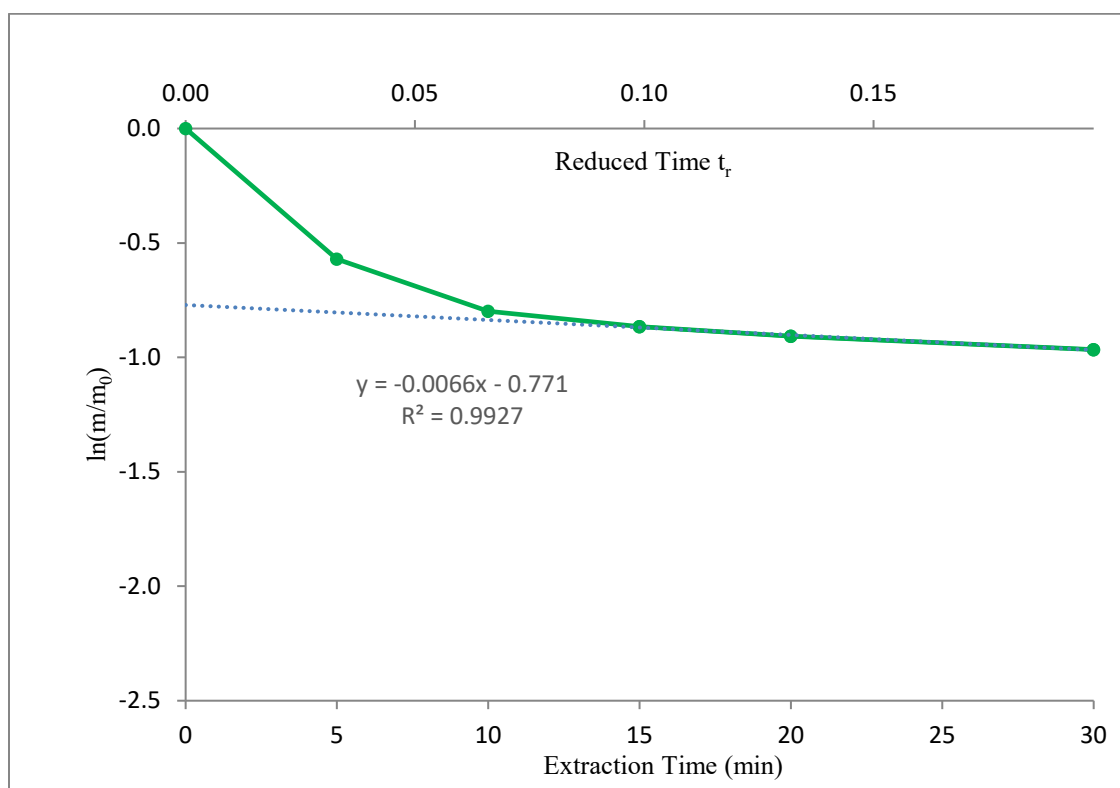


Figure 3.6 Plot of $\ln(m/m_o)$ vs. extraction time for *n*-hexane scaled to the reduced time (t_r) to compare with the hot-ball model.

The linear regression of the trend line is 0.9927, and the slope of the line -0.0066. The intercept on $t = 0$ axis is -0.771. From this data, the diffusion coefficient of extraction of soybean oil in the CEM prototype extractor is calculated to be $7.3 \times 10^{-9} \text{ cm}^2\text{s}^{-1}$. This is close to diffusion coefficient obtained for *n*-hexane in ASE, $5.9 \times 10^{-9} \text{ cm}^2\text{s}^{-1}$. The time required for the recovery of 99% of oil using *n*-hexane is 816 min.

The identity of soybean oil extracted in CEM's prototype extractor using *n*-hexane is confirmed by IR spectroscopy. **Figure 3.7** shows that the IR peaks for C=O, sp^3 C-H, sp^2 C-H, C=C, and C-O stretching frequencies of triglycerides in extracted soybean oil match with the IR peaks of commercial soybean oil.

The GC-MS chromatogram also confirms the identity of fatty acids in the *n*-hexane extracted soybean oil (**Figure 3.8**). For four major fatty acid methyl esters in the extracted oil has a relative abundance that matches with the theoretical relative ratio of the four fatty acids soybean sample.

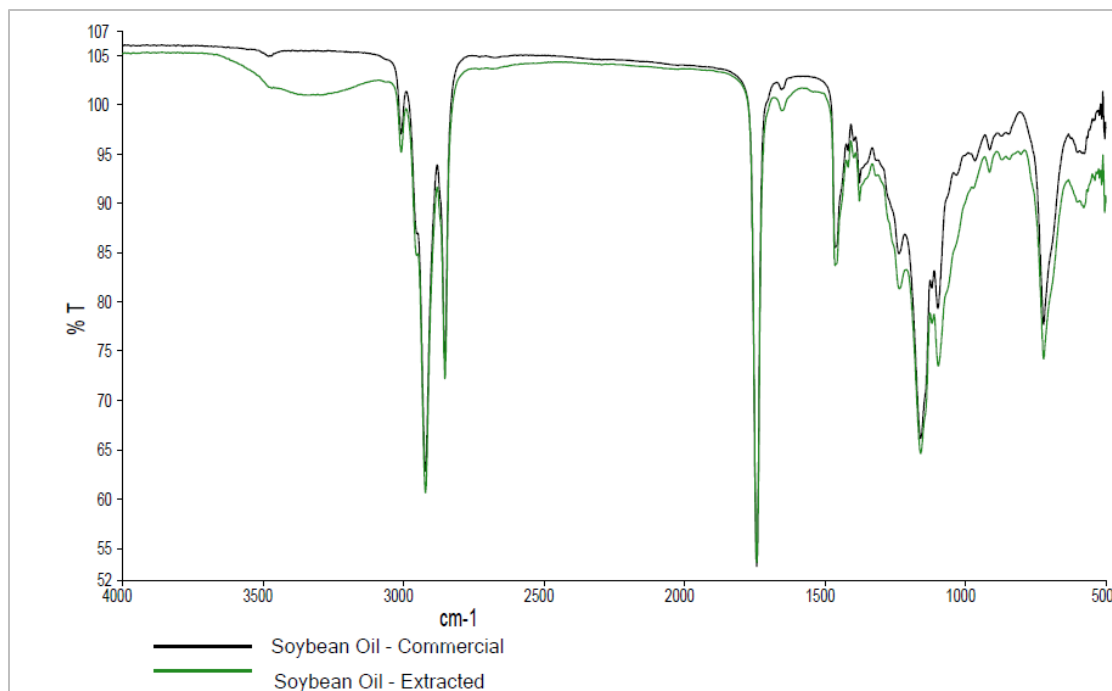


Figure 3.7 Comparison of IR spectra of commercial soybean oil and soybean oil extracted in the CEM prototype extractor using *n*-hexane.

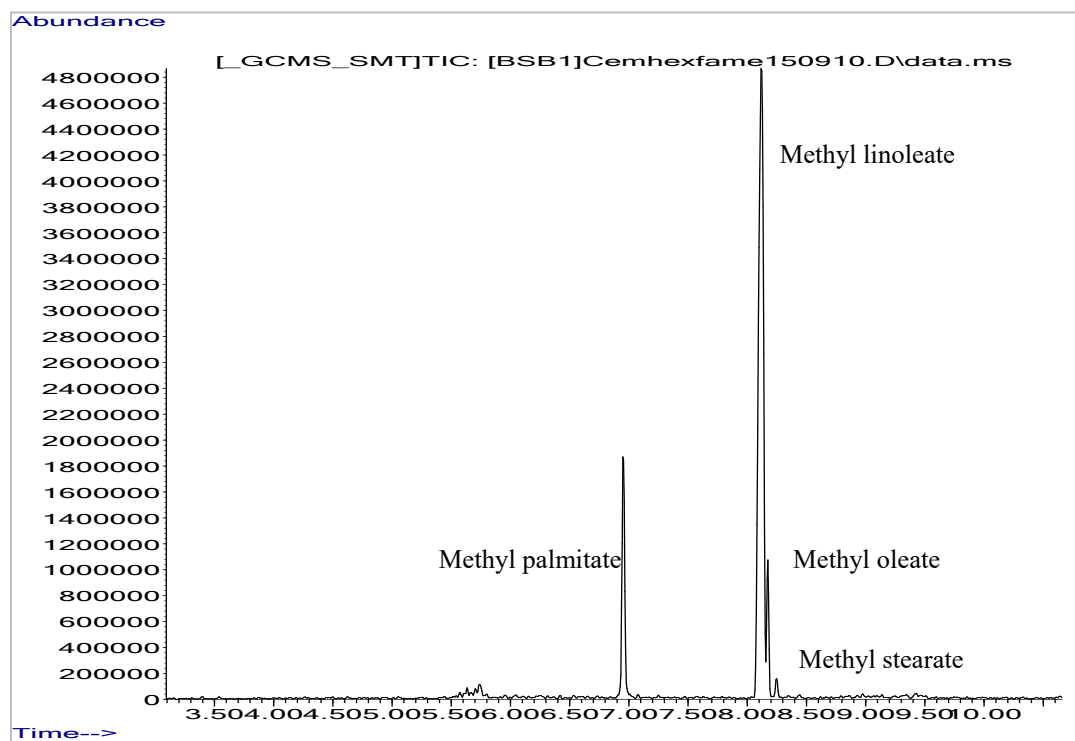


Figure 3.8 Gas chromatogram shows the presence of fatty acid methyl ester derivatives from soybean oil extracted in the CEM prototype extractor using *n*-hexane.

3.3.2 Comparison of Extraction Efficiency of ASE and the CEM Prototype

Extractor

Efficiency of two extraction systems, Dionex™ ASE-350 from Thermo-Fisher, Sunnyvale, CA and a prototype automated extraction system (EDGE) from CEM Corporation, Matthews, NC, was compared.

It is significant to note that the two extraction systems work under a similar mechanisms. Dionex™ ASE-350 applies a pressurized fluid extraction method, where a highly pressurized solvent at an elevated temperature elutes through the solid sample. This would result an escalated extraction rate. The CEM prototype extractor applies a related extraction method, where a solvent at a relatively lower pressure is in constant contact with the solid sample for a set time. Comparing these extraction results will confirm the related extraction mechanisms.

In both ASE and the CEM prototype extractor, the following parameter were kept constant: solvent (*n*-hexane), volume of solvent (30 mL), soybean particle size (513 μm), weight of sample (1 g), weight of dispersing agent (2 g), temperature (100 °C), and extraction time (5 - 30 min). The pressure maintained in the two extraction systems vary drastically; in ASE the pressure is 1500 psi and in the CEM prototype extractor it is 6 psi, enough to raise the solvent boiling point.

Figure 3.9 compares the percent recovery of soybean oil at different extraction times for the two methods. Both curves fit with the hot-ball model, but evidently, ASE yields the higher recovery at all extraction times, a result of the extractor configuration.

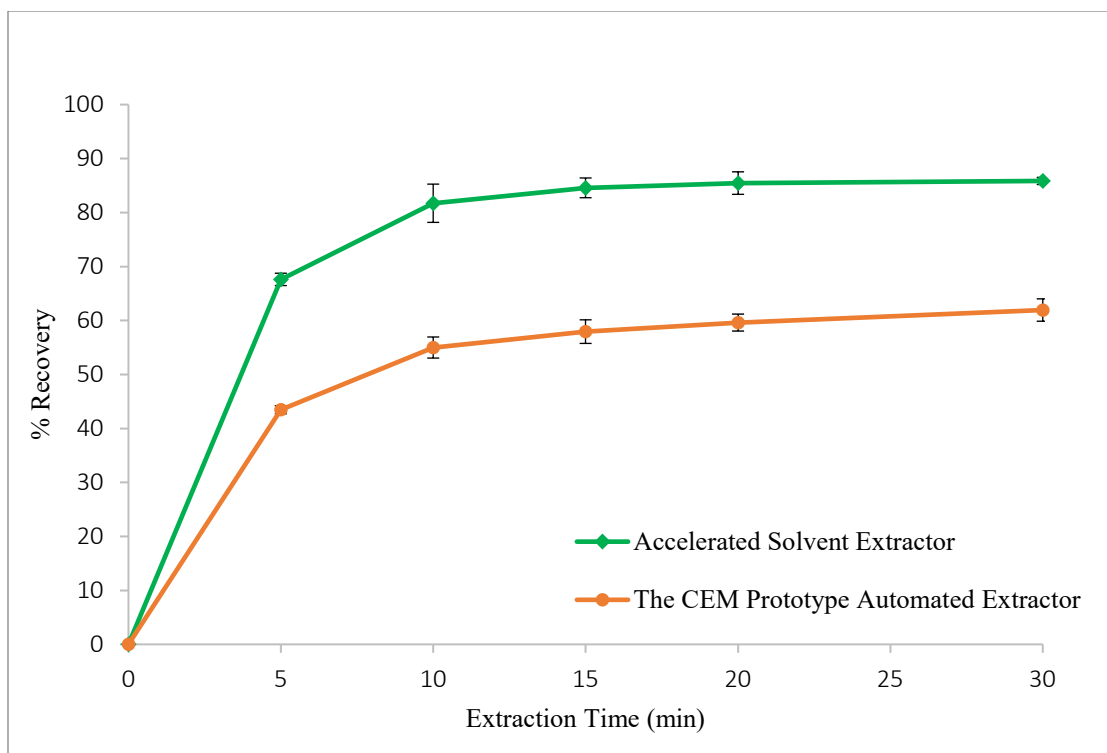


Figure 3.9 Comparison of percent recovery from ASE and CEM’s prototype extractor.

The initial steep equilibrium region ends at 5 min for both curves. At 5 min, ASE recovers $67.62 \pm 1.14\%$ of soybean oil, whereas the prototype extractor recovers only 43%. The difference in percent recovery during this solubility driven part of extraction process can be highly influenced by the solvent flow mechanism of the ASE instrument, resulting in a greater solvent volume. The high temperature provides a high solubility, while the high pressure facilitates a high penetration of solvent into the sample matrix.⁸⁴

The trend in the equilibrium region persists in the transition region (10-15 min) of the extraction curve. At 15 min, ASE recovers $84.58 \pm 1.83\%$ of oil, whereas the prototype extractor recovers only $57.94 \pm 2.19\%$.

The diffusion region of the extraction curve starts at 15 min for both methods, where the rate of extraction is levelled off and predominantly driven by a slow diffusion of solute into the solvent. The slopes for both methods are very close (-0.0066 and -

00053). The slightly steeper slope for the CEM prototype may be due to the fact the concentration gradation is high during the diffusion region or an artifact of the instrument design. That is, the ratio of concentration of unextracted oil in the soybean particle to the concentration of oil in extracted in the solvent is high. The diffusion coefficient for ASE extraction ($5.9 \times 10^{-9} \text{ cm}^2\text{s}^{-1}$) and the CEM prototype extraction ($7.3 \times 10^{-9} \text{ cm}^2\text{s}^{-1}$) are not very different. This suggests that the diffusion occurs during both extraction methods are not affected by the extraction mechanism.

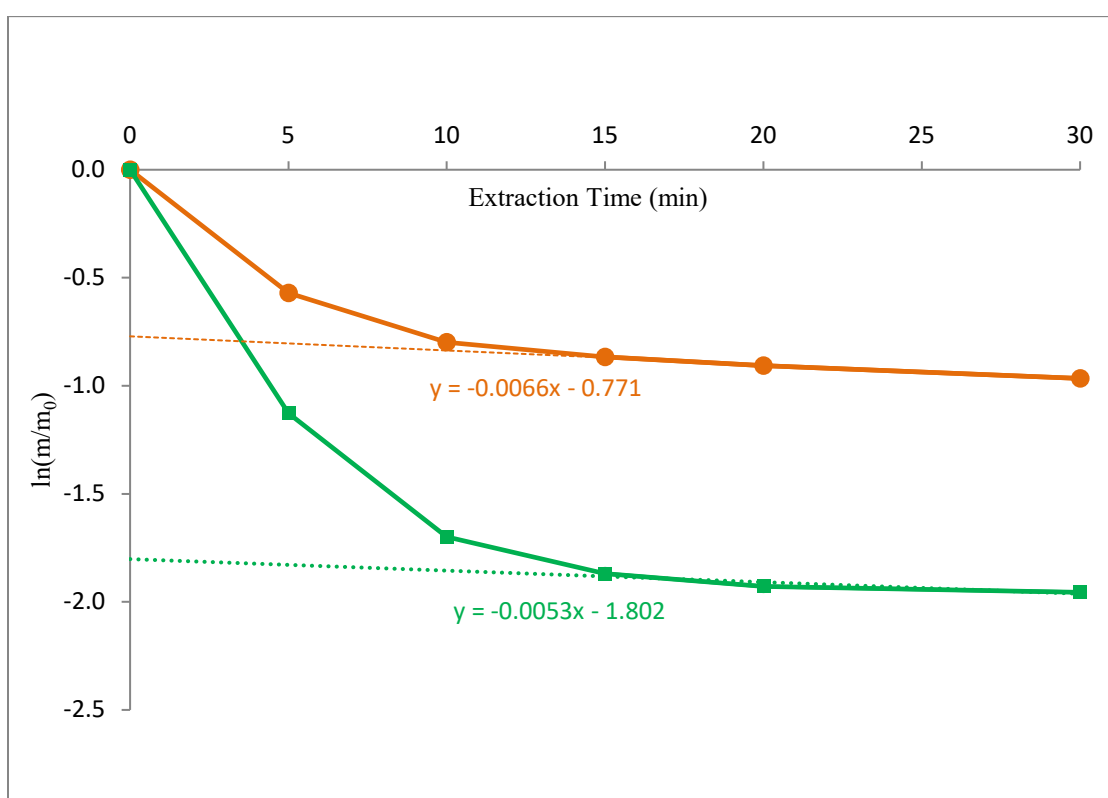


Figure 3.10 Comparison of $\ln(m/m_0)$ curves from ASE and the CEM prototype extractor.

3.4 Summary and Conclusions

A prototype automatic extractor from CEM Corporation was explored and investigated for extracting soybean oil. The results indicate that the extraction system from CEM is less efficient than ASE in terms of amount of oil extracted from soybean during short extraction times 5 – 30 min. Although it fits in the hot-ball model, the percent recovery of soybean oil in the prototype extractor is about 25% less than that of ASE. One possible reason for this difference in recovery is that the penetration of solvent through the sample matrix is high in the pressurized fluid extraction (in ASE), which allows a better solvent-sample interaction. It is significant to note that the two extraction systems may have their advantages and disadvantages with regard to the cost of instruments, cost of operation, ease of handling, energy consumption, and extraction time for multiple samples. But they are both more automatic and greener than the traditional solid-liquid extraction methods.

4 EFFICIENCY OF ADSORBENTS IN ACCELERATED SOLVENT EXTRACTION

4.1 Introduction

Selectivity of modern extraction techniques can be improved by the addition of adsorbents to the system. Treating the extract with adsorbents before chromatographic analysis would eliminate additional clean-up steps, improve selectivity, and ease automation.⁷ Because ASE is an exhaustive extraction technique, extracts obtained from complex samples would often include undesired compounds called co-extractant. These co-extracted substances can interfere with the determination and application of the desired analytes. The ability to extract the most amount of analytes with little or no interfering co-extracts would boost the desirability of ASE. This selective extraction can be achieved by choosing right solvents, using adsorbents, and manipulating the extraction conditions such as temperature.⁸⁵ This chapter discusses the efficiency of different adsorbents in retaining (or adsorbing) oil contents such as saturated and unsaturated fatty acid triglycerides during ASE extraction.

4.1.1 Use of Adsorbents in Extraction

Adsorption is a phenomenon where the concentration of a solute at the surface of a solid becomes greater than the concentration throughout the solution. The driving force for adsorption is the subsequent decrease in surface tension between the solid and solution. Physical adsorption is promoted by a weak van der Waals force of attraction between the adsorbent and the adsorbate molecules. This attraction force is similar to the condensation of gas molecules into their liquid state. Chemical adsorption, or chemisorption, is promoted by a relatively stronger dipole-dipole attraction between the

surface of the adsorbent and the adsorbate molecule.⁸⁶ In many cases both physical and chemical adsorption take place, and it is hard to distinguish them.

Adsorbents are widely used in solid-phase extraction (SPE) technique. SPE is based on chromatographic principles, where the solvent carrying extract is treated with adsorbents to improve the analyte fractionation. Optimizing the functional group interaction of sample, solvent, and adsorbent would enable precise separation of desired compounds from the co-extracts. In addition to conventional SPE columns, several other ways are used to improve the selectivity of extraction.

QuEChERS (Quick, Easy, Cheap, Effective, Rugged, and Safe) is one of the popular methods used for rapid screening of large number of samples, mainly for analyzing pesticide residue in food and agricultural products. Dispersive solid phase extraction (d-SPE) is included as a simple and novel clean-up step in the QuEChERS technique to process the extracts from fruit, vegetables, oil, sediment, soil, etc.⁸⁷⁻⁸⁸ Apart from QuEChERS, dispersive solid phase extraction has evolved as an independent sample preparation and extraction technique in recent years.⁶

The main advantages of d-SPE are its simplicity, repeatability, low cost, speed and wide applicability to different types of samples and analytes.⁸⁹⁻⁹³ Saito *et al* reported the use of d-SPE to pretreat extremely small amount of biological samples in analyzing overdose of drugs.⁹⁴ Cerqueira *et al* have used d-SPE in QuEChERS to determine the pesticides and pharmaceutical and personal care products in drinking water treatment sludge with a quantification limit of 1 to 50 $\mu\text{g kg}^{-1}$.⁹⁵ Fontana *et al* have successfully applied d-SPE to determine several pesticides and other contaminants, such as

sulfonamides, polychlorinated biphenyls (PCBs) and PBDEs in diverse types of food and environmental samples.⁸⁸

Recent developments in automation of SPE and d-SPE support the trend toward green chemistry, miniature experiments, and high extraction efficiency.^{6, 96-97} A complete automation of d-SPE pose significant challenges as it is difficult to couple this with other techniques. Isolating sorbents from sample solution usually require centrifugation. In case of sorbent-free extraction, filtration can be used in place of centrifugation. A filter vial d-SPE concept may be adopted for sorbent-free extraction. Despite these limitations, automated d-SPE is desirable when a large number of extractions are performed in short time. Some commercial automated d-SPE available in market can handle several extractions simultaneously at high efficiency. Another way to selectivity is to add a cartridge of sorbents downstream of existing extraction systems such as ASE.

4.1.2 In-Cell Cleanup during Accelerated Solvent Extraction

The versatility of accelerated solvent extraction can be extended by inserting a compartment of adsorbents for cleanup.⁷ Options are available to couple the extraction cell with simple adapters loaded with adsorbents. But often the extraction cell can be segmented for sample and adsorbents to achieve simultaneous extraction and in-cell cleanup or fractionation. This would reduce the solvent usage, labor, and extraction cost, and at the same time increase the quality of the analysis. As the extract obtained is ready for instrumental analysis, this more automated method falls in line with the current trend in green analytical chemistry.⁹⁸

Emon *et al.* developed a selective pressurized liquid extraction (SPLE) procedure to effectively extract pesticides from complex indoor house dust without post-extraction

cleanup.⁹⁹ The extraction was performed using dichloromethane in a Dionex ASE-200 system at 120 °C and 2000 psi. Acidic and neutral silica were used as the adsorbents. The ASE extraction cell was segmented and packed with dispersant, sample and adsorbents. Among the different ratios of sample to adsorbents tested, a maximum of 85% recovery was obtained for 1:0.8:8 sample, acidic silica and neutral silica ratio. It was also reported that silica gives best recovery compared to florisil and alumina. The sample throughput of SPLE is estimated to be 50% higher than the step-wise extraction and cleanup procedure. This higher efficiency can be translated to reduction in overall analytical cost, and this robust method can be considered for routine laboratory analysis for large numbers of samples.

Kim *et al.* call it a one-step PLE procedure.¹⁰⁰ They used Na₄EDTA as the adsorbent for cleanup during ASE extraction of polycyclic aromatic hydrocarbons (PAHs) from sediments. The extraction cell was loaded with a cellulose filter, sea sand, anhydrous Na₂SO₄, sample and adsorbent. Among different ratios tested, a maximum recovery was obtained for 1:0.05 sample to adsorbent ratio. A 4% increase in recovery, along with an improved precision, and reduction in solvent usage and manual handling was reported.¹⁰⁰

Also found in several articles¹⁰¹⁻¹⁰³ that the efficiency of an adsorbent varies with different sample. An adsorbent ideal for interacting with one functional group may not do well with other functional groups. Thus, a survey of different adsorbents could be a suitable start for developing a new extraction procedure. Liao *et al.* examined the performance of different adsorbents such as sand, florisil, alumina, graphitized carbon and diatomaceous earth in cleaning up of ethyl carbamate extracted from fermented solid

food.¹⁰¹ When dichloromethane was used as the solvent, florisil is the front-runner adsorbent for retaining co-extracts and producing 85% recovery of ethyl carbamate. On the other hand, alumina is the prominent adsorbent with 80% recovery when methanol was the solvent. These results bring in the notable effect of solvent on choosing the suitable adsorbent for a particular extraction.

Effect of temperature is another major factor that affects the sample-solvent-adsorbent interaction. It is difficult to correlate the temperature to the efficiency of an adsorbent, when several other factors are involved. A common practice is to identify the appropriate temperature for each combination of sample-solvent-adsorbent. Pintado *et al.* reported the influence of temperature in the extraction of organic pollutants from costal sediments. Upon testing alumina as the adsorbent for five different solvents at three different temperatures, no common trend was identified among the recoveries of different organic pollutants. For instance the maximum recoveries of octocrylene and homosalate were obtained at 70 °C, the maximum recoveries of celestolide and tris-p-tolylphosphate were obtained at 100 °C, and the maximum recoveries of other pollutants such as ethion, deltamethrin, and anthracene were obtained at the higher temperature of 130 °C.¹⁰²

To our knowledge the efficiency of adsorbents for simultaneous ASE extraction and in-cell cleanup for soybean oil has not been studied. The aim of this study is to develop a simple analytical method for comparing the oil adsorption efficiency of a few common adsorbents. This can be done by assessing the percent of oil adsorbed by the different adsorbents, at different temperature and different concentration of adsorbents. The adsorbents used in this study are listed below.

Silica or silica gel is an amorphous form of silicon dioxide (SiO_2), and is one of the most commonly used adsorbents in chromatography. It is a polymer in which the silicon atom is covalently bonded to four oxygen atoms in a tetrahedral geometry. The terminal hydroxide groups in silica enables it to form hydrogen bonding with polar compounds. Silica gel possessing average pore size greater than about 60 Å is used to adsorb phospholipids and soap in the process of oil purification and bleaching.¹⁰⁴⁻¹⁰⁵

Florisil is a commercially prepared magnesium silicate (MgO_3Si). The common applications are as column packing material in column chromatography, as an adsorbent in gas chromatography with electron capture detector (GC/ECD), and in clean-up procedures in GC-MS. The average particle size of the florisil we used in this study is 149-250 µm, and the average pore size is 4-8nm.¹⁰⁶ It is used as adsorbent for separation of lipids.¹⁰⁷

Activated charcoal is a highly porous adsorbent material traditionally used to remove toxic substances from plants and natural produce. Powdered activated charcoal or activated carbon has particle size synthesized to 25 µm. The average pore diameter of the activated carbon varies widely in nanometer scale.¹⁰⁸⁻¹⁰⁹ This enables the external surface for adsorption of lipids and pigments in vegetable oil.¹¹⁰⁻¹¹¹

Alumina or aluminum oxide (Al_2O_3) is a mesoporous adsorbent material. The average particle size is 5-6 µm and the pore size 3.8 nm.¹¹² Alumina is used to adsorb phospholipids during the post extraction process of vegetable oil.¹¹²⁻¹¹⁴

Diatomaceous earth or Celite® (SiO_2) is a soft silica sediment that is natural occurring. Because of its high porosity this half-white powdery substance has very low

density. The typical particle size of commercially available diatomaceous earth range from 10 to 100 nm, and the pore size is varies widely from 244 – 11000 Å.¹¹⁵⁻¹¹⁶

4.2 Experimental Methods

4.2.1 Materials and Reagents

Silica gel (Davisil™, grade 7.10) was purchased from Aldrich. The mesh size is 4-20 μ , and the pore diameter is about 60 Å. Florisil (mesh size is 60-100 μ), activated carbon (Darco® G-60), and alumina (aluminum oxide anhydrous) were purchased from Fisher Chemicals. Diatomaceous earth was purchased from Dionex. Before used for adsorption study, all adsorbents were placed in oven at about 100 °C for 24 hrs to remove moisture. Then they were cooled to room temperature and stored in dry containers.

n-hexane was purchased from Thermo-Fischer Scientific. Purified soybean oil (Nutrioli®) was purchased from a local supermarket. Extractions were performed using the pressurized fluid extraction instrument Dionex™ ASE-350 (Thermo-Fisher, Sunnyvale, CA), and the prototype automated extraction system named Energized Dispersive Guided Extractor (EDGE) from CEM Corporation (Matthews, NC).

4.2.2 Oil Adsorption Study in ASE

Dry adsorbents were weighted with no or minimal exposure to moisture and transferred into a 33-mL stainless steel ASE extraction cell containing a 30 mm Whatman cellulose filter. Density of the soybean oil was calculated by measuring its weight and volume. The amount of soybean oil used in this study was chosen to be close to the amount of oil extracted from 1 g of ground soybean (as seen in Section 2.3.8). Based on the desired adsorbent to oil ratio given in **Table 4.1** and **Table 4.2**, a measured amount of soybean oil was added on top of the adsorbents. Void space was filled with glass beads, and the cell was sealed with the end cap as show in **Figure 4.1**. The extraction vessel was placed into the ASE system and the extraction was conducted using *n*-hexane. The

pressure was maintained at 1500 psi, and the desired temperature was set for each run. Triplicate extractions were performed for each experiment, and the results were studied gravimetrically. Then solvent recovery was done in a rotatory evaporator or distillation under low pressure. After the distillation of solvent, the extracted oil was dried under nitrogen flushing. The nitrogen drying and weighing process were repeated until two consecutive weights consistent to within ± 0.0009 grams were obtained.

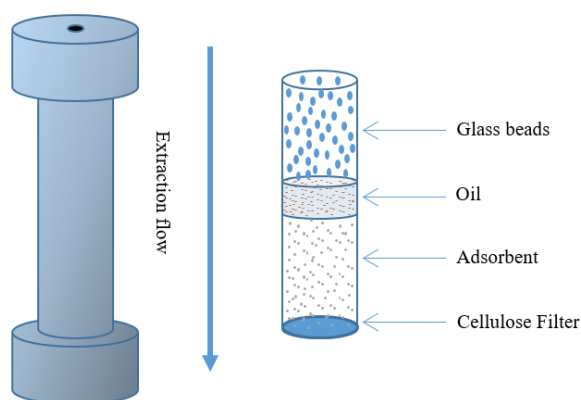


Figure 4.1 Schematic image shows the sample and adsorbent packing in ASE extraction cell.

The mass obtained from the triplicate were plotted. After each experiment, the extraction cells were thoroughly washed, rinsed with acetone, and dried before using for next experiment.

Table 4.1 Amount of Adsorbent and Oil used for Initial Study of selectivity of adsorbents

Adsorbents	Ratio of adsorbent to oil	Mass of soybean oil (g)	Mass of adsorbent (g)
Silica	10:1	0.5	5
Florisil	10:1	0.5	5
Activated carbon	10:1	0.5	5
Diatomaceous earth	10:1	0.5	5
Alumina	10:1	0.5	5

Table 4.2 Amount of adsorbents and oil used to study the effect of temperature and the effect of adsorbent's concentration on adsorption efficiency.

Adsorbent	Adsorbent to oil ratio	Mass of adsorbent (g)	Mass of soybean oil (g)	Volume of solvent (mL)	Extraction Temperature (°C)
Silica	1:5	1.25	0.25	30	50
Silica	1:5	1.25	0.25	30	75
Silica	1:5	1.25	0.25	30	100
Silica	1:5	1.25	0.25	30	150
Florisil	1:5	1.25	0.25	30	50
Florisil	1:5	1.25	0.25	30	75
Florisil	1:5	1.25	0.25	30	100
Florisil	1:5	1.25	0.25	30	150
Activated carbon	1:5	1.25	0.25	30	50
Activated carbon	1:5	1.25	0.25	30	75
Activated carbon	1:5	1.25	0.25	30	100
Activated carbon	1:5	1.25	0.25	30	150
Silica	1:15	3.75	0.25	30	50
Silica	1:15	3.75	0.25	30	75
Silica	1:15	3.75	0.25	30	100
Silica	1:15	3.75	0.25	30	150
Florisil	1:15	3.75	0.25	30	50
Florisil	1:15	3.75	0.25	30	75
Florisil	1:15	3.75	0.25	30	100
Florisil	1:15	3.75	0.25	30	150
Activated carbon	1:15	3.75	0.25	30	50
Activated carbon	1:15	3.75	0.25	30	75
Activated carbon	1:15	3.75	0.25	30	100
Activated carbon	1:15	3.75	0.25	30	150
Silica	1:20	5	0.25	30	50
Silica	1:20	5	0.25	30	75
Silica	1:20	5	0.25	30	100
Silica	1:20	5	0.25	30	150
Florisil	1:20	5	0.25	30	50
Florisil	1:20	5	0.25	30	75
Florisil	1:20	5	0.25	30	100
Florisil	1:20	5	0.25	30	150
Activated carbon	1:20	5	0.25	30	50
Activated carbon	1:20	5	0.25	30	75
Activated carbon	1:20	5	0.25	30	100
Activated carbon	1:20	5	0.25	30	150

4.2.3 Oil Adsorption Study in CEM Prototype Extractor

In a cellulose thimble, an accurately weighed amount of adsorbents and soybean oil were added as give in **Table 4.1**. Care was taken not to expose the adsorbent to moisture atmosphere. The thimble was then placed into an extraction chamber that can be sealed and lowered into a heating block using the linear actuator switch. The temperature was maintained at 100 °C and the pressure at 6 psi. The extraction was conducted with 30 mL of *n*-hexane. This prototype extractor can handle only one extraction at a time. Each run was triplicated. Once the extraction was completed, the extracts were collected in a pre-weighed glass vial. Then solvent recovery was done in rotatory evaporator or distillation under low pressure. After the distillation of solvent, the extracted oil was dried under nitrogen flushing. The nitrogen drying and weighing process were repeated until two consecutive weights consistent to within ± 0.0009 grams were obtained. The mass obtained from the triplicate were plotted.

4.3 Results and Discussion

As adsorption is a complex phenomenon, and meticulous studies are required to understand its mechanism. Experiments are limited to only compare oil adsorption efficiency of five adsorbents. During the adsorption of vegetable oil by silica, florisil, activated carbon, diatomaceous earth, and alumina, both physical and chemical adsorption play a part. Chemical adsorption requires a close interaction and is generally responsible for a single layer of adsorbed molecule. Physical adsorption force can be exerted from the first layer to attract further layers. Thus with multilayers physical adsorption is more common than chemisorption especially at a low temperature and high pressure. But both types of adsorption depend on the nature of the adsorbents, the components of the oil, the relative concentration of adsorbent and oil, and the condition of their contact. Some combinations of these factors work to give a predictable adsorption, but some would conflict to give unpredictable results.¹¹⁷

Temperature and concentration of adsorbent are the two significant parameters that affect adsorption. In order to find the best adsorbents for these triglycerides, we tested three adsorbents at three different concentrations and four different temperatures. Thus a $3 \times 3 \times 4$ multifactor experimental design was used in this study. *n*-Hexane was used as the solvent for all adsorption studies.

4.3.1 Efficiency of Different Adsorbents in ASE Extraction

ASE extraction was used to compare the oil adsorption efficiency of five common adsorbent such as silica, florisil, activated carbon, diatomaceous earth, and alumina. The results shown below in **Figure 4.2** indicate how much each adsorbent retained the pure

soybean oil during the ASE extraction at 100 °C. Major fatty acid triglycerides in soybean oil don't possess a strong hydrogen bond donor character (refer **Figure 2.11**), but they all have a long hydrocarbon chain that can exert non-polar interaction. This hints that a physical adsorption could predominantly take place between triglycerides and the surface of adsorbents. The results show that the polarity of adsorbents did not have much impact on the adsorption capacity. Silica and alumina are both highly polar, but they demonstrated notably different oil adsorption capacity in this study.

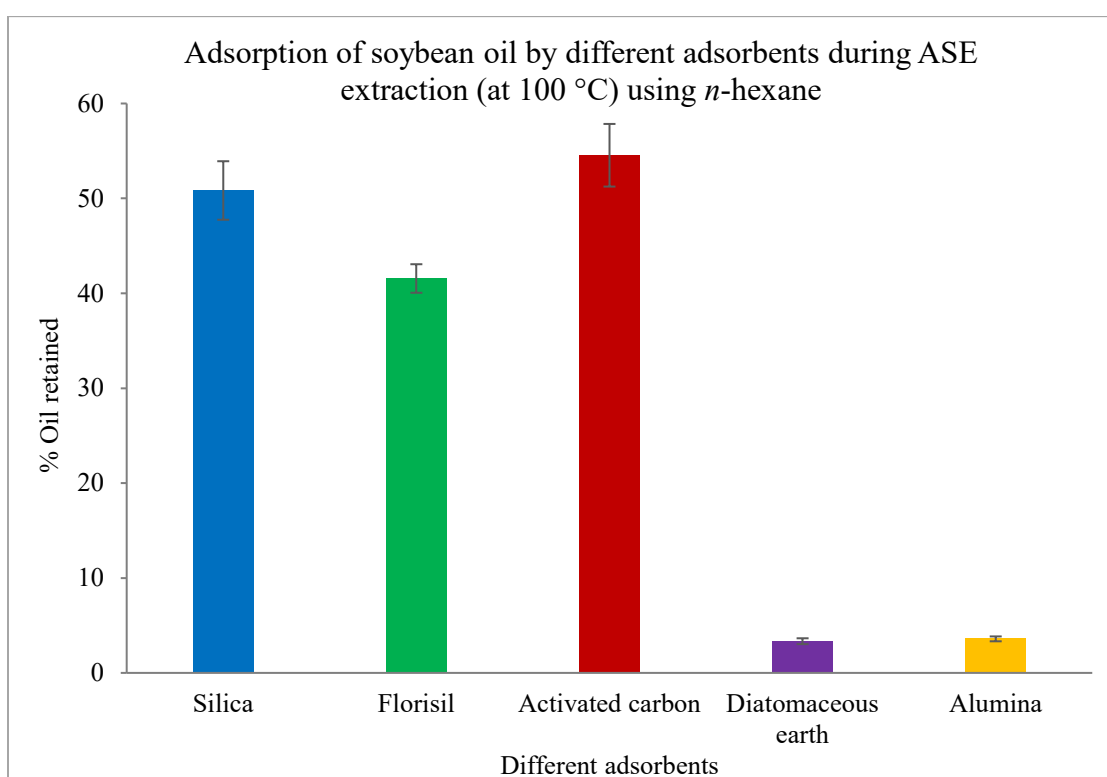


Figure 4.2 Adsorption of soybean oil by different adsorbents during ASE extraction (at 100 °C) using *n*-hexane.

Silica retained $51.83 \pm 3.07\%$ of soybean oil, while alumina retained only $3.59 \pm 0.26\%$. Performance of activated carbon is slightly higher than silica with $54.55 \pm 3.29\%$ that makes it the best adsorbent for oils in ASE extraction. Next to

activated carbon and silica, the third rank performer is florisil with $41.55 \pm 1.50\%$ oil retained. Oil adsorption capacity of diatomaceous earth is only $3.34 \pm 0.31\%$.

Although the limited study we conducted could not establish a proper justification for the poor performance of alumina and diatomaceous earth, a viable reason may be the smaller pore size and pore volume in these adsorbent materials are insufficient to retain triglycerides. Also, since the experiments were performed in an elevated temperature ($100\text{ }^{\circ}\text{C}$) and pressure (1500 psi), the solubility of oil in *n*-hexane could have outplayed the adsorption capacity of the adsorbents. The adsorbent to oil ratio used in this initial study was 10:1 (5 g to 0.5 g), and the volume of *n*-hexane solvent is 30 mL.

4.3.2 Efficiency of Different Adsorbents in CEM Extraction

As an affirmation for the previous results from ASE extraction, the efficiency of adsorbents was tested in the CEM prototype extractor. Except the pressure in CEM (6 psi) all extraction conditions were kept same. The CEM results, only with a slight deviation, verified that alumina and diatomaceous earth are the poor adsorbents with $3.17 \pm 0.19\%$ and $17.05 \pm 3.15\%$ oil retention, respectively. The results also endorsed the high adsorption efficiency of silica, activated carbon and florisil. The performance of silica leaped from $\sim 50\%$ in ASE to $95.64 \pm 2.79\%$ in the prototype extractor. Roughly the same trend was observed for the other adsorbents except for alumina. As the precise reason for the increased adsorption efficiency is not obvious, the solvent flow design that makes ASE a more complete extraction may also retard solute adsorption.

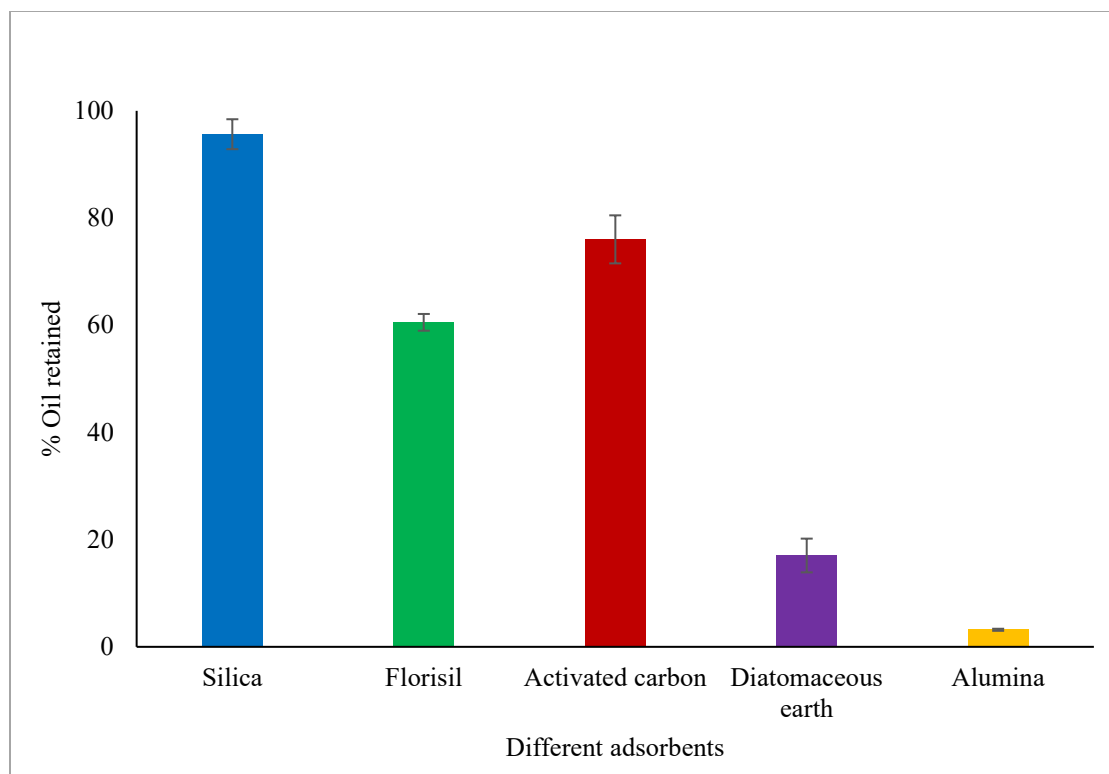


Figure 4.3 Adsorption efficiency of five different adsorbents during the CEM extraction.

4.3.3 Effect of Temperature on the Performance of Adsorbents

The adsorption of triglyceride contents of soybean oil on silica, florisil, and activated carbon was studied at different temperatures using *n*-hexane in ASE. These three adsorbents were chosen based on their performance in the initial ASE and CEM extractions at 100 °C. A multifactor design was used to investigate the influence of temperature on the performance of different adsorbents at different concentration. In this study, our aim is to compare the oil adsorption capacity of the three popular adsorbents at different temperatures. To fully understand the mechanism and thermodynamics of the soybean oil adsorption, a detailed investigation would be required.

Generally, an increase in temperature would decrease the adsorption, due to the increased kinetic energy of solute molecules which may overcome the binding energy

with the adsorbents. The effect of temperature is not universal, but greatly depend on the structure of adsorbents.⁸⁶ Because several factors affect the adsorption efficiency, it would be hard to distinguish between the influence of temperature on activating the adoption sites and the influence of temperature on the solubility of sample in solvent. As the balance between these two independent and conflicting influences cannot be easily predicted, a trial of different temperatures were studied for different adsorbents. As linoleic acid is the major component of soybean oil, and the structural alteration of this polyunsaturated fatty acid would likely occur at about 160 °C, our experiments were carried out below that temperature.

The following results show one common trend for all three adsorbents. The oil adsorption capacity of silica, florisil, and activated carbon decreases with increase in temperature. This indicates that the influence of temperature on the solvation and diffusion of soybean oil into *n*-hexane solvent is more predominant than activating the adsorption sites in the adsorbents. Also as the temperature rises, van der Waals forces between oil and adsorbent are increasingly disrupted and that contributes to a decreased adsorption.

For all different concentration of adsorbents, the adsorption efficiency of silica, florisil, and activated carbon decreased invariably with the increase in temperature.

Figure 4.4 shows that the % oil retained by silica (at 5:1, 15:1, and 20:1 adsorbent-oil ratio) gradually decreased as the temperature increased through 50, 75, 100, and 150 °C. A steeper slope was observed between 75 and 100 °C. **Figure 4.5**, and **Figure 4.6** show a similar trend for florisil and activated carbon. Also, it is adsorbed that the influence of

temperature is more prominent in florisil, where about 30% of retention dropped between 50 °C and 150 °C for all florisil concentrations.

As the results show the important role of temperature in achieving overall oil adsorption efficiency of these adsorbents, care should be taken to adjust the temperature during the purification step. If the target adsorbate compound is a triglycerides, a higher concentration of adsorbent and a lower temperature are preferred for a better retention.

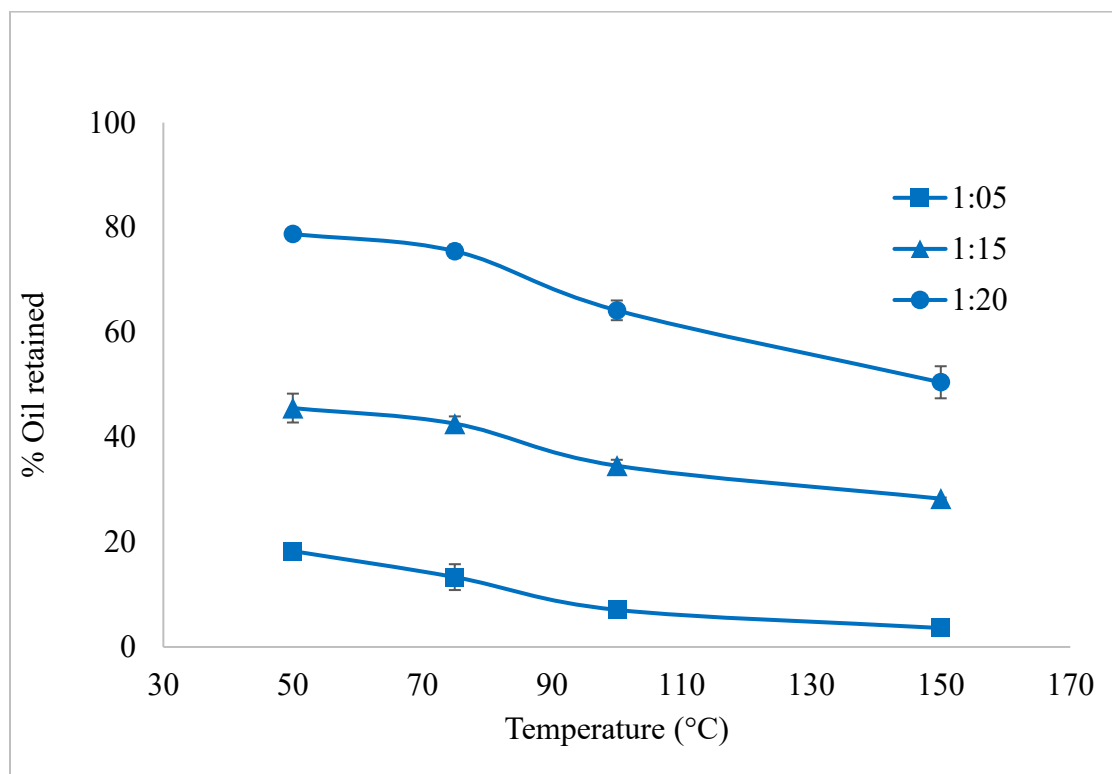


Figure 4.4 Effect of temperature on the performance of silica in adsorbing soybean oil during ASE extraction as a function of adsorbent:oil.

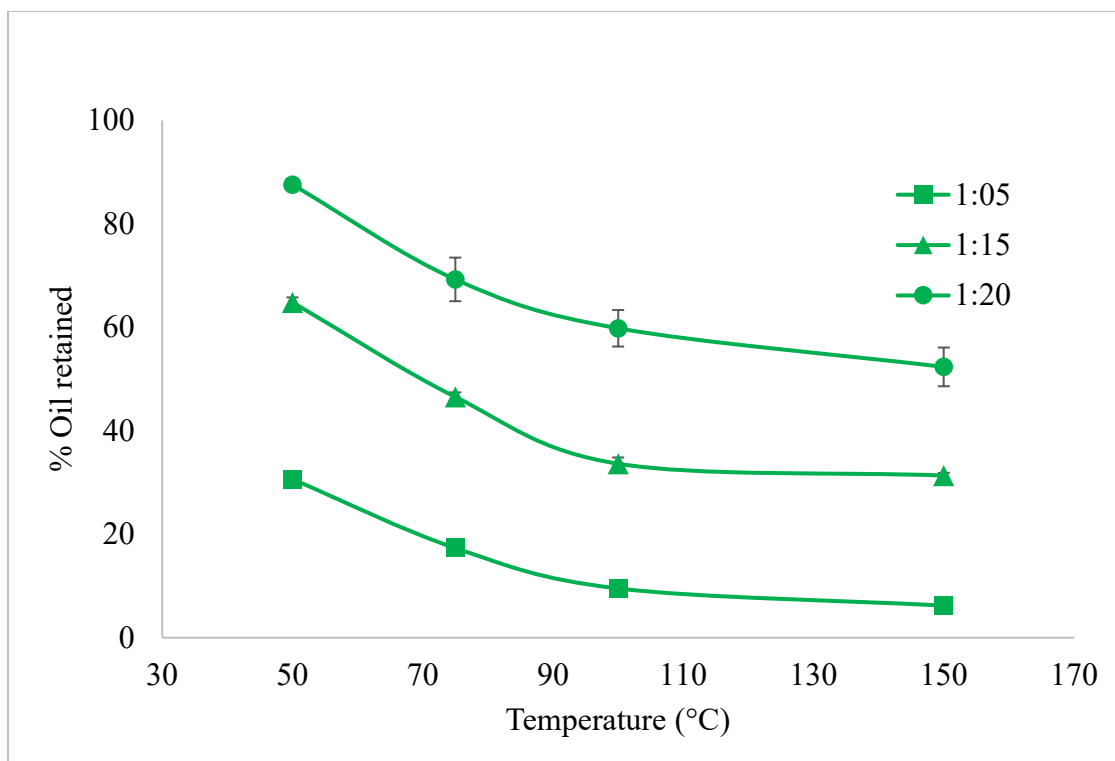


Figure 4.5 Effect of temperature on the performance of florisol in adsorbing soybean oil during ASE extraction as a function of adsorbent:oil .

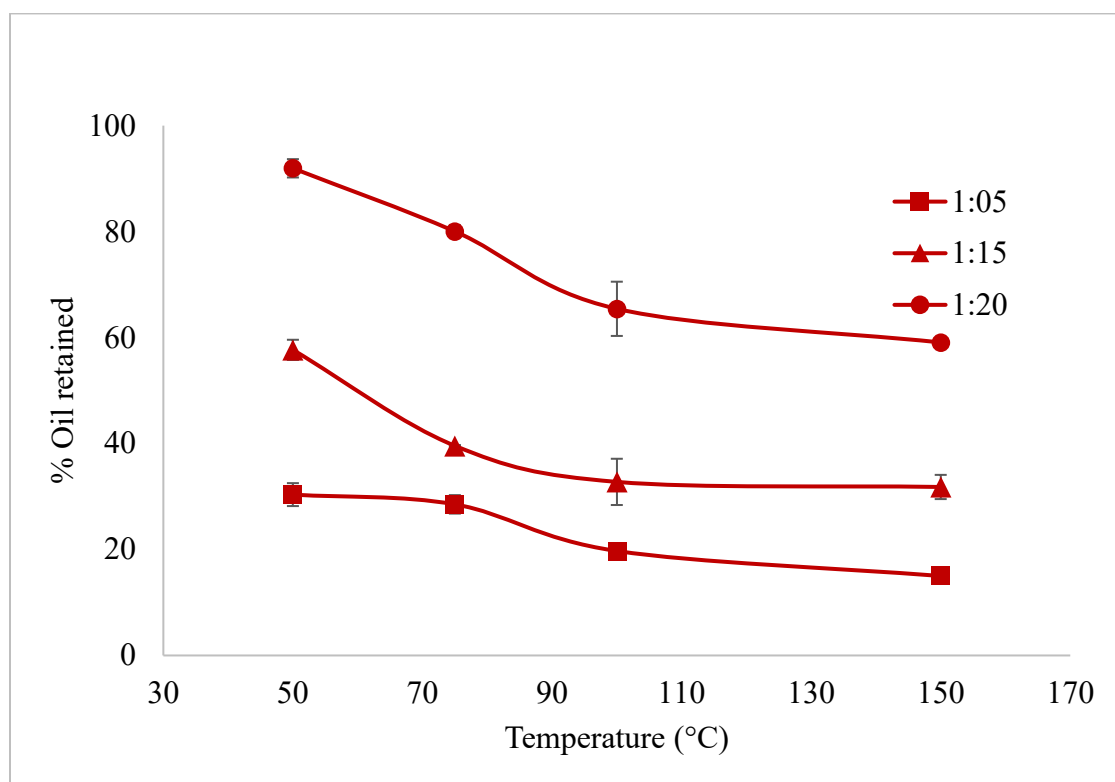


Figure 4.6 Effect of temperature on the performance of activated carbon in adsorbing soybean oil during ASE extraction as a function of adsorbent:oil.

4.3.4 Effect of Adsorbent Concentration on the Performance of Adsorbents

The general understanding is that use of more adsorbents aid a better separation. But this depends on the affinity of the sample to the surface of the adsorbent, and the sample solubility in the solvent. Adding more adsorbent may or may not be useful. Also, the increased concentration of adsorbents would retain not only more interfering substances, but also the useful extracts. This would significantly lower the percent recovery. In order to identify how much adsorbent is ideal for a given purification process, different concentrations of adsorbents need to be tested. As our study targets the adsorbents for triglycerides of fatty acids in soybean oil, we tested different weight ratios of adsorbents to a constant oil weight.

The results show that % oil retention increases with the increase in adsorbent concentration. This implies an increase in collision frequency occur between the molecules of oil and adsorbent with an increase in concentration of adsorbents. A maximum of $91.95 \pm 1.90\%$ oil retention was observed for the activated carbon at 20:1 adsorbent to oil weight ratio at 50 °C (**Figure 4.9**). A gentle slope connecting the performance of adsorbents at 5:1 and 15:1 adsorbent to oil indicates that no sudden change in adsorption mechanism, but the increased surface area of adsorbents opens up more adsorbing sites for the oil content. Except a few deviations, the concentration effect follows a similar trend for all adsorbents. The peak performance of silica ($78.76 \pm 0.66\%$) and florisil ($87.60 \pm 0.54\%$) were observed for 20:1 adsorbent:oil ratio at 50 °C.

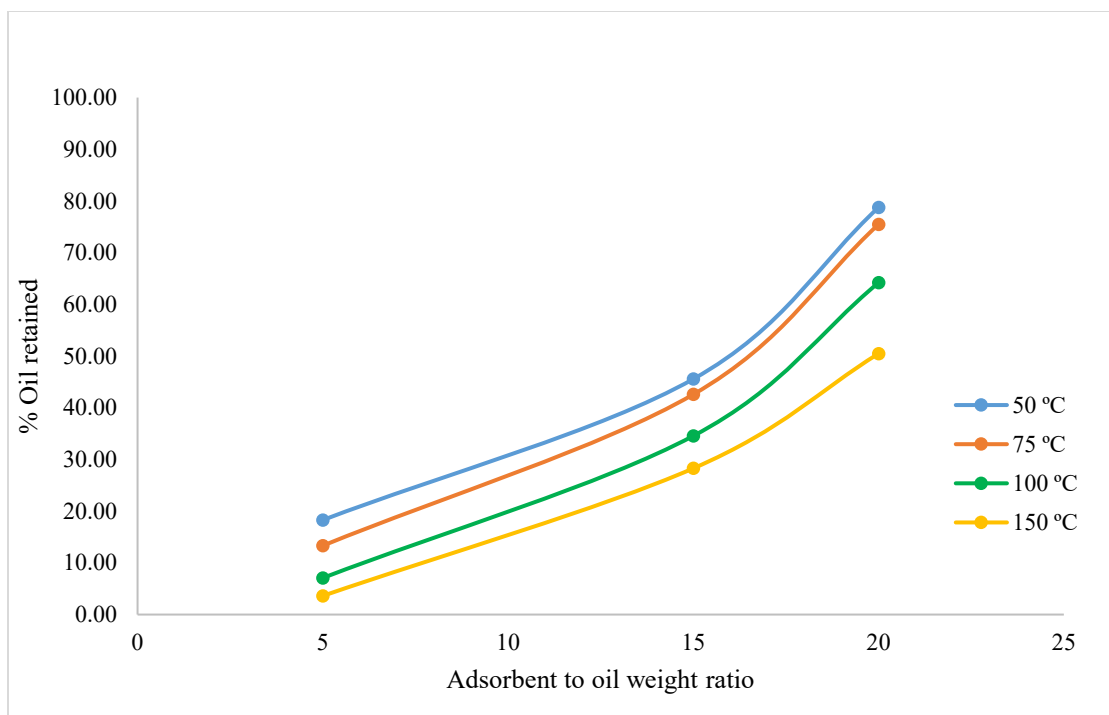


Figure 4.7 Effect of oil to adsorbent weight ratio on the performance of silica at different temperatures.

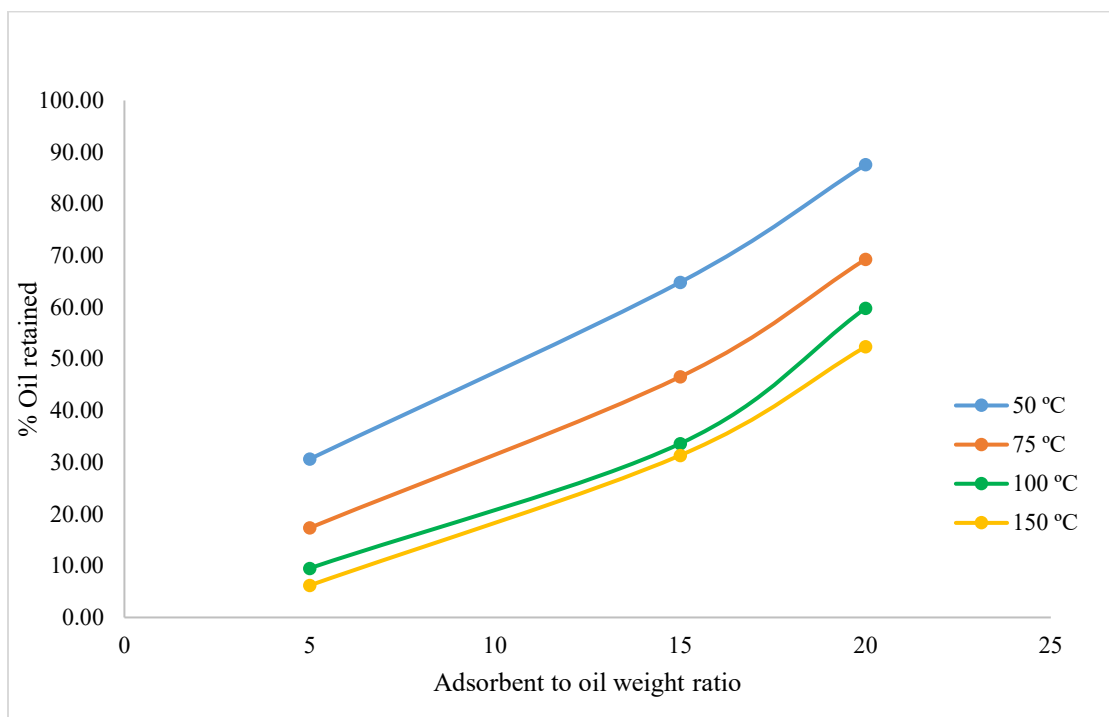


Figure 4.8 Effect of oil to adsorbent weight ratio on the performance of florisol at different temperatures.

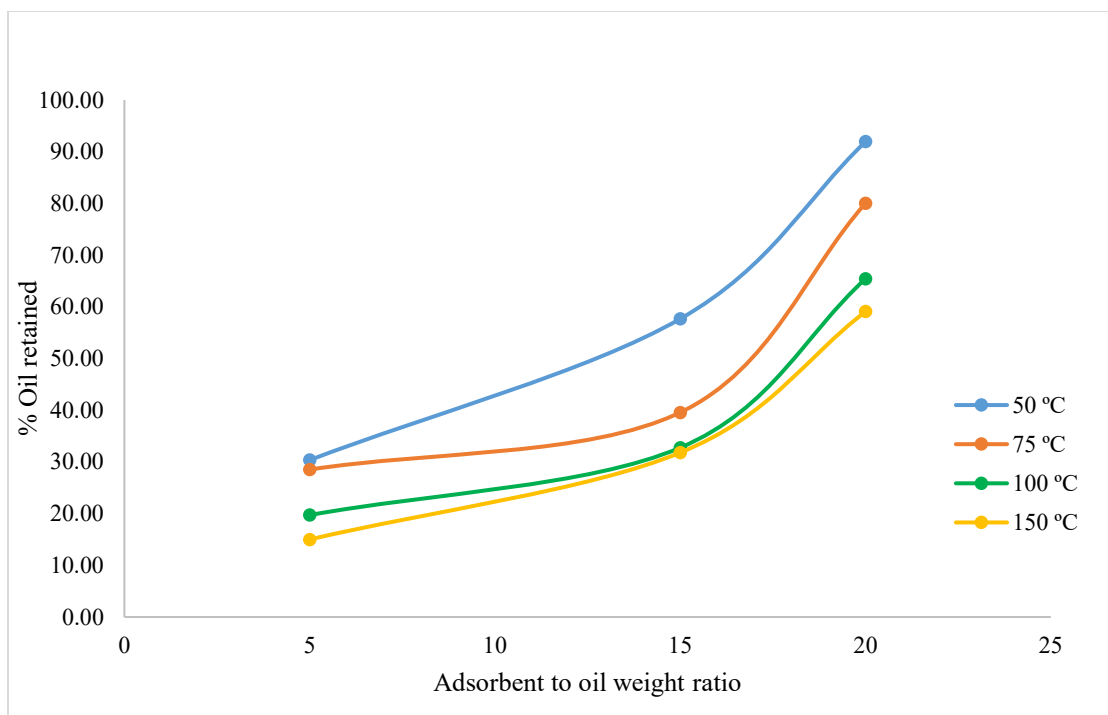


Figure 4.9 Effect of oil to adsorbent weight ratio on the performance of activated carbon at different temperatures.

Table 4.3 ASE extraction results for different adsorbents

Oil to adsorbent ratio	Adsorbent	Temperature (°C)	Average Oil retained per 0.25 g of oil (g)	Percent Oil retained (%)	Standard Deviation (n=3) (%)
1:5	Silica	50	0.0457	18.28	1.32
1:5	Silica	75	0.0333	13.32	2.75
1:5	Silica	100	0.0177	7.08	0.66
1:5	Silica	150	0.0090	3.61	1.00
1:5	Florisil	50	0.0766	30.64	0.96
1:5	Florisil	75	0.0433	17.33	0.54
1:5	Florisil	100	0.0238	9.52	2.16
1:5	Florisil	150	0.0155	6.20	1.91
1:5	Activated carbon	50	0.0759	30.36	1.73
1:5	Activated carbon	75	0.0713	28.52	2.47
1:5	Activated carbon	100	0.0493	19.72	1.38
1:5	Activated carbon	150	0.0375	15.00	1.25
1:15	Silica	50	0.1139	45.56	1.03
1:15	Silica	75	0.1065	42.59	0.87
1:15	Silica	100	0.0864	34.56	4.22
1:15	Silica	150	0.0707	28.28	1.74
1:15	Florisil	50	0.1621	64.84	0.15
1:15	Florisil	75	0.1164	46.56	1.17
1:15	Florisil	100	0.0841	33.64	0.66
1:15	Florisil	150	0.0784	31.36	1.14
1:15	Activated carbon	50	0.1442	57.68	1.88
1:15	Activated carbon	75	0.0989	39.57	0.74
1:15	Activated carbon	100	0.0819	32.76	1.20
1:15	Activated carbon	150	0.0795	31.80	3.53
1:20	Silica	50	0.1969	78.76	0.50
1:20	Silica	75	0.1887	75.48	4.36
1:20	Silica	100	0.1605	64.20	5.12
1:20	Silica	150	0.1262	50.48	0.38
1:20	Florisil	50	0.2190	87.60	0.21
1:20	Florisil	75	0.1732	69.28	3.06
1:20	Florisil	100	0.1496	59.83	1.15
1:20	Florisil	150	0.1309	52.36	0.50
1:20	Activated carbon	50	0.2299	91.95	3.75
1:20	Activated carbon	75	0.2001	80.04	1.08
1:20	Activated carbon	100	0.1636	65.43	2.28
1:20	Activated carbon	150	0.1477	59.08	0.12

4.4 Summary and Conclusions

Oil-adsorption efficiency of five adsorbents, silica, florisil, activated carbon, alumina, and diatomaceous earth, were investigated. An initial study using ASE and CEM prototype extractor indicated that silica, florisil, and activated carbon were the top performers in terms of % oil retention. Further investigation with various temperatures signified that the adsorption efficiency of these three adsorbents notably decreased with an increase in temperature. Temperature promoted solubility of oil in hexane could be a reason for this drop in oil retention percent. An increase in concentration of adsorbent displayed an increase in oil retention capacity, which may be due to the opening of new adsorbing sites, and an overall increase in pore volume. A highest oil retention percent ($91.95 \pm 1.73\%$) was observed for activated carbon at $50\text{ }^\circ\text{C}$ at 20:1 adsorbent to oil (w/w) ratio. At the same temperature and concentration, florisil showed an $87.60 \pm 0.54\%$ and silica showed a $78.76 \pm 0.66\%$.

Since the refining and purification of seed oil becomes a large-scale operation in recent years, comparison of oil-adsorption efficiency of common adsorbents was chosen for study. It should be noted that the adsorption efficiency of an adsorbent may vary considerably from one oil to another. Thus developing a simple method for assessing adsorption efficiency was deemed to be necessary prior to choosing an adsorbent. The method reported in this work imitates the recently evolved ASE in-cell cleanup process. This study on adsorption efficiency during ASE extraction align with the current trends in green analytical chemistry and a step towards an automated post-extraction cleanup. This development of integration of techniques could offer advantages such as simplicity, reduced cost, and low solvent consumption.¹⁰¹

5 CONCLUSION AND FUTURE WORK

The primary focus of this dissertation is to propose and validate an efficient green solvent extraction method for soybean oil. Five solvents (2-MeTHF, *alpha*-pinene, CPME, ethyl lactate, and TBME) were identified via literature survey as green alternatives to the commonly used petroleum-based extraction solvent, *n*-hexane. Based on a solvent indexing system, the relative impact of the solvents on waste, health, environment, fire hazard, reactivity, and lifecycle were assessed. Then, the ability of these solvent to dissolve triglycerides of soybean was theoretically predicted with the aid of a computer program. The solubility of triglycerides in these green solvents was predicted to be high, except for ethyl acetate. Then, the experimental study on viscosity of the green solvents at different temperature indicated that, except ethyl lactate (0.9 cP at 100 °C) and *alpha*-pinene (0.7 cP at 100 °C), the majority of green solvent have low viscosity (~0.5 cP), which is close to that of *n*-hexane.

On the other side, soybean samples were prepared and the effect of particle size on the percent oil recovery was studied in ASE extraction using the reference solvent *n*-hexane. Results showed that the percent recovery increases as the particle size decreases. To be exact, a maximum of 0.2 g of oil was extracted from one gram of 513- μ m particles, whereas only 0.1 g was extracted from one gram of 1200 μ m particles.

As a main focus of the dissertation, the results of ASE extraction of soybean oil using green solvents were validated using the hot-ball model and the extraction efficiencies were compared. All five green solvents showed fit to the hot-ball model, despite of the irregular shape of the soybean particles. The initial steep extraction curve, followed by a flat region at around the reduced time, $t_r = 0.5$, validated the experimental

data of ASE extraction to be reliable. The extrapolation of the linear portion of the curves of all solvents gave y-intercepts less than -0.5, which indicates that 513- μm soybean particles were nonspherical and irregular shapes. Then the experimental results were quantitatively analyzed to calculate the diffusion coefficient and the time required for maximum extraction.

Based on the results, this dissertation proposes CPME, 2-MeTHF, ethyl lactate, and TBME as potential green alternatives to *n*-hexane for soybean oil extraction. Cyclopentyl methyl ether (CPME) demonstrated an excellent overall performance in both the solubility-controlled and diffusion-controlled extraction regions. Remarkably, the diffusion coefficient of CPME ($5.1 \times 10^{-8} \text{ cm}^2\text{s}^{-1}$) is almost ten times greater than that of the petroleum-based solvent *n*-hexane ($5.9 \times 10^{-9} \text{ cm}^2\text{s}^{-1}$). The time required to recover 99% of the soybean oil, was calculated to be 30 min for CPME. The next high efficient alternate solvents were 2-MeTHF with 112 min, TBME with 244 min, and ethyl acetate with 447 min time required for 99% oil recovery. The time required for *n*-hexane for 99% soybean oil recovery is 531 min. alpha-Pinene takes 920 min for that, hence it is less efficient than *n*-hexane.

A knowledge of diffusion coefficient and thus the extraction efficiency of a solute-solvent system would definitely add weight to the quantitative analytical approach in designing both economic and environmentally friendly extraction methods. The exponential behavior of the green solvent extraction can be extrapolated to obtain quantitative analytical information within a brief extraction duration that can be applied for a large-scale extraction.

This dissertation furthers the research area (green solvent extraction of vegetable oils) by examining the method, validating the results, and measuring the efficiency. The experiments were designed with an emphasis on comparing the efficiency of green solvents based on their diffusion coefficient and the time required for maximum oil extraction. The experimental design proposed in this dissertation can be adapted to other green solvents, samples, and extraction techniques. Also, this dissertation opens up an avenue for future works; (i) indexing green solvents based on their performance and behavior during extraction, (ii) developing methods to identify sample-solvent systems for high extraction efficiency, (iii) predicting extraction time and conditions for enhanced recovery.

The second part of this dissertation aimed to test a prototype green extraction technique. The automated Soxhlet type extractor from CEM uses much less solvent than the conventional Soxhlet extraction, and a rapid extraction is promoted by the heat assisted dispersion of analytes. It uses a membrane to filter the extract from solid sample matrix. The pressure setting in this extractor (6 psi) is much less than pressure in ASE (1500 psi). The results indicate that the automatic Soxhlet type extraction system from CEM is 25% less efficient than ASE in terms of amount of oil extracted from soybean during 5 – 30 min. Nevertheless, the extraction results fit in the hot-ball model, and the operating cost, solvent consumption, and extraction time are less than traditional solid-liquid extraction techniques. This examination of new extraction techniques line up with the intention of green analytical chemistry, and future work could focus on developing schemes to compare and highlight the greenness of wide range of extraction techniques.

In-cell cleanup in ASE extraction is a promising strategy to reduce solvent consumption, energy, labor, cost, and time in post extraction procedures. In the last part of this dissertation, oil adsorption efficiency of five different adsorbents was tested at different concentration and temperature. Among the various adsorbents, silica, florisil, activated carbon, alumina and diatomaceous earth, the best performance was observed for activated carbons in terms of % oil retention. Also, the results show that the adsorption ability of these adsorbents decreased with an increase in temperature, which may be attributed to the promoted solubility of oil in hexane at high temperature. The effect of adsorbent concentration suggests that the opening of new adsorbing sites and an overall increase in pore volume would increase the oil retention. Future work in this area may further diversify the use of adsorbents in other extraction techniques. In comparison to the current post-extraction clean-up procedures, the single-step in-cell cleanup method would give more selective extraction free of interfering substances. Developing and documenting adsorbents profiles for various sample-solvent systems could expand the application to large scale.

6 REFERENCES

1. Anastas, P.; Warner, J., *Green Chemistry: Theory and Practice*. Oxford Univ Press: 1998; p 160 pp.
2. Armenta, S.; Garrigues, S.; Esteve-Turrillas, F. A.; de la Guardia, M., Green extraction techniques in green analytical chemistry. *TrAC, Trends Anal. Chem.* **2019**, *116*, 248-253.
3. Keith, L. H.; Gron, L. U.; Young, J. L., Green Analytical Methodologies. *Chemical Reviews* **2007**, *107* (6), 2695-2708.
4. Tobiszewski, M.; Mechlinska, A.; Namiesnik, J., Green analytical chemistry. Theory and practice. *Chem. Soc. Rev.* **2010**, *39* (8), 2869-2878.
5. Armenta, S.; Garrigues, S.; de la Guardia, M., The role of green extraction techniques in Green Analytical Chemistry. *TrAC, Trends Anal. Chem.* **2015**, *71*, 2-8.
6. Tang, S.; Chia, G. H.; Chang, Y.; Lee, H. K., Automated Dispersive Solid-Phase Extraction Using Dissolvable Fe₃O₄-Layered Double Hydroxide Core-Shell Microspheres as Sorbent. *Anal. Chem. (Washington, DC, U. S.)* **2014**, *86* (22), 11070-11076.
7. Huie, C. W., A review of modern sample-preparation techniques for the extraction and analysis of medicinal plants. *Anal. Bioanal. Chem.* **2002**, *373* (1-2), 23-30.
8. Berton, P.; Lana, N. B.; Rios, J. M.; Garcia-Reyes, J. F.; Altamirano, J. C., State of the art of environmentally friendly sample preparation approaches for determination of PBDEs and metabolites in environmental and biological samples: A critical review. *Anal Chim Acta* **2016**, *905*, 24-41.
9. Constable, D. J. C.; Jimenez-Gonzalez, C.; Henderson, R. K., Perspective on Solvent Use in the Pharmaceutical Industry. *Organic Process Research & Development* **2007**, *11* (1), 133-137.
10. Lee, C. K.; Khoo, H. H.; Tan, R. B. H., Life Cycle Assessment Based Environmental Performance Comparison of Batch and Continuous Processing: A Case of 4-d-Erythronolactone Synthesis. *Organic Process Research & Development* **2016**, *20* (11), 1937-1948.
11. Jiménez-González, C.; Curzons, A. D.; Constable, D. J. C.; Cunningham, V. L., Cradle-to-gate life cycle inventory and assessment of pharmaceutical compounds. *The International Journal of Life Cycle Assessment* **2004**, *9* (2), 114-121.
12. Gissi, A.; Lombardo, A.; Roncaglioni, A.; Gadaleta, D.; Mangiatordi, G. F.; Nicolotti, O.; Benfenati, E., Evaluation and comparison of benchmark QSAR models

to predict a relevant REACH endpoint: the bioconcentration factor (BCF). *Environ Res* **2015**, *137*.

13. Candidate list of substances of very high concern for authorisation. European Chemicals Agency (ECHA): 2005.
14. Byrne, F. P.; Jin, S.; Paggiola, G.; Petchey, T. H. M.; Clark, J. H.; Farmer, T. J.; Hunt, A. J.; Robert McElroy, C.; Sherwood, J., Tools and techniques for solvent selection: green solvent selection guides. *Sustainable Chemical Processes* **2016**, *4* (1), 7.
15. Tobiszewski, M.; Tsakovski, S.; Simeonov, V.; Namieśnik, J.; Pena-Pereira, F., A solvent selection guide based on chemometrics and multicriteria decision analysis. *Green Chemistry* **2015**, *17* (10), 4773-4785.
16. Mandalakis, M.; Atsarou, V.; Stephanou, E. G., Airborne PBDEs in specialized occupational settings, houses and outdoor urban areas in Greece. *Environmental Pollution* **2008**, *155* (2), 375-382.
17. de la Cal, A.; Eljarrat, E.; Barceló, D., Determination of 39 polybrominated diphenyl ether congeners in sediment samples using fast selective pressurized liquid extraction and purification. *Journal of Chromatography A* **2003**, *1021* (1), 165-173.
18. Lacorte, S.; Ikonou, M. G.; Fischer, M., A comprehensive gas chromatography coupled to high resolution mass spectrometry based method for the determination of polybrominated diphenyl ethers and their hydroxylated and methoxylated metabolites in environmental samples. *Journal of Chromatography A* **2010**, *1217* (3), 337-347.
19. Echols, K. R.; Peterman, P. H.; Hinck, J. E.; Orazio, C. E., Polybrominated diphenyl ether metabolism in field collected fish from the Gila River, Arizona, USA – Levels, possible sources, and patterns. *Chemosphere* **2013**, *90* (1), 20-27.
20. Bayen, S.; Lee, H. K.; Obbard, J. P., Determination of polybrominated diphenyl ethers in marine biological tissues using microwave-assisted extraction. *Journal of Chromatography A* **2004**, *1035* (2), 291-294.
21. Vilaplana, F.; Ribes-Greus, A.; Karlsson, S., Microwave-assisted extraction for qualitative and quantitative determination of brominated flame retardants in styrenic plastic fractions from waste electrical and electronic equipment (WEEE). *Talanta* **2009**, *78* (1), 33-39.
22. Shin, M.; Svoboda, M. L.; Falletta, P., Microwave-assisted extraction (MAE) for the determination of polybrominated diphenylethers (PBDEs) in sewage sludge. *Analytical and Bioanalytical Chemistry* **2007**, *387* (8), 2923-2929.
23. Picó, Y., Ultrasound-assisted extraction for food and environmental samples. *TrAC Trends in Analytical Chemistry* **2013**, *43*, 84-99.

24. Sun, J.; Liu, J.; Liu, Q.; Qu, G.; Ruan, T.; Jiang, G., Sample preparation method for the speciation of polybrominated diphenyl ethers and their methoxylated and hydroxylated analogues in diverse environmental matrices. *Talanta* **2012**, *88*, 669-676.
25. Martínez-Moral, M. P.; Tena, M. T., Focused ultrasound solid-liquid extraction and gas chromatography tandem mass spectrometry determination of brominated flame retardants in indoor dust. *Analytical and Bioanalytical Chemistry* **2012**, *404* (2), 289-295.
26. Rodil, R.; Carro, A. M.; Lorenzo, R. A.; Cela Torrijos, R., Selective Extraction of Trace Levels of Polychlorinated and Polybrominated Contaminants by Supercritical Fluid-Solid-Phase Microextraction and Determination by Gas Chromatography/Mass Spectrometry. Application to Aquaculture Fish Feed and Cultured Marine Species. *Analytical Chemistry* **2005**, *77* (7), 2259-2265.
27. Xie, S.; Paau, M. C.; Li, C. F.; Xiao, D.; Choi, M. M. F., Separation and preconcentration of persistent organic pollutants by cloud point extraction. *Journal of Chromatography A* **2010**, *1217* (16), 2306-2317.
28. Zhao, A.; Wang, X.; Ma, M.; Wang, W.; Sun, H.; Yan, Z.; Xu, Z.; Wang, H., Temperature-assisted ionic liquid dispersive liquid-liquid microextraction combined with high performance liquid chromatography for the determination of PCBs and PBDEs in water and urine samples. *Microchimica Acta* **2012**, *177* (1), 229-236.
29. Li, Y.; Hu, J.; Liu, X.; Fu, L.; Zhang, X.; Wang, X., Dispersive liquid-liquid microextraction followed by reversed phase HPLC for the determination of decabrominated diphenyl ether in natural water. *Journal of Separation Science* **2008**, *31* (13), 2371-2376.
30. Li, Y.; Wei, G.; Hu, J.; Liu, X.; Zhao, X.; Wang, X., Dispersive liquid-liquid microextraction followed by reversed phase-high performance liquid chromatography for the determination of polybrominated diphenyl ethers at trace levels in landfill leachate and environmental water samples. *Analytica Chimica Acta* **2008**, *615* (1), 96-103.
31. Driver, J. L. Investigations into Chemical Analysis: Assessing Greenness, Quantifying Isomers, and Modeling Diffusion. South Dakota State University Brookings, SD, 2009.
32. Gachumi, G. APPLICATION OF SUPERCRITICAL CARBON DIOXIDE IN AGRICULTURAL PRODUCTS PROCESSING. South Dakota State University, Brookings, SE, 2015.
33. D.E.Raynie, The Role of Selectivity in Extractions: A Case Study. *LC/GC* **2014**, *32* (6), 396-403.

34. Richter, B. E.; Raynie, D., 2.06 - Accelerated Solvent Extraction (ASE) and High-Temperature Water Extraction. In *Comprehensive Sampling and Sample Preparation*, Pawliszyn, J., Ed. Academic Press: Oxford, 2012; pp 105-115.
35. Lopez-Avila, V.; Bauer, K.; Milanés, J.; Beckert, W. F., *J. AOAC Int.* **1993**, *76*, 880.
36. Abu-Sumra, A.; Morris, J. S.; Koirtiyohann, S. R., *Anal. Chem.* **1975**, *47*, 1477.
37. Chatol, G.; Casteynaro, M.; Roche, J. L.; Fantanges, R., *Anal. Chim. Acta* **1971**, *53*, 265.
38. Oostdyk, T. S.; Grob, R. L.; Snyder, J. L.; McNally, M. E., *Anal. Chem.* **1993**, *65*, 600.
39. Richter, B. E.; Jones, B. A.; Ezzell, J. L.; Porter, N. L.; Avdalovic, N.; Pohl, C., Accelerated Solvent Extraction: A Technique for Sample Preparation. *Analytical Chemistry* **1996**, *68* (6), 1033-1039.
40. Ezzell, J. L., *Pressurized Fluid Extractions: Non-Environmental Applications - Encyclopedia of Separation Science*. Academic Press: New York, 2000; Vol. 8.
41. Pitzer, K. S.; Brewer, L., *Thermodynamics*. 1961.
42. Fick, A., *Ann. Phys. (Leipzig)* **1855**, *170*, 65.
43. Pena-Pereira, F.; Kloskowski, A.; Namieśnik, J., Perspectives on the replacement of harmful organic solvents in analytical methodologies: a framework toward the implementation of a novel generation of eco-friendly alternatives. *Green Chem* **2015**, *17*.
44. Clark, J. H.; Farmer, T. J.; Hunt, A. J.; Sherwood, J., Opportunities for bio-based solvents created as petrochemical and fuel products transition towards renewable resources. *Int J Mol Sci* **2015**, *16*.
45. Abou-Shehada, S.; Clark, J. H.; Paggiola, G.; Sherwood, J., Tunable solvents: shades of green. *Chem Eng Process* **2016**, *99*.
46. Hossaini, R.; Chipperfield, M. P.; Montzka, S. A.; Rap, A.; Dhomse, S.; Feng, W., Efficiency of short-lived halogens at influencing climate through depletion of stratospheric ozone. *Nat Geosci* **2015**, *8*.
47. World Health Organization (2015) IARC monographs on the evaluation of carcinogenic risks to humans. <http://monographs.iarc.fr/ENG/Classification/index.php>. Accessed 18 Dec 2015.
48. European Chemicals Agency (2015) List of restrictions. <http://echa.europa.eu/addressing-chemicals-of-concern/restrictions/list-of-restrictions>. Accessed 9 Sept 2015.

49. Capello, C.; Fischer, U.; Hungerbühler, K., What is a green solvent? A comprehensive framework for the environmental assessment of solvents. *Green Chem* **2007**, *9*.
50. Royal Society of Chemistry (2011) GSK solvent selection guide 2009 (supplementary information relating to reference 43).
<http://www.rsc.org/suppdata/gc/c0/c0gc00918k/c0gc00918k.pdf>. Accessed 12 Feb 2017.
51. Henderson, R. K.; Jiménez-González, C.; Constable, D. J. C.; Alston, S. R.; Inglis, G. G. A.; Fisher, G.; Sherwood, J.; Binks, S. P.; Curzons, A. D., Expanding GSK's solvent selection guide – embedding sustainability into solvent selection starting at medicinal chemistry. *Green Chemistry* **2011**, *13* (4), 854-862.
52. Tanzi, C. D.; Vian, M. A.; Ginies, C.; Elmaataoui, M.; Chemat, F., Terpenes as green solvents for extraction of oil from microalgae. *Molecules* **2012**, *17*, 8196-8205.
53. Breil, C.; Meullemiestre, A.; Vian, M.; Chemat, F., Bio-based solvents for green extraction of lipids from oleaginous yeast biomass for sustainable aviation biofuel. *Molecules* **2016**, *21* (2), 196/1-196/14.
54. Greener Solvent Alternatives: Supporting the Advancement of Chemistry through Sound Environmental, Social & Fiscal Responsibilities. *Sigma-Aldrich boucher*.
55. Yara-Varon, E.; Fabiano-Tixier, A. S.; Balcells, M.; Canela-Garayoa, R.; Bily, A.; Chemat, F., Is it possible to substitute hexane with green solvents for extraction of carotenoids? A theoretical versus experimental solubility study. *RSC Adv.* **2016**, *6* (33), 27750-27759.
56. Watanabe, K.; Yamagiwa, N.; Torisawa, Y., Cyclopentyl Methyl Ether as a New and Alternative Process Solvent. *Organic Process Research & Development* **2007**, *11* (2), 251-258.
57. D'Archivio, A. A.; Maggi, M. A.; Ruggieri, F., Extraction of curcuminoids by using ethyl lactate and its optimization by response surface methodology. *J. Pharm. Biomed. Anal.* **2018**, *149*, 89-95.
58. Aparicio, S.; Alcalde, R., The green solvent ethyl lactate: an experimental and theoretical characterization. *Green Chemistry* **2009**, *11* (1), 65-78.
59. Lores, M.; Pajaro, M.; Alvarez-Casas, M.; Dominguez, J.; Garcia-Jares, C., Use of ethyl lactate to extract bioactive compounds from *Cytisus scoparius*: Comparison of pressurized liquid extraction and medium scale ambient temperature systems. *Talanta* **2015**, *140*, 134-142.

60. Matyash, V.; Liebisch, G.; Kurzchalia, T. V.; Shevchenko, A.; Schwudke, D., Lipid extraction by methyl-tert-butyl ether for high-throughput lipidomics. *J. Lipid Res.* **2008**, *49* (5), 1137-1146.
61. Earl G. Hammond, L. A. J., Caiping Su, Tong Wang, and Pamela J. White, Soybean Oil. *Bailey's Industrial Oil and Fat Products, Sixth Edition* **2005**, *6*, 577-654.
62. Dobarganes Nodar, M.; Molero Gómez, A.; Martínez de la Ossa, E., Characterisation and Process Development of Supercritical Fluid Extraction of Soybean Oil. *Food Science and Technology International* **2002**, *8* (6), 337-342.
63. Alder, C. M.; Hayler, J. D.; Henderson, R. K.; Redman, A. M.; Shukla, L.; Shuster, L. E.; Sneddon, H. F., Updating and further expanding GSK's solvent sustainability guide. *Green Chem* **2016**.
64. L. A. Johnson and E. W. Lusas, *J. Amer. Oil Chem. Soc.* **1983**, *60*, 181A-193A.
65. Stahl, E.; Schuetz, E.; Mangold, H. K., Extraction of seed oils with liquid and supercritical carbon dioxide. *J. Agric. Food Chem.* **1980**, *28* (6), 1153-7.
66. Friedrich, J. P.; List, G. R., Characterization of soybean oil extracted by supercritical carbon dioxide and hexane. *J. Agric. Food Chem.* **1982**, *30* (1), 192-3.
67. Phan, L.; Brown, H.; White, J.; Hodgson, A.; Jessop, P. G., Soybean oil extraction and separation using switchable or expanded solvents. *Green Chemistry* **2009**, *11* (1), 53-59.
68. Raynie, D. E., "A Fundamental Understanding of the Chemical Extraction Process," Encyclopedia of Separation Science - (Extraction) - Academic Press. *Extraction* **2000**, 118-128.
69. Bartle, K. D.; Clifford, A. A.; Hawthorne, S. B.; Langenfeld, J. J.; Miller, D. J.; Robinson, R., A model for dynamic extraction using a supercritical fluid. *J. Supercrit. Fluids* **1990**, *3* (3), 143-9.
70. Bartle, K. D.; Boddington, T.; Clifford, A. A.; Hawthorne, S. B., The effect of solubility on the kinetics of dynamic supercritical-fluid extraction. *J. Supercrit. Fluids* **1992**, *5* (3), 207-12.
71. Taniguchi, M.; Tsuji, T.; Shibata, M.; Kobayashi, T., Extraction of oils from wheat germ with supercritical carbon dioxide. *Agric. Biol. Chem.* **1985**, *49* (8), 2367-72.
72. Basics of viscometry. <https://wiki.anton-paar.com/en/basic-of-viscometry/>.
73. Zabaloy, M. S.; Vasquez, V. R.; Macedo, E. A., Viscosity of pure supercritical fluids. *J. Supercrit. Fluids* **2005**, *36* (2), 106-117.

74. Christie, W. W., Gas chromatography-mass spectrometry methods for structural analysis of fatty acids. *Lipids* **1998**, *33* (4), 343-53.
75. Jensen, W. B., The origin of the Soxhlet extractor. *J. Chem. Educ.* **2007**, *84* (12), 1913-1914.
76. Wang, P.; Zhang, Q.; Wang, Y.; Wang, T.; Li, X.; Ding, L.; Jiang, G., Evaluation of Soxhlet extraction, accelerated solvent extraction and microwave-assisted extraction for the determination of polychlorinated biphenyls and polybrominated diphenyl ethers in soil and fish samples. *Anal. Chim. Acta* **2010**, *663* (1), 43-48.
77. Sporring, S.; Bowadt, S.; Svensmark, B.; Bjoerklund, E., Comprehensive comparison of classic Soxhlet extraction with Soxtec extraction, ultrasonication extraction, supercritical fluid extraction, microwave assisted extraction and accelerated solvent extraction for the determination of polychlorinated biphenyls in soil. *J. Chromatogr. A* **2005**, *1090* (1-2), 1-9.
78. Hawthorne, S. B.; Grabanski, C. B.; Martin, E.; Miller, D. J., Comparisons of Soxhlet extraction, pressurized liquid extraction, supercritical fluid extraction and subcritical water extraction for environmental solids: recovery, selectivity and effects on sample matrix. *J. Chromatogr. A* **2000**, *892* (1+2), 421-433.
79. Luque de Castro, M. D.; Garcia-Ayuso, L. E., Soxhlet extraction of solid materials. An outdated technique with a promising innovative future. *Anal. Chim. Acta* **1998**, *369* (1-2), 1-10.
80. Manirakiza, P.; Covaci, A.; Andries, S.; Schepens, P., Automated Soxhlet extraction and single step clean-up for the determination of organochlorine pesticides in soil by GC-MS or GC-ECD. *Int. J. Environ. Anal. Chem.* **2001**, *81* (1), 25-39.
81. Chen, G. G.; Luo, G. S.; Sun, Y.; Xu, J. H.; Wang, J. D., A ceramic microfiltration tube membrane dispersion extractor. *AIChE Journal* **2004**, *50* (2), 382-387.
82. Majors, R. E., A review of EPA sample preparation techniques for organic compound analysis of liquid and solid samples. *LCGC North Am.* **2001**, *19* (11), 1120-1130.
83. EDGE Energized Dispersive Guided Extraction - Brochure. Corporation, C., Ed. <http://cem.com/uk/edge-energized-dispersive-guided-extraction>: 2019.
84. Duarte, K.; Justino, C. I. L.; Gomes, A. M.; Rocha-Santos, T.; Duarte, A. C., Chapter 4 - Green Analytical Methodologies for Preparation of Extracts and Analysis of Bioactive Compounds. In *Comprehensive Analytical Chemistry*, Rocha-Santos, T.; Duarte, A. C., Eds. Elsevier: 2014; Vol. 65, pp 59-78.
85. Kettle, A., Use of Accelerated Solvent Extraction with In-Cell Cleanup to Eliminate Sample Cleanup During Sample Preparation. *Thermo Fisher Scientific - White Paper* **2013**, (70632).

86. El-Hamidi, M.; Zaher, F. A., Comparison between some common clays as adsorbents of carotenoids, chlorophyll and phenolic compounds from vegetable oils. *Am. J. Food Technol.* **2016**, *11* (3), 92-99.
87. Anastassiades, M.; Lehotay, S. J.; Stajnbaher, D.; Schenck, F. J., Fast and easy multiresidue method employing acetonitrile extraction/partitioning and "dispersive solid-phase extraction" for the determination of pesticide residues in produce. *J. AOAC Int.* **2003**, *86* (2), 412-431.
88. Fontana, A. R.; Camargo, A.; Martinez, L. D.; Altamirano, J. C., Dispersive solid-phase extraction as a simplified clean-up technique for biological sample extracts. Determination of polybrominated diphenyl ethers by gas chromatography–tandem mass spectrometry. *Journal of Chromatography A* **2011**, *1218* (18), 2490-2496.
89. Lehotay, S. J.; Mastovska, K.; Yun, S. J., Evaluation of two fast and easy methods for pesticide residue analysis in fatty food matrixes. *J. AOAC Int.* **2005**, *88* (2), 630-638.
90. Kmellar, B.; Fodor, P.; Pareja, L.; Ferrer, C.; Martinez-Uroz, M. A.; Valverde, A.; Fernandez-Alba, A. R., Validation and uncertainty study of a comprehensive list of 160 pesticide residues in multi-class vegetables by liquid chromatography-tandem mass spectrometry. *J. Chromatogr. A* **2008**, *1215* (1-2), 37-50.
91. Dagnac, T.; Garcia-Chao, M.; Pulleiro, P.; Garcia-Jares, C.; Llompart, M., Dispersive solid-phase extraction followed by liquid chromatography-tandem mass spectrometry for the multi-residue analysis of pesticides in raw bovine milk. *J. Chromatogr. A* **2009**, *1216* (18), 3702-3709.
92. Nguyen, T. D.; Yu, J. E.; Lee, D. M.; Lee, G.-H., A multiresidue method for the determination of 107 pesticides in cabbage and radish using QuEChERS sample preparation method and gas chromatography mass spectrometry. *Food Chem.* **2008**, *110* (1), 207-213.
93. Patil, S. H.; Banerjee, K.; Dasgupta, S.; Oulkar, D. P.; Patil, S. B.; Jadhav, M. R.; Savant, R. H.; Adsule, P. G.; Deshmukh, M. B., Multiresidue analysis of 83 pesticides and 12 dioxin-like polychlorinated biphenyls in wine by gas chromatography-time-of-flight mass spectrometry. *J. Chromatogr. A* **2009**, *1216* (12), 2307-2319.
94. Saito, K.; Kikuchi, Y.; Saito, R., Solid-phase dispersive extraction method for analysis of benzodiazepine drugs in serum and urine samples. *Journal of Pharmaceutical and Biomedical Analysis* **2014**, *100*, 28-32.
95. Cerqueira, M. B. R.; Caldas, S. S.; Primel, E. G., New sorbent in the dispersive solid phase extraction step of quick, easy, cheap, effective, rugged, and safe for the extraction of organic contaminants in drinking water treatment sludge. *Journal of Chromatography A* **2014**, *1336*, 10-22.

96. Rodriguez-Mozaz, S.; Lopez de Alda, M. J.; Barcelo, D., Picogram per Liter Level Determination of Estrogens in Natural Waters and Waterworks by a Fully Automated On-Line Solid-Phase Extraction-Liquid Chromatography-Electrospray Tandem Mass Spectrometry Method. *Anal. Chem.* **2004**, *76* (23), 6998-7006.
97. Louter, A. J. H.; Brinkman, U. A. T.; Ghijzen, R. T., Fully automated water analyzer based on online solid phase extraction-gas chromatography. *J. Microcolumn Sep.* **1993**, *5* (4), 303-15.
98. Haglund, P.; Spinnel, E., A modular approach to pressurized liquid extraction with in-cell cleanup. *LCGC North Am.* **2011**, (Suppl.), 66-72.
99. Van Emon, J. M.; Chuang, J. C., Development of a simultaneous extraction and cleanup method for pyrethroid pesticides from indoor house dust samples. *Anal. Chim. Acta* **2012**, *745*, 38-44.
100. Kim, J. H.; Moon, J. K.; Li, Q. X.; Cho, J. Y., One-step pressurized liquid extraction method for the analysis of polycyclic aromatic hydrocarbons. *Anal. Chim. Acta* **2003**, *498* (1-2), 55-60.
101. Liao, Q. G.; Luo, L. G., Fast and Selective Pressurized Liquid Extraction with Simultaneous In-Cell Cleanup for the Analysis of Ethyl Carbamate in Fermented Solid Foods. *Chromatographia* **2014**, *77* (13-14), 963-967.
102. Pintado-Herrera, M. G.; Gonzalez-Mazo, E.; Lara-Martin, P. A., In-cell clean-up pressurized liquid extraction and gas chromatography-tandem mass spectrometry determination of hydrophobic persistent and emerging organic pollutants in coastal sediments. *J. Chromatogr. A* **2016**, *1429*, 107-118.
103. Krstić, V.; Urošević, T.; Pešovski, B., A review on adsorbents for treatment of water and wastewaters containing copper ions. *Chemical Engineering Science* **2018**, *192*, 273-287.
104. Ezzell, J. L.; Richter, B. E.; Felix, W. D.; Black, S. R.; Meikle, J. E., A comparison of accelerated solvent extraction with conventional solvent extraction for organophosphorus pesticides and herbicides. *LC-GC* **1995**, *13* (5), 390-8.
105. Bogdanor, W., In *77th AOCS Annual Meeting*, Honolulu, Hawaii, 1986.
106. Rashid, I.; Daraghmeh, N. H.; Al Omari, M. M.; Chowdhry, B. Z.; Leharne, S. A.; Hodali, H. A.; Badwan, A. A., Chapter 7 - Magnesium Silicate. In *Profiles of Drug Substances, Excipients and Related Methodology*, Brittain, H. G., Ed. Academic Press: 2011; Vol. 36, pp 241-285.
107. Gomez-Ariza, J. L.; Bujalance, M.; Giraldez, I.; Velasco, A.; Morales, E., Determination of polychlorinated biphenyls in biota samples using simultaneous pressurized liquid extraction and purification. *J. Chromatogr. A* **2002**, *946* (1-2), 209-219.

108. Okhovat, A.; Ahmadpour, A.; Ahmadpour, F.; Khaki Yadegar, Z., Pore Size Distribution Analysis of Coal-Based Activated Carbons: Investigating the Effects of Activating Agent and Chemical Ratio. *ISRN Chemical Engineering* **2012**, 2012, 10.
109. Ilomuanya, M. O.; Nashiru, B.; Ifudu, N. D.; Igwilo, C. I., Effect of pore size and morphology of activated charcoal prepared from midribs of *Elaeis guineensis* on adsorption of poisons using metronidazole and *Escherichia coli* O157:H7 as a case study. *Journal of Microscopy and Ultrastructure* **2017**, 5 (1), 32-38.
110. Nording, M.; Sparring, S.; Wiberg, K.; Bjoerklund, E.; Haglund, P., Monitoring dioxins in food and feedstuffs using accelerated solvent extraction with a novel integrated carbon fractionation cell in combination with a CAFLUX bioassay. *Anal. Bioanal. Chem.* **2005**, 381 (7), 1472-1475.
111. Haglund, P.; Sparring, S.; Wiberg, K.; Bjoerklund, E., Shape-Selective Extraction of PCBs and Dioxins from Fish and Fish Oil Using In-Cell Carbon Fractionation Pressurized Liquid Extraction. *Anal. Chem. (Washington, DC, U. S.)* **2007**, 79 (7), 2945-2951.
112. National Center for Biotechnology Information. PubChem Database. pp Source=Sigma-Aldrich, SID=24873970, <https://pubchem.ncbi.nlm.nih.gov/substance/24873970>.
113. Ezzell, J.; Richter, B.; Francis, E., Selective extraction of polychlorinated biphenyls from fish tissue using accelerated solvent extraction. *Am. Environ. Lab.* **1996**, 8 (10), 12-13.
114. Ezzell, J.; Richter, B. E.; Felix, W. D.; Meikle, J.; Black, S., *LC/GC* **1995**, 13 (5), 398.
115. Drake, L. C.; Ritter, H. L., Pore-size distribution in porous materials. II. Macropore size distributions in some typical porous substances. *Ind. Eng. Chem., Anal. Ed.* **1945**, 17, 787-91.
116. Leon y. Leon, C. A., New perspectives in mercury porosimetry. *Adv. Colloid Interface Sci.* **1998**, 76-77, 341-372.
117. List, G. R., 3.1.1 Mineral Types. In *Bleaching and Purifying Fats and Oils - Theory and Practice (2nd Edition)*, AOCS Press.